UNIVERSITY OF CALGARY

The Upper Cretaceous Horseshoe Canyon Formation: using paleosols to reconstruct ancient environments, climates, and record of sea level change in a dinosaur-dominated terrestrial ecosystem

by

Ann Quinney

A THESIS

SUBMITTED TO THE FACULTY OF GRADUATESTUDIES

IN PARTIAL FULFILMENT OF THE REQUIREMENTS FOR THE

INTERDISCIPLINARY DEGREE OF MASTER OF SCIENCE

DEPARTMENT OF GEOSCIENCE

CALGARY, ALBERTA

AUGUST, 2011

Abstract

Paleosols are investigated to reconstruct Late Cretaceous paleoenvironments and paleoclimates of the Horseshoe Canyon Formation. Based on hydrology, degree of development, and pedogenic features, paleosols record the transition from wetland environments to well-drained environments and back to poorly-drained environments through the formation. Paleoclimatic reconstructions indicate that the lower half of the formation was warm and humid, but a period of cooling and drying occurred in the middle of the formation. A complex relationship exists between paleoenvironmental and paleoclimatic changes and a terrestrial vertebrate faunal turnover within the Horseshoe Canyon Formation.

The distribution of paleosols was also compared to sequence stratigraphic interpretations of the HCFm to determine if paleosols recorded evidence of base level changes. Although HCFm paleosols do record some marine transgressive-regressive cycles, the ability to resolve these cycles depends on the distance to the shoreline and the magnitude of the sea-level change.

ACKNOWLEDGEMENTS

Thank you to everyone who helped me with this thesis. Special thanks to my supervisors, Dr. François Therrien and Dr. Darla Zelenitsky for all the research support, feedback, and time you have invested into this project. Thank you to Dr. David Eberth for granting me access to your measured sections and for your endless insight into the Horseshoe Canyon Formation. I would also like to thank Dr. Dennis Braman for sharing his perspectives on the Horseshoe Canyon Formation and for supplying additional samples. Thank you to Amanda McGee, Kohei Tanaka, and Kate Zubin-Stathopolous for teaching my how to use the microscope and various software in the lab. To Jeff Quinney, Jan Quinney, Katie Quinney and Malcolm Williamson, thank you for your continuous support, suggestions, grammatical and technological savvy, and even more support!

I would also like to extend my thanks to all the institutions and societies whose funding made this project possible. Geochemical analyses were funded by the Royal Tyrrell Museum Cooperating Society and funding for thin section preparation was granted by the Dinosaur Research Institute. Additional funding was supplied by an Alberta Graduate Scholarship, a Queen Elizabeth II Graduate Scholarship, and the Natural Sciences and Engineering Research Council of Canada (NSERC).

TABLE OF CONTENTS

LIST OF TABLES

LIST OF FIGURES

Chapter One: Introduction

1.1 Introductory Statement

The Upper Cretaceous Horseshoe Canyon Formation (HCFm) exposed in south-central Alberta preserves a diverse assemblage of terrestrial vertebrate fauna whose paleoenvironmental context, although often inferred, has not been rigorously studied. Several attempts have been made to reconstruct the ancient environments and ancient climates of the HCFm based on palynology, sedimentology, and floral and faunal assemblages (Srivastava, 1970; Wolfe and Upchurch, 1987; Brinkman, 2003; Eberth, 2004; Brinkman and Eberth, 2006). These methods suggest that the lowermost HCFm was subtropical and humid, that aridification occurred throughout the middle part of the formation leading to a subtropical temperate climate, and that a return to more humid conditions occurred in the uppermost HCFm (Srivastava, 1970; Wolfe and Upchurch, 1987; Brinkman, 2003; Eberth, 2004; Brinkman and Eberth, 2006). Inferences regarding climate based on lithology are limited as numerous other factors, including accommodation, subsidence and sediment supply, can influence sedimentation (Bartek et al., 1991; Gordon, 1993; Prosser, 1993; Wright and Marriott, 1993; Miall, 1996; Yoshida et al., 1996; O'Mara, 1999; Goodbred and Kuehl, 1999; Blum and Tornqvist, 2000; Eberth, 2004; Greb et al., 2008). In turn, climatic inferences based on vertebrate fossil evidence are limited by the incompleteness of the terrestrial fossil record (Fastovsky and Weishampel, 2005) and the presence of temperature-sensitive taxa. Finally, climatic inferences based on fossils plants may affected by the potential presence of a lag time in the response of plants to climate change (Davis, 1958; Pennington, 1986). Nevertheless, some authors have suggested that inferred cooling and drying throughout the HCFm is responsible for a documented faunal turnover in vertebrate species, whereby the ankylosaur *Edmontonia* and ceratopsian dinosaurs disappear, the hadrosaur *Edmontosaurus* is replaced by the basal ornithopod *Parksosaurus* and by the hadrosaurs *Hypacrosaurus* and *Saurolophus*, and turtle diversity is reduced (Eberth et al., 2001; Brinkman and Eberth, 2006; Brinkman, 2003). Claims

associating climate change and the faunal turnover have not yet been tested by means independent of fossil occurrences.

The paleoclimatic and paleoenvironmental conditions of the HCFm can be reconstructed through the study of paleosols, or ancient soils, that are preserved in the rock record (Drees and Wilding, 1987; PiPujol and Buurman, 1994, 1997; Ludvigson et al., 1998; Krause, 1999; Retallack, 1994, 1997, 2001; Nordt et al., 2002, 2003; Sheldon et al., 2002; Driese et al, 2005; Therrien et al., 2009; Sheldon and Tabor, 2009). Because the HCFm was deposited in a terrestrial setting, it has the potential to preserve numerous paleosols throughout its stratigraphic interval. Detailed study of the lithological and geochemical features of HCFm paleosols will provide information on the environments and climates that prevailed during deposition. By considering the stratigraphic context in which each paleosol occurs, a record of paleoenvironmental and paleoclimatic change from the late Campanian (73 Ma) to the early Maastrichtian (67 Ma) (Lerbekmo, 2002; Lerbekmo and Braman, 2002) can be produced.

Finally, paleosols have also been used as sequence stratigraphic markers to document changes in base level (e.g., Currie, 1997; McCarthy and Plint, 1998, 1999; McCarthy et al., 1999; Atchley et al., 2004; Bennett et al., 2006). Changes in the hydrology and degree of development of paleosols are inferred to reflect various systems tracts (McCarthy and Plint, 2003). By comparing the record of sea level change to the occurrence paleosol types, the utility of paleosols as indicators of base level can be tested.

1.2. Geologic Setting

A complex depositional history influenced by tectonic activity, eustatic sea level change, and climate change has been proposed for the HCFm (Jerzykiewicz, 1992; Catuneanu and Sweet, 1999; Catuneanu et al., 2000; Eberth et al., 2001; Straight and Eberth, 2002; Eberth, 2004; Hamblin, 2004; Brinkman and Eberth, 2006; Dawson et al, 1994). The HCFm was deposited in the Western Canada Sedimentary basin as part of an eastward thinning clastic wedge of marginal marine to non-marine sediments known as the Edmonton Group. The latest Campanian-earliest Paleocene Edmonton Group is conformably underlain by the

upper Campanian marine Bearpaw Formation and unconformably overlain by the upper Paleocene fluvial Paskapoo Formation. This Group has a long and complex history of stratigraphic subdivisions (Fig. 1.1) but is now generally recognized to consist of four constituent formations: the Horseshoe Canyon, Battle, and Scollard formations (Eberth, 2004; Hamblin, 2004). Sediments of the Edmonton Group are terrestrially-derived from the concurrently-forming Rocky Mountains to the west. Loading of the lithosphere occurred via episodic accretion of terranes along the western margin of Canada, which caused downwarping of the lithosphere and created accommodation space for the accumulation of sediments (Cant and Stockmal, 1989; Cant, 1989; Catuneanu, 1997; Catuneanu et al., 2000). Deposition of the Edmonton Group within the basin is synchronous, in part, with the accretion of the Pacific Rim-Chugah Terrane during the Maastrichtian (Cant and Stockmal, 1989).

The HCFm was deposited on the western edge of the Bearpaw Sea, a broad, northwest-southeast trending seaway that developed between the Canadian Shield to the east and the actively-forming Rocky Mountains to the west (Stott, 1984). The HCFm overlies and partially interfingers with the upper Bearpaw Formation (Fig. 1.2), recording the marine to non-marine transition (Leckie and Smith, 1992; Ainsworth, 1994; Dawson et al., 1994; Eberth, 2004; Hamblin, 2004). The Bearpaw Formation retrogrades to the south and east up section, showing the overall and final regression of the Bearpaw Sea (Ainsworth, 1994; Dawson et al., 1994; Eberth, 2004; Hamblin, 2004). The HCFm is stratigraphically equivalent to the St. Mary River Formation, the upper Wapiti Formation, and the upper Brazeau Formation to the north and the west (Brinkman, 2003; Hamblin, 2004), and to the Eastend and Fox Hills formations to the southeast (Eberth, 2004; Hamblin, 2004) (Fig. 1.2).

In the Drumheller area, the average thickness of the HCFm is approximately 250-275 metres (Eberth, 2004). Over the years, several attempts have been made to subdivide the HCFm into smaller units, based mainly on the relative abundance of coal (Fig. 1.1). Recent studies have aimed at subdividing the HCFm based on lithological differences inferred to represent eustatic, tectonic, and/or climatic controls. Hamblin (2004) proposed that the regressive HCFm can be subdivided into five informal units based on hypothesized

flooding surfaces related to the Bearpaw Formation. In contrast, Eberth (2004) subdivided the HCFm into five informal sub-units (Fig. 1.3) based on lithological differences inferred to reflect tectonic, marine and climatic processes that would have influenced deposition: the lower half of the formation appears to be mainly influenced by changes in relative sea level, whereas the upper half appears to be dominated by climatic and tectonic influences. The stratigraphic scheme of Eberth (2004), which is followed in this thesis, is outlined in Fig. 1.3.

1.2.1. Unit 1

The basal unit of the HCFm, approximately 150-160 m thick, consists of brown, grey, and green mudstones interbedded with siderite layers and laterally extensive carbonaceous mudstones and sandstones (Eberth, 2004). At least 10 laterally-extensive coal intervals, formed by single beds or swarms of multiple beds of subbituminous grade, have been recorded within this unit (Allan and Sanderson, 1945; Ower, 1960; Stelck et al., 1976; Gibson, 1977; McCabe et al, 1989). Following the nomenclature of Gibson (1977), these coals are numbered consecutively from 0-9. Below Coal 7, deposits are tabular and laterally extensive, sandstones are generally fine-grained, and isolated, lenticular, single-storied sandstone bodies are dominant (Eberth, 2004). Numerous bonebeds and articulated dinosaur remains have been recovered from this interval (Eberth, 2004; Brinkman and Eberth, 2006). Above Coal 7, deposits become strongly tapered eastwards, sandstone grain size increases from fine to medium in localized outcrops, stacked paleochannels become more prolific, and rare extra-basinal pebbles are observed (Eberth, 2004).

Unit 1 has been interpreted to represent a paralic depositional environment (Shepheard and Hills, 1970; McCabe et al., 1989; Rahmani, 1988; Lavigne, 1999; Eberth, 2004; Hamblin, 2004; Lerbekmo and Braman, 2005), where the coal seams formed within vertically-aggrading to weakly prograding parasequences (Eberth, 2004). The lower-most part of Unit 1 is inferred to have been strongly influenced by the marine-to-non-marine transition associated with the Bearpaw Sea regression (Leckie and Smith, 1992; Ainsworth, 1994; Dawson et al., 1994; Eberth, 2004; Hamblin, 2004). Below coal 7, lithologic features

suggest that sedimentation occurred during a period of moderate-to-high accommodation, dominated by vertical aggradation (Eberth, 2004). In contrast, the upper part of Unit 1 (above Coal 7) is inferred to have been deposited during a period of increased sediment supply and possibly subsidence (Eberth, 2004).

1.2.2. Unit 2

This unit, approximately 30 m thick, consists of olive green to grey-green mudstones interbedded with laterally-extensive sandstones. This unit differs from the underlying Unit 1 in that beds are thinner, paleochannels are smaller, organic horizons are rare, and ripple-laminated sandstones are common (Eberth, 2004, Hamblin, 2004). These changes suggest that sediment supply, accommodation space, and rates of subsidence have decreased relative to Unit 1 (Eberth, 2004). A stratigraphic interval of variable thickness containing a single coal bed (Coal 10) and numerous occurrences of brackish-water pelecypods in the middle of Unit 2 are associated with a significant marine transgression referred to as the "Drumheller Marine Tongue." Coincidentally, the Campanian-Maastrichtian boundary occurs stratigraphically close to the Drumheller Marine Tongue in the Drumheller area (Lerbekmo and Braman, 2002).

1.2.3. Unit 3

This unit, approximately 10-20 m thick, is a non-coaly interval that consists predominantly of laterally extensive, light brown, fine-grained stacked channels and shoreline sandstones (Eberth, 2004). Finer-grained deposits, interpreted as lacustrine and paludal facies, are uncommon (Eberth, 2004). This architecture has led to the interpretation that deposition of the unit occurred at a time of decreased accommodation during a marine highstand (Straight and Eberth, 2002; Eberth, 2004).

1.2.4. Unit 4

This unit, approximately 25 m thick, is a non-coaly interval that consists of light green to green-grey mudstones and fine-grained sandstones represented in subequal proportions (Eberth, 2004). Unlike Unit 3, channel deposits in Unit 4 are single-storied and well

separated by overbank deposits. This stratigraphic architecture has been interpreted as evidence that Unit 4 was deposited during a period characterized by greater accommodation, low depositional gradients, and reduced sediment supply (Eberth, 2004). This change from Unit 3 may have been induced by an orogenic pulse to the west, as suggested by the presence of coarse-grained volcanic ash and well-separated fluvial sandstones (Eberth, 2010).

1.2.5. Unit 5

The uppermost unit of the HCFm, approximately 20 m thick, consists of light grey mudstones interbedded with laterally-extensive sandstone bodies (Hamblin, 2004; Eberth, 2004). At least two coal swarms occur within this stratigraphic interval. Thick paleochannel deposits with fine- to medium-grained sandstone fills (Hamblin, 2004; Eberth, 2004), some preserving extra-formational pebbles (Eberth, 2004), are present in this unit. The processes leading to the formation of coal beds within Unit 5 have been a topic of debate. Whereas Hamblin (2004) suggested that coal formation is related to sea level rise, Eberth (2004) argued that it is due to an increase in basin subsidence coincident with the return to humid climatic conditions. An increase in grain size relative to Unit 4, the abundance of alluvial sediments, and the presence of extra-formational pebbles suggest that Unit 5 formed during a period of increased sediment supply and accommodation that was likely tectonically-driven by foredeep rebound in proximal portions of the basin (Catuneanu et al., 2000; Eberth, 2004; see also Eberth and Hamblin, 1993).

1.3. Previous Paleoenvironmental Reconstructions of the Horseshoe Canyon Formation

Early attempts to conduct paleoenvironmental reconstructions in the HCFm were based on the relative abundance of coals and dinosaur bones, as well as the presence of environmentally-sensitive fossil plants. The abundance of coal deposits, dinosaur bones, and fossil sequoia trees led to the general interpretation that the HCFm was deposited under a warm, humid to temperate climatic regime (Allan and Sanderson, 1945; Furnival, 1950; Nurkowski and Rhamani, 1984). Other authors took under consideration the diversity of

sporo-pollen assemblages, the size and shape of fluvial channels, and the distribution of vertebrate taxa to refine these paleoenvironmental interpretations (Srivastava, 1970; Russell and Chamney, 1967; Eberth et al., 2001; Russell and Manabe, 2002; Brinkman, 2003; Brinkman and Eberth, 2006; Larson et al., 2010). Similar studies have been undertaken in the correlative St. Mary River Formation by Jerzykiewicz and Sweet (1988) who examined sedimentological and palynological evidence for climate change. Although these authors used different stratigraphic frameworks to produce their paleoenvironmental reconstructions, their interpretations are compiled here into the HCFm stratigraphic framework of Eberth (2004).

1.3.1. Unit 1

Based on the abundance of coal beds and the presence of large fluvial channels, Unit 1 is generally regarded as having formed under humid conditions (Brinkman, 2003; Eberth, 2004; Brinkman and Eberth, 2006). This interpretation is supported by the inferred presence of histosols and gleysols, which form in poorly-drained environments (Nadon, 1988, Hamblin, 2004). Subtropical, humid climatic conditions are inferred from the diverse palynological assemblage of the *Pulcheripollenites krempii* zone of Unit 1 (Srivastava, 1970).

1.3.2. Unit 2

The abrupt disappearance of coal beds at the base of Unit 2, concurrent with a decrease in the number and size of fluvial channels, has been attributed to rapid aridification across the Unit 1/ Unit 2 boundary (Brinkman, 2003; Eberth, 2004, Brinkman and Eberth, 2006; Hamblin, 2004). Abundant paleosols, such as vertisols, with deep vertical root traces suggest improved drainage relative to Unit 1 (Eberth, 2004; Hamblin, 2004). Drying across the Unit 1/Unit 2 boundary appears to be accompanied by subsequent cooling, based on the transition to the *Manicorpus vancampoi* palynological zone above the Drumheller Marine Tongue. This palynological zone is characterized by a reduction in sporo-pollen diversity, such that the paleoclimate becomes subtropical and temperate above the Drumheller Marine Tongue (Srivastava, 1970). Inference of a cooler, drier climate is also supported by

a decline in the relative abundance of crocodiles, champsosaurs and turtles, vertebrates inferred to be climatically sensitive (Eberth, 2004).

1.3.3. Unit 3

This unit is inferred to have formed under the same climatic (and tectonic) conditions interpreted for Unit 2, but was deposited during a marine highstand (Eberth, 2004). Ergo, Unit 3 is inferred to have also been characterized by a drier climate than Unit 1.

1.3.4. Unit 4

Relatively dry climatic conditions are maintained through Unit 4 based on the absence of coals (Eberth, 2004). Forkner (2002) described incipiently-developed paleosols that suggest moderate seasonality of precipitation and/or drainage. Towards the top of Unit 4, however, he noted the occurrence of a periodically-drained hydromorphic paleosol. The appearance of a hydromorphic paleosol at the top of Unit 4 may represent the onset of the humid climatic conditions that prevailed through Unit 5 (Forkner, 2002).

1.3.5. Unit 5

The recurrence of coaly deposits and large paleochannel deposits in Unit 5 suggests a more humid climatic phase relative to Unit 4 (Brinkman and Eberth 2006; Eberth, 2004). A wetter climate is also suggested by the palynological assemblage, whereby the base of Unit 5 also represents the onset of the *Manicorpus gibbus* zone. Climatic conditions in Unit 5 are thus inferred to have reverted to Unit 1-like climatic conditions.

1.4. Paleoprecipitation and Paleotemperature Estimates for the Horseshoe Canyon Formation

Through the study of fossil plant material recovered in the Oldman and Dinosaur Park formations (late Campanian), the Scollard Formation (late Maastrichtian), and similar-aged formations from the western United States, Wolfe and Upchurch (1987) were able to derive paleoprecipitation estimates for the Upper Cretaceous of North America. In Alberta, such

paleoprecipitation estimates are uncertain, but the diminutive leaf size, the rarity of drip tips, the presence of some emarginate apices (notched tip of leaf), and the absence of liana-type leaves suggest that precipitation may have been limited during the Upper Cretaceous (Wolfe and Upchurch, 1987). Modern analogues of Upper Cretaceous North American vegetation are found in eastern Australia and eastern Asia (Webb, 1959; Wolfe, 1979; Wolfe and Upchurch, 1987), suggesting that Upper Cretaceous Alberta experienced a similar precipitation regime, where rainfall approached 1000-1400 mm/year and was evenly distributed throughout the year.

Foliar physiognomy and leaf assemblages have also been used to infer a cooling trend throughout the Campanian and early Maastrichtian and to estimate the paleotemperature of Upper Cretaceous Alberta (Wolfe and Upchurch, 1987). Based on the correlation between dicotyledont leaf margin type and temperature (Bailey and Sinnott, 1915; Wolfe and Upchurch, 1987; Spicer et al., 2004, 2009; Jaques et al., 2011), Wolfe and Upchurch (1987) derived paleotemperature estimates for Upper Cretaceous fossil plant assemblages from paleolatitudes ranging as far north as 50°N. They presented their results in the form of a standardized paleotemperature estimate for a paleolatitude of 30°N, and provided a paleotemperature latitudinal gradient for Upper Cretaceous North America. For the purposes of this study, paleotemperature estimates have been recalculated for a paleolatitude of 60°N (Fig. 1.4), the proposed paleolatitude of the HCFm (Smith et al., 1981), using the Upper Cretaceous latitudinal temperature gradient of 0.3^{o} C per degree of latitude (Amiot et al., 2004; Wolfe and Upchurch, 1987). Based on leaf physiognomy, paleotemperatures are believed to have been equable and mildly seasonal during the Upper Cretaceous in North America (Wolfe and Upchurch, 1987). Climate, however, would have undergone a cooling trend from approximately 17°C in the late Santonian to 15°C in the Campanian. Temperature remained constant throughout the Campanian, followed by a marked decrease during the early Maastrichtian to a minimum of 13°C. A subsequent warming trend occurred during the late Maastrichtian to a peak temperature estimate of 18°C (Fig. 1.4).

Mean annual paleotemperature estimates have also been derived from isotopic analyses of latest Campanian-early Paleocene (71-63.6 Ma) pedogenic carbonate from west Texas, which would have been located at 35°N paleolatitude. Their results have been standardized to a paleolatitude of 60°N using the latitudinal gradient of 0.4^{o}C per degree of latitude derived by Nordt et al. (2003), from a comparison on their paleotemperature estimates to the paleotemperature estimates of Wilf et al. (2003) for latest Cretaceous plants of North Dakota. The latitude-corrected paleotemperature estimates indicate that a cooling trend occurred across the Campanian-Maastrichtian boundary, where paleotemperature dropped from 9°C to 4°C (Fig. 1.4). A brief warming event occurred during the earliest Maastrichtian, where temperature rose to 13°C. Temperature subsequently returned to latest Campanian levels, with occasional fluctuations.

A third set of paleotemperature estimates during the Campanian-Maastrichtian interval have been derived from isotopic analyses of fossil molluscan shells from the Bearpaw Seaway in Saskatchewan. The shells are inferred to represent the near-surface water temperatures of the Bearpaw Sea (He et al., 2005). These authors provide mean annual temperature estimates of approximately 13°C for the early Campanian, 20°C for the middle to late Campanian, and 14°C for the early Maastrichtian (He et al., 2005). Maximum temperatures are correlated with a peak transgression.

1.5. Faunal Assemblage of the Horseshoe Canyon Formation

The Horseshoe Canyon Formation preserves a diverse faunal assemblage (Table 1.1) and produces numerous new fossil discoveries each year. Articulated, associated, and isolated remains are all documented from the HCFm. Bonebeds are especially common in Unit 1, but also occur in Unit 4: three bonebeds of *Edmontosaurus* have been studied from Unit 1 and one bonebed of *Albertosaurus* has been studied from Unit 4 (Eberth et al., 2001; Eberth and Currie, 2010; Larson et al., 2010).

A faunal turnover has been documented among some ornithischian dinosaurs within the HCFm: ceratopsians, *Edmontosaurus,* and *Edmontonia* disappear at the level of Coal 10 within Unit 2, and *Saurolophus, Hypacrosaurus*, and *Parksosaurus* first appear at the base

of Unit 3 (Eberth et al., 2001). Based on the paleoenvironmental reconstructions discussed above and the occurrence of *Hypacrosaurus* and *Parksosaurus* in dry facies of the Judith River Group, this faunal turnover has been attributed to the transition to a drier climate above Unit 1 (Eberth et al., 2001). It has been suggested that occurrence of *Saurolophus osborni* in the upper HCFm may be related to a faunal invasion by Asian dinosaurs during this time (Russell, 1993; Eberth et al., 2001), as a closely related species, *Saurolophus angustirostris*, is known from the Campanian to Maastrichtian Nemegt Formation of Mongolia (Weishampel et al., 2004).

In addition to the changes in dinosaur assemblage, changes in turtle diversity have also been documented in the HCFm (Brinkman and Eberth, 2006). Whereas four different turtle taxa are known from the basal unit of the HCFm (a macrobaenid, a chelydrid, *Basilemys*, and *Aspideretoides* sp.), turtle diversity decreases significantly in overlying units: turtles are not known from Unit 2 and only one taxon (a primitive eucryptodire) is known from Unit 3 and Unit 4. Another turnover in the turtle assemblage takes place in Unit 5, where *Adocus* replaces the taxon known from underlying units (Brinkman and Eberth, 2006). It has been suggested that the pattern of change in turtle diversity preserved in the HCFm may reflect latitudinal changes in temperature over time, as modern turtles are sensitive to changes in temperature (Tarundo et al., 1998; Brinkman, 2003). Temperature may have thus played an important role in controlling turtle diversity in the HCFm (Brinkman, 2003; Brinkman and Eberth, 2004), as the decline in turtle taxa appears to coincide with the decrease in temperature proposed by Wolfe and Upchurch (1987, 1993).(.

1.6. Paleosols as Indicators of Sea Level Changes

In addition to being paleoclimatic and paleoenvironmental indicators, paleosols can also been used as sequence stratigraphic markers to document changes in sea level (e.g., Currie, 1997; McCarthy and Plint, 1998, 1999; McCarthy et al., 1999; Atchley et al., 2004; Bennett et al., 2006). Sequence stratigraphy is most often applied to shallow-marine deposits due to the obviousness of stratigraphic surfaces representing sea level change (McCarthy and Plint, 1998), although several attempts have been made to find correlative surfaces in

terrestrial deposits (e.g., Shanley and McCabe, 1991, Aitken and Flint, 1995; Kamola and Van Wagoner, 1995; Straight and Eberth, 2002; Blum and Tornqvist, 2000; Bennett et al, 2006; McCarthy and Plint, 1998). In addition to paleosols, terrestrial expression of sequence boundaries includes surfaces associated with fining upward packages (Blum and Tornqvist, 2000), the base of incised valley fills, crevasse splays, coal seams, and fossiliferous horizons (Straight and Eberth, 2002). Interfluve paleosols in coastal settings are commonly thought to represent the sequence boundary equivalent of incised channel scours occurring at the same stratigraphic position (McCarthy and Plint, 1998).

McCarthy and Plint (2003: fig. 20) developed a model that correlates the degree of development and hydrology of interfluve paleosols to the various system tracts associated with sea level change, with lateral variation in the paleosols reflecting catenary relationships. Three sequence stratigraphic phases can be recorded in paleosols of coastal and alluvial settings:

1. An aggradational phase, related to normal alluvial sedimentation (transgressive-highstand).
2. A phase of non-deposition or degradation, related to valley incision (falling stage-lowstand).
3. An aggradational phase, related to valley-filling, flooding, and renewed sedimentation on the flood-plain (transgressive).

During a marine highstand (phase 1), the watertable is high, resulting in a poorly-drained coastal plain that is subject to frequent flooding. Flooding should result in the formation of thick, cumulic, hydromorphic soils with organic-rich surficial deposits. During the falling stage and subsequent marine lowstand (phase 2), incised valleys are carved in response to the lowering of base level. While ground drainage improves towards the margins of incised valleys, areas located farther from the edge of the valley remain poorly-drained. As a result, soils that formed in phase 1 become thicker and better developed in phase 2, and those located at the margin of an incised valley will be better-drained than other floodplain soils. Finally, after the incised valleys fill with sediment during the subsequent transgressive

phase (phase 3), watertable rises and the interfluves are once again subject to flooding. Renewed sedimentation, as a result of flooding, is focused along the margins of the valleys and produces cumulic soils with organic-rich surface horizons. In more distal locations, sediment supply may be restricted, leading to the development of thick coal horizons on pre-existing hydromorphic soils.

A similar four-phase model has been proposed by Wright and Marriott (1993: fig. 1), which consists of:

1. A lowstand phase consisting primarily of coarser-grained (possibly braided) channel deposits with restricted aerial extent. Consistent with phase 2 of the McCarthy and Plint (2003) model, well-developed and well-drained soils develop on terrace surfaces.

2. An early transgressive phase involves the slow creation of accommodation space and development of multi-storey sandstone bodies that may be subject to reworking. In response to base-level rise, hydromorphic soils will likely develop. This phase is equivalent to phase 3 of McCarthy and Plint (2003).

3. A late transgressive phase is characterized by an increase in accommodation and the preservation well-separated channel deposits within the floodplain. Rapid vertical accretion allows weakly-developed and well-drained soils to develop. While more mature soils may develop on the floodplain in the latest stages, preservation is unlikely due to the slow creation of accommodation space. An equivalent phase is not noted by McCarthy and Plint (2003).

4. A highstand phase is associated with reduced accommodation and floodplain accretion, producing high-density channel deposits through sediment reworking. Soil preservation is uncommon in this phase. While McCarthy and Plint also note a highstand phase (phase 1), it is thought to be aggradational, producing thick, cumulic, and poorly-drained soils.

To date, sequence stratigraphic work on the HCFm has focused on facies distribution, stratigraphic architecture, and the recognition of sequence bounding surfaces (see Catuneanu and Sweet, 1999; Catuneanu et al., 1999, 2000; Straight and Eberth, 2002; Eberth, 2004; Hamblin, 2004). These authors suggest that the Bearpaw-Horseshoe Canyon succession represents a third-order regressive cycle that is overprinted by up to fourth or fifth-order cycles. This thesis will test the utility of paleosols as sequence stratigraphic markers in the HCFm by comparing the paleosol record to previously identified sequence stratigraphic markers in order to determine if sea level changes based on different methods can be correlated.

1.7. Objectives of this Study

While climatic controls on the changes in ornithischian dinosaur and turtle diversity have been hypothesized for the HCFm, these claims have not been rigorously tested by methods independent of fossil preservation. To assess the potential correlation between faunal turnover and climatic change during the Upper Cretaceous, this thesis will examine the paleosols preserved in the HCFm. A detailed paleoenvironmental reconstruction for the entire HCFm will be established by studying paleosols from each of the five units. The stratigraphic distribution of the HCFm faunal assemblages will then be compared to that of the paleosols to see if changes in faunal assemblage coincide with paleoenvironmental changes.

This thesis will also test the utility of paleosols as sequence stratigraphic markers in the HCFm. The stratigraphic distribution of paleosols in the HCFm will be compared to previously identified sequence stratigraphic markers in order to determine if the occurrence of certain paleosol types coincide with previously established indicators of sea level changes.

1.8. Organization of this thesis

This thesis has been written as two main chapters, each intended for publication in a peer-reviewed journal following the successful defense of this thesis. Chapters 3 and 4 are,

therefore, intended to be complete written works of scientific inquiry. As such, these chapters each contain an abstract, introduction, geologic setting, and materials and methods section. Some overlap exists in the information provided in these sections as a result of this format.

TABLE CAPTIONS

Table 1.1: Vertebrates of the Horseshoe Canyon Formation. Based on Eberth et al. (2001), Weishampel et al. (2004), Longrich and Currie (2009), Brinkman et al. (2007), Newbrey at al. (2009), and Larson et al. (2010)

FIGURE CAPTIONS

Figure 1.1: Historical attempts at subdivision of the Horseshoe Canyon Formation (modified from Hamblin, 2004)

Figure 1.2 Correlation of the Edmonton Group with stratigraphically-equivalent formations (modified from Hamblin, 2004).

Figure 1.3: Stratigraphic architecture of the Horseshoe Canyon Formation (modified from Eberth, 2004)

Figure 1.4: Mean annual temperature curves of Nordt et al. (2003) and Wolfe and Upchurch (1987) for the latest Cretaceous, standardized to a paleolatitude of 60°N, presented with the climatic divisions of Srivastava (1970) (marked by an asterisk).

TABLES

CHAPTER ONE

Table 1.1		
Class	**Order**	**Family (*Genus/ species*)**
Chondrichthyes	Elasmobranchii	Euselachii (*Lamna* sp.) Rhinobatoidea (Family incertae sedis) (*Myledaphus bipartitus*)
Osteichthyes	Acipenseriformes Aspidorhychiformes Lepisosteiiformes Amiiformes ?Semionotiformes Elopiformes Ellimmichthyformes	Acipenseridae (Gen. et sp. indet.) Polydontidae (Gen. et sp. indet.) Aspidorhychidae (*Belonostromus longirostris)* Lepisosteiidae (*Atractosteus occidentalis*) Amiidae (*Cyclurus* sp., Gen. et sp. indet.) (Gen. et sp. indet.) Phyllodontidae (*Paralbula casei*) Family indet. (Gen. et sp. indet.) Sorbinichthyidae (*Horseshoeichthys armaserratus*)
Amphibia	Caudata Anura	Scapherpetontidae (*Scapherpeton tectum*) (Gen. et. sp. indet.)
Reptilia	Cryptodira Eucryptodira Chorisotodera Sauropterygia Squamata Crocodylia Pterosauria Theropoda	Nanhsiungchelyidae (*Basilemys* sp.) Trionychidae (*Aspideretoides* sp. cf. *A. faveatus*) Chelydridae (Gen. et sp. indet.) Macrobaenidae (Gen. et sp. indet.) *Adocidae* (*Adocus*) (Gen. indet.) Champsosauridae (*Champsosaurus albertensis*) Elasmosauria (*Leurospondylus ultimus*) Varanidae (*Palaeosaniwa canadensis*) Alligatoroidea (*Leidyosuchus* sp., *Stangerochampsa mccabei*) (Gen. et sp. indet.) Tyrannosauroidea (*Aublysodon* sp., *Daspletosaurus* sp., *Albertosaurus sarcophagus,* Tyrannosauridae indet.) Dromeosauridae (*Atrociraptor marshalli*, *Sauronitholestes* sp., *Dromaeosaurus* sp. new) Troodontidae (cf. *Troodon* sp.,? Troodontidae indet.) Coelurosauria incertae sedis (*Richardoestesia gilmorei*, cf. *Richardoestesia isosceles)* Ornithomimosauria (*Ornithomimus edmontonicus*, *Struthiomimus altus*,

	Ornithopoda Pachycephalosauria Ankylosauria Ceratopsia	Ornithomimidae indet.) Oviraptorosauria (*Caenagnathidae* sp., *Chirostenotes pergracilis*) Alvarezsauridae (*Albertonykus borealis*) Avialae indet. *Parksosaurus warreni* *Thescelosaurus neglectus* Hadrosauridae (*Edmontosaurus regalis, Hypacrosaurus altispinus, Saurolophus osborni*) *Stegoceras brevis* *Stegoceras edmontonense* Ankylosauridae (*Euoplocephalus tutus*) Nodosauridae (*Panoplosaurus* sp., *Edmontonia longiceps*) *Anchiceratops ornatus, Arrhinoceratops brachyops, Pachyrhinosaurus canadensis,* Ceratopsidae indet., *Eotriceratops xerinsularis*
Mammalia	Multituberculata Marsupialia	Gen. et sp. indet. *Didelphodon coyi*, Gen. et sp. indet.

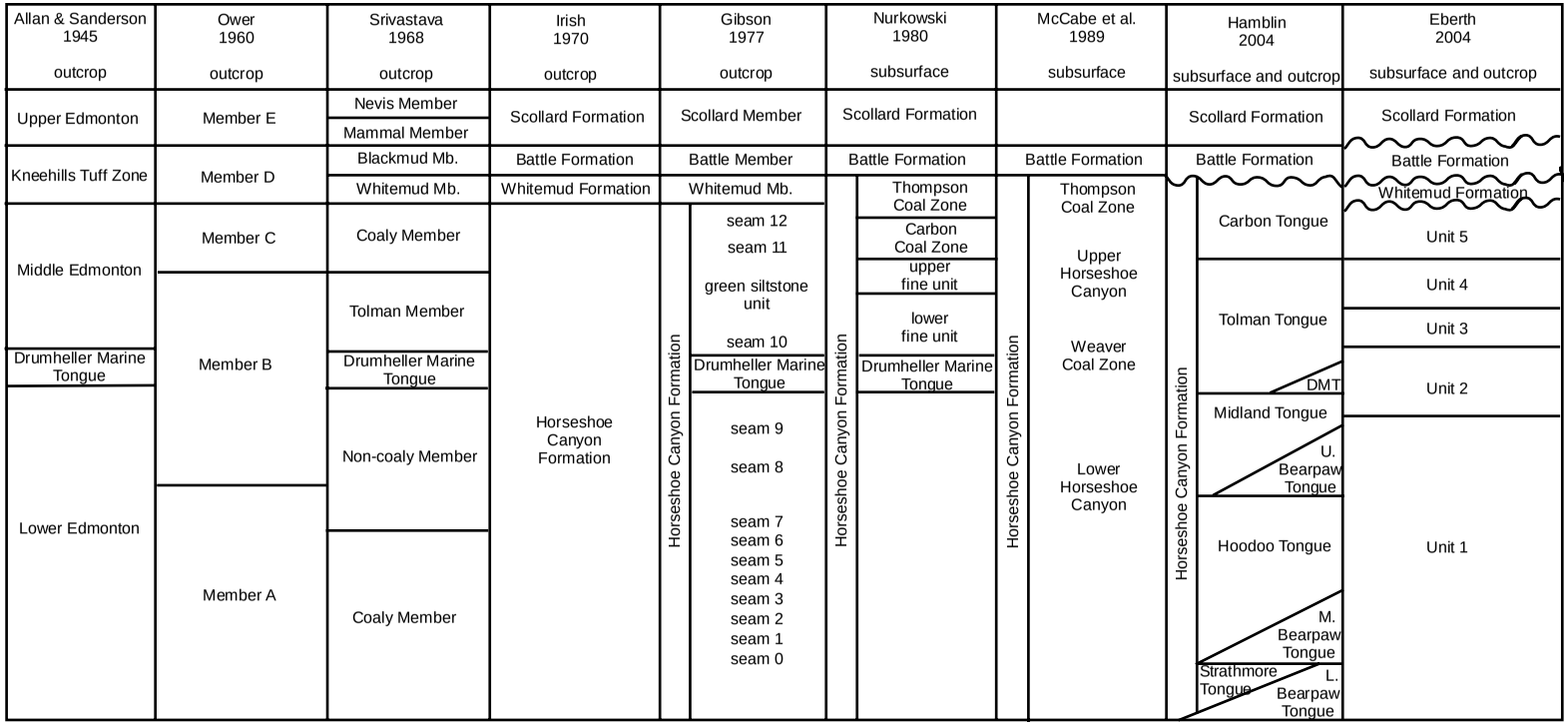
Allan & Sanderson 1945 outcrop
Ower 1960 outcrop
Srivastava 1968 outcrop
Irish 1970 outcrop
Gibson 1977 outcrop
Nurkowski 1980 subsurface
McCabe et al. 1989 subsurface
Hamblin 2004 subsurface and outcrop
Eberth 2004 subsurface and outcrop
Upper Edmonton
Member E
Nevis Member
Mammal Member
Scollard Formation
Scollard Member
Scollard Formation
Scollard Formation
Scollard Formation
Kneehills Tuff Zone
Member D
Blackmud Mb.
Whitemud Mb.
Battle Formation
Whitemud Formation
Battle Member
Whitemud Mb.
Battle Formation
Battle Formation
Battle Formation
Battle Formation
Whitemud Formation
Middle Edmonton
Member C
Coaly Member
Member B
Tolman Member
Drumheller Marine Tongue
Drumheller Marine Tongue
Non-coaly Member
Lower Edmonton
Member A
Coaly Member
Horseshoe Canyon Formation
Horseshoe Canyon Formation
seam 12
seam 11
green siltstone unit
seam 10
Drumheller Marine Tongue
seam 9
seam 8
seam 7
seam 6
seam 5
seam 4
seam 3
seam 2
seam 1
seam 0
Horseshoe Canyon Formation
Thompson Coal Zone
Carbon Coal Zone
upper fine unit
lower fine unit
Drumheller Marine Tongue
Horseshoe Canyon Formation
Thompson Coal Zone
Upper Horseshoe Canyon
Weaver Coal Zone
Lower Horseshoe Canyon
Horseshoe Canyon Formation
Carbon Tongue
Tolman Tongue
DMT
Midland Tongue
U. Bearpaw Tongue
Hoodoo Tongue
M. Bearpaw Tongue
Strathmore Tongue
L. Bearpaw Tongue
Unit 5
Unit 4
Unit 3
Unit 2
Unit 1

Figure 1.1

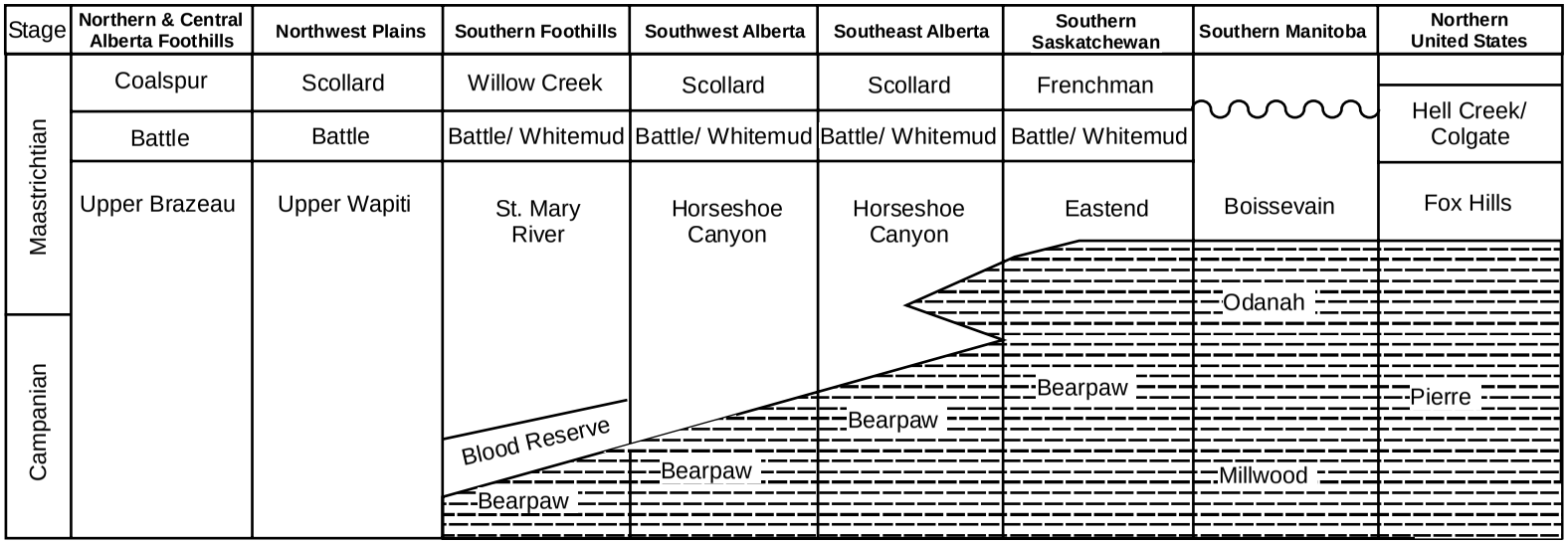
Stage
Northern & Central Alberta Foothills
Northwest Plains
Southern Foothills
Southwest Alberta
Southeast Alberta
Southern Saskatchewan
Southern Manitoba
Northern United States
Maastrichtian
Campanian
Coalspur
Scollard
Willow Creek
Scollard
Scollard
Frenchman
Hell Creek/ Colgate
Battle
Battle
Battle/ Whitemud
Battle/ Whitemud
Battle/ Whitemud
Battle/ Whitemud
Upper Brazeau
Upper Wapiti
St. Mary River
Horseshoe Canyon
Horseshoe Canyon
Eastend
Boissevain
Fox Hills
Odanah
Bearpaw
Pierre
Blood Reserve
Bearpaw
Bearpaw
Millwood
Bearpaw

Figure 1.2

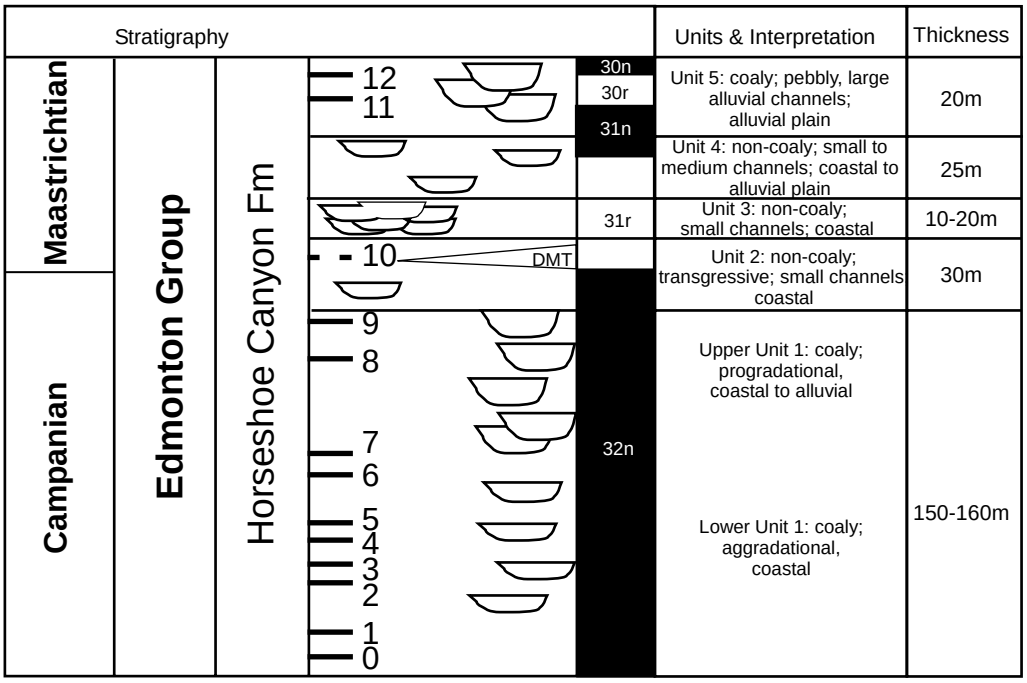
Stratigraphy
Units & Interpretation
Thickness
Maastrichtian
Campanian
Edmonton Group
Horseshoe Canyon Fm
12
11
10
9
8
7
6
5
4
3
2
1
0
DMT
30n
30r
31n
31r
32n
Unit 5: coaly; pebbly, large alluvial channels; alluvial plain
20m
Unit 4: non-coaly; small to medium channels; coastal to alluvial plain
25m
Unit 3: non-coaly; small channels; coastal
10-20m
Unit 2: non-coaly; transgressive; small channels coastal
30m
Upper Unit 1: coaly; progradational, coastal to alluvial
Lower Unit 1: coaly; aggradational, coastal
150-160m

Figure 1.3

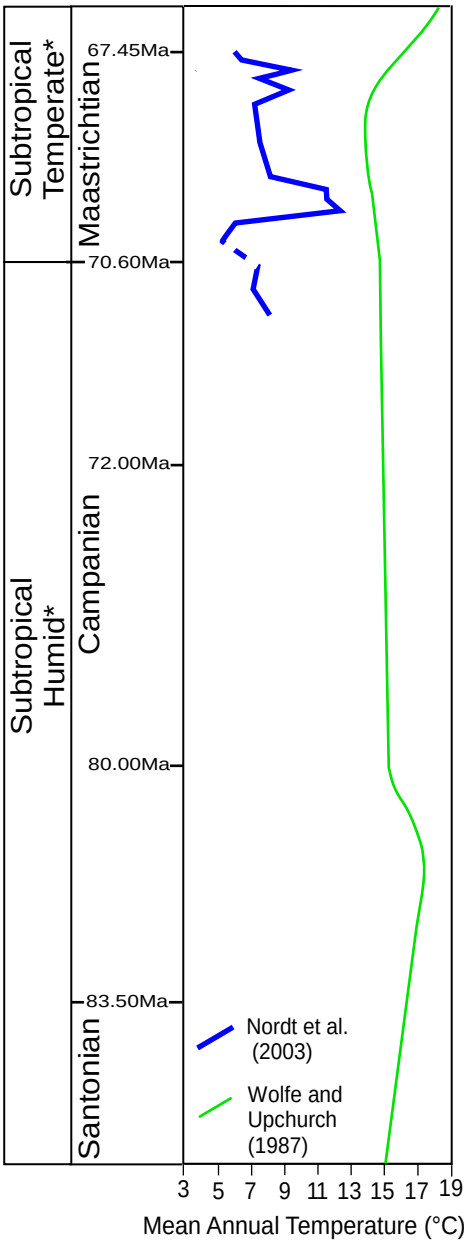
Subtropical Temperate*
Subtropical Humid*
Maastrichtian
Campanian
Santonian
67.45Ma
70.60Ma
72.00Ma
80.00Ma
83.50Ma
Nordt et al. (2003)
Wolfe and Upchurch (1987)
3 5 7 9 11 13 15 17 19
Mean Annual Temperature (°C)

Figure 1.4

Chapter Two: Materials and Methods

To more fully understand the late Campanian-early Maastrichtian paleoenvironments of the Horseshoe Canyon Formation (HCFm), paleosols preserved in these terrestrial deposits were studied. Eight stratigraphic sections spanning the entire stratigraphic interval of the HCFm were measured within the Red Deer River Valley, Alberta: two sites (East Coulee and Hoodoos) are located south-east of the town of Drumheller, two sites (Settling Ponds, Ski Hill) within the town itself, and four sites (Kirkpatrick, Horsethief Canyon, Morrin Bridge, Tolman Bridge) were visited north-west of Drumheller (Fig. 2.1). Two stratigraphic sections (Ski Hill and Tolman Bridge) were measured with a measuring tape and Brunton compass for the purposes of this study; the other six sections were measured by Eberth (2004). The stratigraphic position of paleosols was documented based on the HCFm stratigraphic scheme of Eberth (2004). Field work was completed in the summer of 2010.

2.1. Field Work

A total of 78 paleosol profiles were identified in the HCFm based on the presence of pedogenic horizons, root traces, and pedogenic features, such as clay coatings and slickensides (for a review, see Retallack [1988, 2001]). Each paleosol was documented in the field in terms of horizon thickness and colour, lithology, macroscopic pedogenic features, sedimentary structures, and stratigraphic position within the HCFm. The paleosols were excavated manually using a pick in order to expose fresh, unweathered rock. Fresh rock samples were collected every 15-20 cm in each paleosol profile for potential petrographic and geochemical study. Where relevant, paleosols were exposed laterally in order to document lateral variation. Thickness measurements were made using a tape measure and a Brunton compass, and colour was documented using the Munsell Soil Colour chart (Munsell, 2005).

Preliminary division of the HCFm paleosols into 14 pedotypes, inferred to represent paleosol profiles that formed under a similar set of paleoenvironmental and paleoclimatic conditions, was done based on conspicuous pedogenic features observed in the field

(Retallack, 1994). One paleosol profile from each preliminary pedotype, selected because they were considered representative of their respective pedotypes, was studied in detail through petrographic and geochemical analyses (see Feakes and Retallack, 1988; Retallack, 1997).

2.2. Horizon identification

Pedogenic horizon identification is based on the relative abundance of organic matter and pedogenic features present (Retallack, 1997). Organic-rich surficial horizons forming coal deposits that lie stratigraphic above pedogenically-modified deposits are called O-horizons. An A horizon can be found at the surface or below an O horizon and often has high organic matter content. Subsurface B horizons can be divided into several types, depending on the features they preserve: Bw horizons are weakly developed with few illuvial features, Bt horizons are well-developed with significant clay accumulation, Bss horizons contain common slickensides, and Bg horizons are gleyed. Finally, C horizons lack illuvial features, exhibit minimal weathering, and are therefore considered the parent material.

The degree of development of a paleosol is based on the presence (or absence) of certain horizons as well as of other pedogenic features. Retallack (1997, 1988) described the degree of paleosol development in terms of stages from very weakly developed to very strongly developed. Very weakly-developed paleosols display root traces, maintain textures inherited from the parent material, and lack an A horizon. Weakly-developed paleosols are rooted, may preserve an A horizon, and show evidence of clay translocation or gley without resulting in the formation of a Bt or Bg horizon. Moderately developed paleosols have a surficial organic horizon with rooting and subsurface horizons that preserve illuvial or eluvial features or gley that result in true Bt or Bg horizons. Finally, well-developed paleosols will have obvious illuvial and eluvial features, a well-developed soil structure, and may have a thick coal horizon.

2.3. Petrographic Analysis

A total of 98 rock samples, one per horizon for each preliminary pedotype, were sectioned by Calgary Rock and Minerals Services and analyzed using a petrographic microscope. The 30 µm-thick thin sections were unstained, constituted with epoxy and affixed with Canadian balsam. Microscopic pedogenic features, including redoximorphic features, slickensides, nodules, root traces, clay coatings, and b-fabric, were documented. The descriptive terminology of Bullock et al. (1985) was employed in this study to describe pedogenic features.

2.4. Geochemical Analysis

Rock samples for each preliminary pedotype were processed for geochemical study. A total of 152 samples were analysed for major and trace elements using X-ray fluorescence spectroscopy (XRF) at SGS Minerals Services Limited in Lakefield, Ontario. These results were used to calculate molecular weathering ratios (Table 2.1), which are used as a geochemical proxy for pedogenic processes (Feakes and Retallack, 1988; Retallack, 1997). Due to the unknown geochemical composition of the parent material(s) of HCFm paleosols, the mass-balance method for paleosol geochemical analysis (e.g., Chadwick et al., 1990; Driese et al., 2000) was not utilized.

Mean annual temperature (MAT) and mean annual precipitation (MAP) can be calculated, based on the geochemical composition of Bt or Bk horizon of well-drained paleosols (Sheldon et al., 2002). Based on correlations observed between the geochemical composition of modern soil horizons and climatic factors, Sheldon et al. (2002) have shown that MAT and MAP can be estimated from the base loss molecular weathering ratio (minus the effect of potash) of Bw and Bt horizons of well-developed lowland paleosols (Equations 1 and 3-5). For poorly-developed paleosols, a correlation exists between temperature and the clayeness molecular weathering ratio, as indicated in Equation 2 (Sheldon, 2006). Among the paleoprecipitation estimation methods, Equation 3 is thought to describe the most robust relationship, giving a more precise and accurate estimate for paleosols lacking a Bk horizon (Sheldon et al., 2002; Sheldon and Tabor, 2009). Consequently, only this equation was used to estimate MAP in this thesis. None of these

equations are valid for soils with near surface evaporites or carbonates, waterlogged soils, or soils from hillslope or montane settings (Sheldon et al., 2002; Sheldon and Tabor, 2009).

$$\text{MAT 1} = 18.516*([K2O+Na_2O]/Al_2O_3) + 17.298 \quad (1)$$

$$\text{MAT 2} = 46.9(Al_20_3/SiO_2) + 4 \quad (2)$$

$$\text{MAP 1} = 221e^{0.0197(100*Al2O3/[Al2O3+CaO+Na2O])} \quad (3)$$

$$\text{MAP 2} = 14.265*(100*Al_2O_3/[Al_2O_3+CaO+Na_2O])-37.632 \quad (4)$$

$$\text{MAP 3} = -259.34\ln([MgO+CaO+Na_2O+K_2O]/Al_2O_3)+759.05 \quad (5)$$

Some of the preliminary pedotypes analyzed possessed thick horizons from which several samples were collected. In order to obtain a mean MAT and MAP estimate for each horizon, the geochemical composition of each sample within the horizon was averaged prior to calculation. In cases where a paleosol profile preserved several Bw and Bt horizons, the MAT and MAP estimates for each horizon were averaged to obtain a single MAT and MAP estimate per paleosol profile. Samples from seven well-drained paleosols that had not originally been submitted for geochemical analyses were also selected for MAT and MAP estimates. A single sample from the best-developed Bt or Bw horizon present in each of these profiles was analyzed for major element composition following the methodology described above.

2.5. Final selection of pedotypes

Following the detailed study of microscopic pedogenic features and molecular weathering ratios, some of the preliminary 14 pedotypes were revealed to be variants of the same pedotype. These results lead to the final recognition of nine pedotypes. Paleoenvironmental and paleoclimatic conditions are reconstructed based solely on the pedogenic features observed in each pedotype, without reference to modern soil taxonomy. The use of modern soil taxonomy with paleosols is not appropriate for several reasons: 1) modern soil taxonomy was developed based on present soil-forming processes that may not

have been active in the distant past (Dahms and Holliday, 1998); 2) ancient soils may not preserve all the features necessary to assign it to a taxonomic group (Fastovsky and McSweeney, 1987; Dahms, 1998; Dahms and Holiday, 1998; Mack et al. 1993); 3) because assignment of a modern soil to a specific taxonomic group is, at least partly, based on the climate in which the soil developed, reconstructions of past climates using paleosol taxonomic affinity will be biased (Fastovsky and McSweeney, 1987; Dahms, 1998; Dahms and Holiday, 1998; Mack et al. 1993).

TABLE CAPTIONS

Table 2.1: Molecular weathering ratios of Feakes and Retallack (1988) and Retallack (1997).

FIGURE CAPTIONS

Figure 2.1: Map of study area showing the location of eight measured section in the Red Deer River Valley near Drumheller, Alberta (inset).

TABLES

CHAPTER TWO

Table 2.1				
Salinization	Calcification	Clayeness	Base Loss	Leaching
Na_2O/K_2O	$(CaO+MgO)/Al_2O_3$	$(Al_2O_3)/Si0_2$	$Al_2O_3/(CaO+MgO+Na_2O+K_2O)$	Ba/Sr

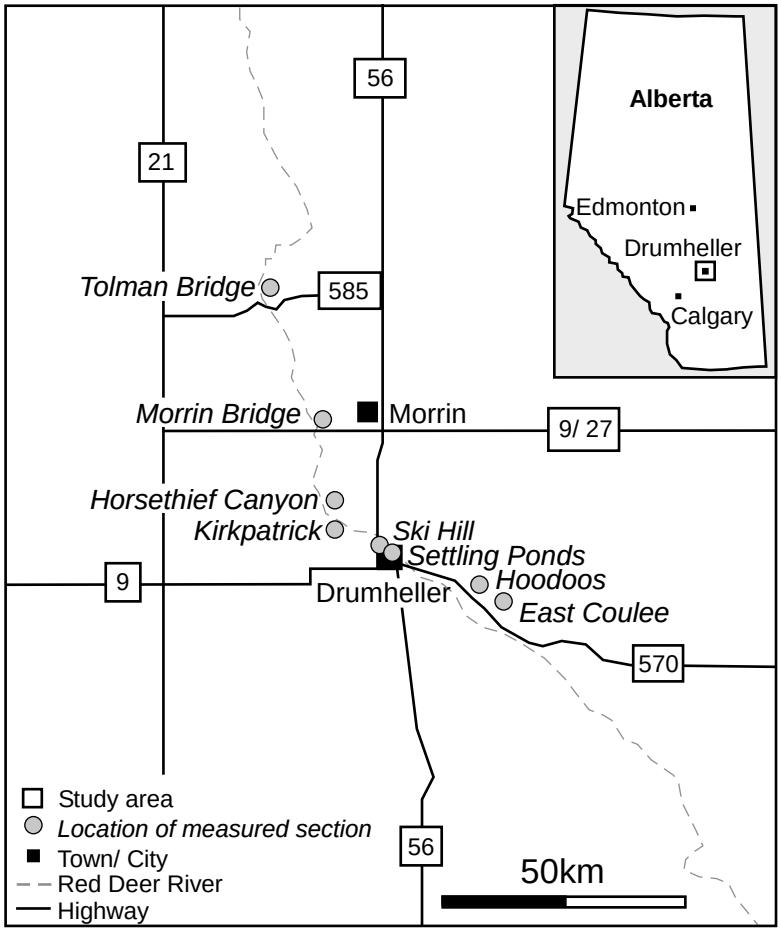
56
21
Alberta
Edmonton
Drumheller
Calgary
Tolman Bridge
585
Morrin Bridge
Morrin
9/ 27
Horsethief Canyon
Kirkpatrick
Ski Hill
Settling Ponds
Hoodoos
East Coulee
9
Drumheller
570
56
50km
Study area
Location of measured section
Town/ City
Red Deer River
Highway

Figure 2.1

Chapter Three: Paleoenvironments and Paleoclimate of the Upper Cretaceous (late Campanian- early Maastrichtian) Horseshoe Canyon Formation (Alberta): using paleosols to study the effect of environmental changes on faunal turnover in a dinosaur-dominated terrestrial ecosystem.

3.1 Abstract

The Upper Cretaceous Horseshoe Canyon Formation (HCFm) produces a wealth of fossil vertebrates each year, some of which are thought to have had strong affinities for specific environmental and climatic conditions. Despite being climatically and environmentally restricted, the details of the paleoenvironmental and paleoclimatic conditions in which these animals lived are not well understood. Pedogenic features and geochemical signatures of paleosols can be used as a proxy for the environmental (i.e. drainage) and climatic conditions under which soils originally formed; abundant paleosols preserved in the overbank deposits of the HCFm are studied to reconstruct the ancient environments and climates that prevailed during the late Campanian to early Maastrichtian. The results of this study are compared with previous paleoenvironmental reconstructions based on sedimentology, lithology, palynology, and floral and faunal assemblages to identify congruencies and differences between methods. The results are also compared to a documented faunal turnover within the HCFm to determine if episodes of environmental and/ or climate change coincide with changes in the HCFm fossil vertebrate assemblage.

The results of this study show that some paleoenvironmental and paleoclimatic changes occurred gradually across the boundary between major lithological units of the HCFm, whereas others occurred relatively rapidly within a lithological unit. Poorly-drained paleoenvironments, predominant in the coal-rich Unit 1, gradually gave way to well-drained paleoenvironments in the coal-poor Unit 2. Climate remained warm and humid during this transition in drainage conditions. Temperature and precipitation dropped suddenly in Unit 2 without concomitant paleoenvironmental changes. A brief return of poorly-drained conditions in Unit 2 coincided with the Drumheller Marine Tongue transgression. Well-drained paleoenvironments, associated with the cool and dry climate

established in Unit 2, persisted through the coal-free Unit 4 and a gradual return to poorly-drained conditions is associated with the transition into the coal-rich Unit 5. Comparison of the results of this study to the documented HCFm faunal turnover reveals a complex association between paleoenvironmental/paleoclimatic changes and faunal changes.

3.2. Introduction

The Upper Cretaceous Horseshoe Canyon Formation (HCFm) is renowned for preserving one of the best vertebrate fossil records near the end of the Cretaceous. Particularly noted for its dinosaur assemblage, the HCFm has produced a wealth of fossils, including tyrannosaurids, hadrosaurs, and ceratopsians (e.g., Eberth et al., 2001; Brinkman and Eberth, 2006; Wu et al., 2007; Eberth and Currie, 2010; Larson et al., 2010). Due to its importance as a record of latest Cretaceous biotic changes and as a natural resources reservoir (coal, conventional gas, and coal-bed methane; Hamblin, 2004), the HCFm has been the subject of paleobotanical, sedimentological, and paleontological studies that aimed to reconstruct the ancient environments and climate under which the formation was deposited (e.g., Srivastava, 1970; Shepheard and Hills, 1970; Wolfe and Upchurch, 1987; Rahmani, 1988; McCabe et al., 1989; Lavigne, 1999; Brinkman, 2003; Eberth, 2004; Hamblin, 2004; Lerbekmo and Braman, 2005; Brinkman and Eberth, 2006). While these studies have documented environmental and climatic trends through the formation, few have sought to determine precise paleoenvironmental parameters (e.g., drainage conditions, paleotemperature, paleoprecipitation) or the precise stratigraphic occurrence of paleoenvironmental changes.

The paleoclimatic and paleoenvironmental conditions of the HCFm can be reconstructed through the study of paleosols, or ancient soils, that are preserved in the rock record (e.g., Drees and Wilding, 1987; PiPujol and Buurman, 1994, 1997; Ludvigson et al., 1998; Kraus, 1999; Retallack, 1994; Nordt et al., 2003; Sheldon et al., 2002; Driese et al, 2005; Sheldon and Tabor, 2009; Therrien et al., 2009; Nordt and Driese, 2010). Detailed study of the lithological and geochemical features of HCFm paleosols can provide valuable information on paleoenvironmental parameters that cannot be evaluated by other methods.

Furthermore, when the paleoenvironmental signal of each paleosol is considered in a stratigraphic context, a detailed record of paleoenvironmental and paleoclimatic changes can be compiled. In this study, the paleoenvironmental and paleoclimatic reconstructions based on paleosols will be compared to previous hypotheses of Upper Cretaceous climate change in order to establish similarities and differences between the methods. Finally, the results will be compared to a documented vertebrate faunal turnover within the HCFm (Russell and Chamney, 1967; Eberth et al., 2001) to determine if episodes of paleoenvironmental and paleoclimatic change coincide with changes in vertebrate diversity.

3.3. Geologic Setting

The depositional history of the HCFm is complex and influenced by tectonic activity, relative sea level change, and climate change (Jerzykiewicz, 1992; Dawson et al, 1994; Catuneanu and Sweet, 1999; Catuneanu et al., 2000; Eberth et al., 2001; Straight and Eberth, 2002; Eberth, 2004; Hamblin, 2004; Brinkman and Eberth, 2006). Deposited in the Western Canada Sedimentary Basin, the HCFm comprises the basal two-thirds of an eastward thinning, clastic wedge of marginal marine to non-marine sediments known as the Edmonton Group. Generally, the Edmonton Group is considered to be composed of four rock formations: the Horseshoe Canyon, Whitemud, Battle, and Scollard formations (Eberth, 2004). Sediments of the Edmonton Group are terrestrially-derived from the concurrently-forming Rocky Mountains to the west, with the accretion of terranes preceding sedimentation into the basin (Cant and Stockmal, 1989; Cant, 1989; Catuneanu, 1997; Catuneanu et al., 2000). Specifically, deposition of the HCFm is synchronous, in part, with the accretion of the Pacific Rim-Chugah Terrane during the Maastrichtian (Cant and Stockmal, 1989). A complex interplay of orogenic pulses and quiescent phases resulted in the creation and reduction, respectively, of accommodation space throughout the deposition of the HCFm (Catuneanu et al. 2000).

The HCFm was deposited during the late Campanian and early Maastrichtian (73 – 67 Ma) (Lerbekmo, 2002; Lerbekmo and Braman, 2002) on the western shore of the Bearpaw Sea, at a paleolatitude of ~60°N (Smith et al., 1981). The Bearpaw Sea was an extensive,

northwest-southeast trending epeiric seaway that developed between the Canadian Shield to the east and the actively-forming Rocky Mountains to the west (Stott, 1984). The Bearpaw Sea is defined as the entire 3rd order, transgressive-regressive cycle of the Bearpaw cyclothem (*sensu* Catuneanu et al. 2000). During the late Campanian, the Bearpaw Sea gradually withdrew and the paralic to alluvial sediments of the HCFm prograded to the south and east. The contact between the Horseshoe Canyon Formation and the underlying marine Bearpaw Formation is conformable and records the overall and final regression of the Bearpaw Sea (Leckie and Smith, 1992; Ainsworth, 1994; Dawson et al., 1994; Eberth, 2004; Hamblin, 2004). The HCFm is stratigraphically equivalent to the St. Mary River, Eastend, and Fox Hills formations, as well as to the upper parts of the Wapiti and Brazeau formations (Brinkman, 2003; Eberth, 2004; Hamblin, 2004).

In the Drumheller area, the HCFm is approximately 250-275 metres thick and consists of interbedded sandstones, siltstones, shales, and coals (Eberth, 2004; Hamblin, 2004). Thirteen coal seams are identified in the HCFm and are numbered consecutively from 0-12 (Gibson, 1977). Whereas early authors subdivided the HCFm into sub-units based mainly on the relative abundance of coal (Allan and Sanderson, 1945; Ower, 1960; Irish, 1970; Gibson, 1977; Nurkowski, 1980; McCabe et al., 1989), recent subdivisions have been based on lithological differences inferred to represent eustatic, tectonic, and/or climatic controls. Using well-log and outcrop data, Hamblin (2004) proposed that the HCFm could be subdivided into five informal units separated by inferred transgressive marine phases. In contrast, Eberth (2004) subdivided the HCFm into five informal sub-units based on lithological differences inferred to reflect tectonic, marine and climatic processes that would have influenced deposition (Fig. 1.3). The latter subdivision scheme is used in this study.

3.4. Materials and Methods

To better understand the Upper Cretaceous paleoenvironments and paleoclimates that prevailed during the deposition of the terrestrial HCFm, paleosols preserved in the abundant overbank deposits were studied. Based on the stratigraphic sections of Eberth

(2004; pers. com., 2010), paleosols were documented at eight sites within the Red Deer River Valley of south-central Alberta (see Fig. 2.1), spanning the entire stratigraphic interval of the HCFm. Paleosol profiles were identified based on the presence of pedogenic horizons, root traces, and macroscopic pedogenic features, such as clay coatings and slickensides (see Retallack, 2001). Each paleosol was documented in the field in terms of horizon thickness and colour, lithology, macroscopic pedogenic features, sedimentary structures, and stratigraphic position within the HCFm. Paleosols were excavated manually, using a pick, in order to expose fresh, unweathered rock. Fresh rock samples were collected at a 15-20 cm interval in each paleosol profile for potential petrographic and geochemical study. Where permissible, paleosols were exposed laterally in order to document lateral variation. Thickness measurements were made using a tape measure and a Brunton compass, and colour was documented using the Munsell Soil Colour chart (Munsell, 2005).

Preliminary division of the HCFm paleosols into 14 pedotypes, inferred to represent paleosol profiles that formed under a similar set of paleoenvironmental and paleoclimatic conditions, was completed based on conspicuous pedogenic features observed in the field and in hand samples (see Retallack, 1994). One paleosol profile from each preliminary pedotype, selected because they were considered representative of their respective pedotypes, was studied in detail through petrographic and geochemical analyses (see Feakes and Retallack, 1988; Retallack, 1997).

3.4.1. Petrographic Analysis

A total of 98 rock samples, one per horizon for each preliminary pedotype, were made into thin sections by Calgary Rock and Minerals Services in Calgary, Alberta. The 30 µm-thick thin sections were unstained, constituted with epoxy, and affixed with Canadian balsam. Thin sections were analyzed using a Leica DM 2500P petrographic microscope and the Leica Application Suite v. 3.6.0 imaging software. Microscopic pedogenic features, including redoximorphic features, slickensides, nodules, root traces, clay and iron coatings, and b-fabric, were documented and described using the descriptive terminology of Bullock et al. (1985).

3.4.2. Geochemical Analysis

Rock samples from each horizon of the preliminary pedotypes were processed for geochemical study. A total of 152 samples were analysed for major and trace elements, using X-ray fluorescence spectroscopy (XRF), at SGS Minerals Services Limited in Lakefield, Ontario. These results were used to calculate molecular weathering ratios, which are used as a geochemical proxy for pedogenic processes (Feakes and Retallack, 1988; Retallack, 1997). Due to the uncertainty surrounding the geochemical composition of the parent material(s) of HCFm paleosols, the mass-balance method for paleosol geochemical analysis (e.g., Chadwick et al., 1990; Driese et al., 2000) was not utilized.

3.4.3. Final selection of pedotypes

Following the detailed study of microscopic pedogenic features and molecular weathering ratios, the preliminary subdivision of HCFm paleosols into fourteen pedotypes was refined into nine pedotypes. Reconstructions of paleoenvironmental and paleoclimatic conditions are based solely on the pedogenic features observed in each pedotype, without reference to modern soil taxonomy. Applying modern soil taxonomy to ancient soils is not appropriate as it relies on many soil characteristics not preserved in paleosols (Dahms and Holliday, 1998). Furthermore, modern soils are often assigned to a taxonomic group based on the climate in which they formed, without regard to the pedogenic features they possess (Soil Survey Staff, 2010). Therefore, applying modern soil taxonomy to paleosols can lead to biased paleoenvironmental reconstructions (Fastovsky and McSweeney, 1987; Dahms, 1998; Dahms and Holiday, 1998; Mack et al. 1993).

3.4.4. Paleotemperature and paleoprecipitation estimates

Because a relationship exists between climatic factors and the geochemical composition of modern soils, this relationship can be applied to ancient soils in order to estimate the mean annual temperature (MAT) and mean annual precipitation (MAP) under which they formed (Sheldon et al., 2002). Specifically, MAT and MAP can be calculated from the base loss molecular weathering ratio (minus the effect of potash) of Bt or Bk horizons in

well-drained, well-developed paleosols (Equations 1, 3, 4, and 5; Sheldon et al., 2002). For poorly-developed paleosols, a correlation exists between temperature and the clayeness molecular weathering ratio (Equation 2; Sheldon, 2006). Equation 3 is considered to document the most robust relationship between precipitation and soil geochemistry, providing a more accurate MAP estimate for paleosols lacking a Bk horizon (Sheldon et al., 2002; Sheldon and Tabor, 2009). As no Bk horizons were documented in the HCFm, preference was given to Equation 3 for MAP estimates.

$$\text{MAT 1} = 18.516*([K2O+Na_2O]/Al_2O_3)+17.298 \quad (1)$$

$$\text{MAT 2} = 46.9(Al_20_3/SiO_2)+4 \quad (2)$$

$$\text{MAP 1} = 221e^{0.0197(100*Al2O3/[Al2O3+CaO+Na2O])} \quad (3)$$

$$\text{MAP 2} = 14.265*(100*Al_2O_3/[Al_2O_3+CaO+Na_2O])-37.632 \quad (4)$$

$$\text{MAP 3} = -259.34\ln([MgO+CaO+Na_2O+K_2O]/Al_2O_3)+759.05 \quad (5)$$

A MAT and MAP estimate was obtained for every Bt and Bw horizon of each well-drained pedotype in the HCFm. In cases where multiple samples were taken from a single horizon, a mean MAT and MAP estimate was obtained by averaging the geochemical composition of every sample within that horizon prior to calculation of estimates. In cases where paleosol profiles contained several Bt or Bw horizons, a single MAT and MAP estimate for the paleosol was calculated by averaging the MAT and MAP estimates from each Bw and/or Bt horizon in that profile. Samples from seven additional, well-drained paleosol profiles within the HCFm were also selected for MAT and MAP estimates. A single sample from the best-developed Bt or Bw horizon present in each additional profile was analyzed for major element composition following the method described above.

3.4.5. Effects of Diagenesis

The effects of diagenesis on HCFm paleosol geochemistry and pedogenic features are considered minor as Horseshoe Canyon paleosols are devoid of diagenetic features in the

form of recrystallization or burial reddening (e.g. Fastovsky and McSweeney, 1987; Retallack, 1991b, 1997). Furthermore, the estimated depth of burial of the HCFm is very shallow, suggesting that diagenetic changes would have been limited. Based on the documented relationship between coal rank and depth of burial, the subbituminous coal beds of the HCFm indicate that the formation would have been buried to a depth of 1176m – 1920m (Nurkowski, 1984). This interpretation is supported by analyses of authigenic clay minerals in sandstones of the overlying Scollard Formation, which concluded a maximum depth of burial of less than 1.5 km and burial temperatures of less than 70°C (Khidir and Catuneanu, 2009). Because the 260-m-thick HCFm lies only 20 m below the Scollard Formation, a depth of burial less than 1.8 km can be inferred. Additionally, studies (Driese et al., 2000, 2007) have demonstrated that many paleosol features are not altered by diagenesis. Consequently, the pedogenic features and geochemical composition of HCFm paleosols are considered to represent the unaltered signature of Upper Cretaceous paleoenvironmental and paleoclimatic conditions.

3.5. Characteristic Features of Horseshoe Canyon Paleosols

3.5.1. Coal

Black coal beds are a prominent feature of the HCFm. Coal beds are common in units 1 and 5, and one coal bed (Coal 10) is present in Unit 2. Coal beds often cap paleosol profiles and, thus, are interpreted as organic-rich (O) surficial horizons (Retallack, 1997). Coal beds can have sharp or gradational bases and root traces occasionally extend from the coal beds into underlying horizons.

3.5.2. Colour

Paleosol colour varies greatly in the HCFm. Whereas paleosols from units 1 and 5 exhibit low chroma (1 to 2) colours in the shades of black, brown, grey, and green-grey, paleosols from units 2 and 4 exhibit colours with chromas greater than 2 in shades of olive green. Significant colour changes are presumably related to varying concentrations of organic matter, iron, and manganese as a result of differences in hydrology (Torrent et al.

1980; Richardson and Daniels, 1993; Schwertmann, 1993). In turn, differences in hydrology are related, in part, to prevailing paleoenvironmental and paleoclimatic conditions (Blodgett et al., 1993; Schwertmann, 1993; Atchley et al., 2004). Whereas low-chroma, "gleyed" colours are interpreted to form under reducing conditions created in poorly-drained soils, bright soil colours are inferred to develop in oxidized, well-drained soils (e.g., Schwertmann, 1993; Wright at al., 2000; Atchley et al., 2004; Richardson and Daniels, 1993).

3.5.3. Microstructure and Fabric of Paleosol Groundmass

Peds represent natural aggregates of soil that formed via the shrink and swell processes caused by alternating wet and dry conditions and rooting in the soil (Retallack, 2001). Although peds were not recognized in outcrops, the presence of peds was inferred from petrographic analysis based on the presence of iron or clay accumulation along distinct surfaces, interpreted as ped surfaces. Because thin sections often preserved only partial peds, it is not always possible to determine the shape and dimensions of the ped.

The orientation of clay particles in a soil groundmass due to pedogenic processes, observable under cross polarized light, is known as b-fabric (Bullock et al. 1985). HCFm paleosols commonly preserve speckled and striated b-fabrics. Two types of speckled b-fabrics occur in HCFm paleosols: 1) stipple-speckled b-fabrics (Fig. 3.1a), formed by randomly arranged, equidimensional, isolated units of optically-oriented clay, and 2) mosaic-speckled b-fabrics (Fig. 3.1b), where the clay units are in contact and produce domains of simultaneous extinction (Bullock et al., 1985). Striated b-fabrics exhibit elongated, birefringent zones with simultaneous extinction produced by the alignment of clays. Clay alignment can be the result of stresses related to shrinking and swelling of clays within the profile (i.e., slickensides) (Nordt and Driese, 2009) or accumulation of clay along features (e.g., clay coatings) (Bullock et al., 1985). Striated b-fabrics of the HCFm may be unistriated, reticulate striated, or granostriated (Fig. 3.1c-e).

3.5.4. Slickensides

Slickensides are shearing planes produced by soil movement due to the shrinking and swelling of clays in response to alternating wet and dry conditions (Smart, 1970; Yaalon and Kalmar, 1978). In thin section, slickensides appear as aligned, birefringent clays (Bullock et al, 1985). Although macroscopic slickensides are not frequently observed in hand samples, striated b-fabrics are common. Well-developed, macroscopic slickensides are common in Unit 2 and weakly-developed, striated b-fabrics (inferred to represent slickensides) are present in Unit 1.

3.4.5. Clay Accumulation

Clay accumulation forms as a result of the translocation of clay, from upper horizons to lower horizons of a soil profile, due to percolation of rainfall through the soil (Brewer, 1960; McKeague, 1983). In the HCFm, clay accumulation occurs as coatings on clastic grains, and along root traces and void walls. Under cross-polarized light, clay coatings will appear as oriented, highly birefringent clay zones, often with subtle laminations (Fig. 3.1f). The presence of clay accumulations in HCFm paleosols indicates that rainfall played an important role in soil development; variability in the degree of development and the frequency of occurrence of clay coatings suggests that the amount of annual precipitation may have varied throughout the deposition of the HCFm, although formation time, parent material, and topography could also have played a role.

3.5.6. Redoximorphic Features and Ferruginous Pedofeatures

Localized depletions and accumulations of iron within the groundmass are called redoximorphic features (formerly called mottles). They form due to the migration and re-precipitation of iron within the soil profile in response to alternating reducing and oxidizing conditions caused by a fluctuating water table (Retallack, 2001; Pipujol and Buurman, 1994; Vepraskas, 1992; Vepraskas and Caldwell, 2008). Redoximorphic features in HCFm paleosols are small and can be difficult to distinguish from the groundmass, depending on the degree of development; consequently, they are often observable only under the microscope (Fig. 3.1g). Depletion redoximorphic features tend to be larger than ferruginous redoximorphic features.

Ferruginous pedofeatures, including iron coatings, hypocoatings, link cappings, and bridges, form via translocation of iron under the alternating oxidizing and reducing conditions produced by cycles of wet and dry conditions during periods of abundant rainfall (Pimentel et al., 1996; Pipujol and Buurman, 1997; Retallack, 2001). Iron oxide will precipitate from ferrous water when oxidizing conditions or a higher pH is encountered in the soil (Pimentel et al. 1996; PiPujol and Buurman, 1997; Retallack; 2001). In HCFm paleosols, iron accumulation occurs as yellow to red coatings and hypocoatings on grains, void edges, organic matter, ped surfaces, and as rare bridges and link cappings between grains (Fig. 3.1h).

3.5.7. Sphaerosiderite

Sphaerosiderite consists of small spherical nodules of iron carbonate. In the HCFm, these nodules are usually less than 20 µm in diameter but can reach up to 30 µm (Fig. 3.1i). The nodules occur in small, grape-like clusters interpreted as coccoid siderite (Driese et al., 2010). This type of siderite forms in fine-grained clay groundmasses or in macropores lined with Fe or Mn oxides under anaerobic conditions related to soil saturation following a period of unimpeded drainage (Ludvigson et al., 1998; Driese et al., 2010).

3.5.8. Pedogenic Carbonate

Pedogenic carbonate is a secondary carbonate accumulation known to form in arid to subhumid climates (Goudie, 1973, 1983; Reeves, 1976). This type of carbonate accumulation is a rare feature of Unit 2 and Unit 4 HCFm paleosols. When present, microscopic carbonate accumulation occurs either as a sparry in-filling of void space or as an amorphous, sparry to micritic accumulation in the groundmass (Fig. 3.1j). Rain water can dissolve and transport carbonate, but limited precipitation prevents the complete removal of carbonate from the soil. Carbonate will precipitate as the water evaporates, forming pedogenic carbonate (Goudie, 1973, 1983; Reeves, 1976; Blodgett, 1988; Retallack, 1994). Whereas pedogenic carbonate is most often micritic (McSweeney and Fastovsky, 1990; Retallack, 1991a,b), sparite can develop pedogenically, given slower calcite precipitation rates within soil fractures (Drees and Wilding, 1987). Periodic showers

during the dry season allow carbonate to precipitate in and around channels where moisture is retained the longest. Repetition of this process results in long growth times, allowing sparite to form (PiPujol and Buurman, 1997).

3.5.9. Bioturbation

Bioturbation is the destruction of original sedimentary structures by the activities of plants and animals (Frey and Pemberton, 1990). Root traces are preserved in paleosols throughout the HCFm as vertically-oriented, carbonaceous filaments that branch downwards. Most root traces are small (1-3 mm in diameter and less than 6 cm long), although larger traces (7 mm in diameter and longer than 10 cm) have been found. Burrows were also observed in HCFm paleosols. Burrow casts most often occur as distinct, sandstone-filled tubules in a clay-rich matrix. The tubules are approximately 1-10 cm long and 0.5-3 cm in diameter, cylindrical, non-branching, and range in orientation from subvertical to subhorizontal. These burrows were likely formed by terrestrial invertebrates, such as worms and insects.

3.6. Results

Seventy-eight paleosol profiles were identified in the HCFm (Fig. 3.2). Paleosols of the HCFm vary between 45 and 185 cm in thickness and range from very weakly-developed to well-developed (see Retallack, 1997). Individual profiles tend to fine upwards and can either be separated vertically by sandstone sheets or stacked, forming compound or composite profiles (e.g. Kraus and Brown, 1986; Birkeland, 1999; Kraus, 1999). Truncated paleosol profiles with erosional upper contacts were also observed, most commonly in units 2 and 4. Although most paleosol profiles are laterally extensive, some profiles developed in lenticular channel fill deposits and are restricted to approximately 20 m in lateral extent. Whereas most HCFm paleosols developed in silty or muddy overbank deposits, a few paleosol profiles developed on sandy parent material. Nine pedotypes are recognized within the Horseshoe Canyon Formation (Fig. 3.3, Table 3.1).

3.6.1. Category 1 paleosols: Gleyed profile capped by coal horizon

Category 1 paleosols consist of brown, grey, or green-grey gleyed horizons overlain by a coal horizon approximately 15- 120cm thick (Fig. 3.3, Table 3.1). Root traces are the only macroscopic pedogenic feature observed in these profiles. Microscopically, clay coatings are common at the base of the paleosol profile but decrease in abundance upward through the profile. The groundmass is generally devoid of iron impregnation. Small iron hypocoatings around gains and along root traces, and voids occur in increasing abundance upward through the profile. Some Category 1 profiles exhibit lateral variation (Fig. 3.4). This pedotype is relatively common in the HCFm and represents 20.5% of the paleosols encountered (n = 16).

Geochemically, these paleosols show limited changes in molecular weathering ratios through the profile (Fig. 3.3). A general decrease in clayeness, base loss, and salinization ratios is observed with increasing depth. The calcification and leaching ratios remain constant throughout the profile.

3.6.1.1. Interpretation

Category 1 paleosols are interpreted as very-well developed hydromorphic paleosols that formed in environments with impeded drainage. The gleyed colour indicates that a high watertable saturated the entire soil profile for three to six months per year (Daniels at al. 1971). The presence of a thick surficial coal, interpreted as an O horizon, suggests that the poorly-drained conditions may have persisted for approximately 3000-12000 years based on coal thicknesses ranging from 30-60cm, a compaction factor of 0.1 times the original thickness, and a peat accumulation rate of 0.5- 1.0mm per year (see Retallack, 1994). The occurrence of ferruginous redoximorphic features around root traces indicates that aeration occurred periodically along voids and fissures while the groundmass remained saturated (PiPujol and Buurman, 1994). The presence of clay coatings also suggests periods of free drainage within the profile (Brewer, 1960; McKeague, 1983, Wright et al., 2000). Lateral variation in Category 1 paleosol profiles can be related to variation in parent material, such as development on lenticular channel deposits (Fig. 3.4).

The various horizons of Category 1 paleosols are poorly differentiated geochemically. Other than the presence of higher clayeness, base loss, and salinization ratios near the top of the profile, presumably due to higher weathering and evaporation at the top of the profile (see Retallack, 1997), the undifferentiated nature of the various ratios suggest limited drainage (e.g., Therrien et al., 2009). An overall history of groundwater saturation punctuated by episodes of soil drying and aeration along pores characterizes Category 1 paleosols.

3.6.2. Category 2 paleosols: Gleyed profiles with a thin, organic-rich surficial horizon

Category 2 paleosols consist of gleyed mudstone to siltstone horizons overlain by an organic-rich mudstone. Category 2 paleosols are divided into three subtypes based on the colour of the subsurface horizons: whereas Category 2a paleosols exhibit brown colours in the lower part of the profile and grey colours in the upper part of the profile, Category 2b paleosols are grey to green-grey throughout the profile, and Category 2c paleosols are grey in the lower part of the profile and brown in the upper part of the profile (Table 3.1). Lateral variation in colour is documented from Category 2 paleosol profiles (Fig. 3.4). Aside from colour, all Category 2 paleosol subtypes display the same pedogenic features: limited clay accumulation in the form of rare clay coatings and faint unistriated b-fabrics in some A and B horizons, a groundmass that is devoid of impregnation, and uncommon ferruginous hypocoatings along root traces, ped surfaces, and voids. Only one representative of the Category 2 profiles is drawn in Fig. 3.3 as the pedogenic features and geochemical profiles are the same for all the subtypes. Category 2 paleosols are extremely common in the HCFm, forming 40% of the paleosols encountered (n=31).

Category 2 paleosols show limited geochemical differentiation between horizons. Only the leaching ratio displays an increasing trend towards the top of the profile (Fig. 3.3), suggesting that more leaching occurs in surface horizons than at depth (Feakes and Retallack, 1988).

3.6.2.1. Interpretation

Category 2 paleosols are interpreted as moderately-developed, hydromorphic paleosols that formed in poorly-drained environments with a high watertable that fluctuated in some profiles (see Wright et al., 2000). Differences in colour and chroma between the three subtypes could reflect differences in organic matter content (see Dobos et al., 1990) as no differences in iron content were observed. Although organic matter content was not quantitatively evaluated, visual inspection indicates that horizons with greater organic matter content may have a chroma greater than 1 and still be interpreted as gleyed. Soil saturation must have persisted for 3 to 6 months per year in order to produce gleyed colours (Daniels at al., 1971). The presence of ferruginous redoximorphic features in voids and along root traces and ped surfaces suggests periodic oxidation of these areas while the groundmass remained saturated (PiPujol and Buurman, 1994). Although rare, the presence of slickensides also suggests alternating wet and dry conditions.

The absence of geochemical differentiation between horizons supports a waterlogged interpretation for Category 2 profiles (e.g., Therrien et al., 2009). Higher values of the leaching ratio near the top of the profiles suggest periods of free drainage in the uppermost horizons (see Feakes and Retallack, 1988).

3.6.3. Category 3 paleosols: Pedogenically-modified sandstone overlain by coal horizon

Category 3 paleosols consist of low-chroma, white to green-grey, fine to medium grained sandstones capped by a thick (30 - 200 cm) coal horizon (Fig. 3.3, Table 3.1). The sandstone horizons exhibit faint, relict sedimentary structures, abundant and well-developed clay coatings, and common external ferruginous hypocoatings on grains, bridges, pendants, and link cappings. The groundmass of these paleosols is devoid of iron impregnation. Category 3 paleosols are moderately common in the HCFm, representing 19.5% of paleosols (n=15).

The horizons of Category 3 paleosols are geochemically undifferentiated, except for the leaching and base loss ratios, which decrease with depth (Fig. 3.3). Furthermore, the leaching ratio of these sandy paleosols is far greater in absolute values than that of muddy paleosol profiles, reaching the highest values observed in any of the HCFm pedotypes.

3.6.3.1. Interpretation

Category 3 paleosols are interpreted as weakly-developed, waterlogged profiles that developed on channel or crevasse splay deposits. The accumulation of coal in these profiles is not interpreted as a thick O horizon but rather as the accumulation of organic matter in ponded areas. The gleyed colours and extensive coal development are indicative of poorly-drained environments, but the clay coatings and iron hypocoatings indicate that drainage improved periodically (e.g. Brewer, 1960; Pipujol and Buurman, 1994; McKeague, 1983).

The sandy nature of Category 3 paleosols may have allowed more rapid drainage through the profile (relative to muddy parent materials) due to greater porosity and permeability (see Boggs, 2006). The greater abundance of clay coatings and redoximorphic features in coarser-grained versions of this pedotype as opposed to finer-grained versions of the same pedotype, supports this interpretation. Accordingly, the unusually high leaching ratio of Category 3 paleosols can also be linked to the sandy parent material. Limited geochemical differentiation between the remaining molecular weathering ratios may be attributed to impeded drainage (e.g., Therrien et al., 2009).

3.6.4. Category 4 paleosols: Profiles with gleyed basal horizons and non-gleyed upper horizons

Category 4 paleosols consist of gleyed, grey to green-grey mudstone horizons in the lower part of the profile and of non-gleyed, olive-coloured mudstone horizons in the upper part (Fig. 3.3, Table 3.1). A variety of macroscopic and microscopic pedogenic features occur in these paleosols. Root traces and rare clay coatings are present in the upper horizons but only clay coatings exist in the lower horizons. Ferruginous redoximorphic features are common in the lower part of the profile and decrease in abundance upward through the profile. Finally, sphaerosiderite is uncommon in these paleosols, occurring as small (5-20 µm in diameter), grape-like clusters in the groundmass, with the largest and most abundant nodules (up to 30 µm in diameter) occurring low in the paleosol profile. Weak to moderate iron impregnation of the groundmass surrounds the sphaerosiderite. Gleyed horizons are devoid of iron impregnation whereas non-gleyed horizons exhibit

weak to moderate iron impregnation. B-fabrics range from stipple speckled to mosaic speckled, with occasional granostriation near the top of the profile. Category 4 paleosols are uncommon in the HCFm, representing 6.5% of the paleosols (n=5).

Geochemical differentiation of horizons is limited in the lower part of the profile, but an increase in the salinization, clayeness and calcification ratios is observed near the top of the profile (Fig. 3.3). Notably, the calcification and leaching ratios are higher and lower, respectively, than in Category 1-3 paleosols.

3.6.4.1. Interpretation

Category 4 paleosols are interpreted as moderately-developed paleosols that formed in moderately-drained environments where the watertable fluctuated during the year (see Wright et al., 2000). The watertable remained low for an extended period of time, as indicated by the gleyed lower horizons (see Daniels et al., 1971) and the presence of sphaerosiderite (see Driese et al., 2010). In contrast, the upper part of the profile was well-drained, as indicated by the non-gleyed colours and the presence of clay and iron coatings.

The molecular weathering ratios reveal that the upper part of the profile was better drained, with higher salinization, clayeness, and calcification ratios than the lower part of the profile, which is geochemically undifferentiated (Fig. 3.3). The increase in the salinization molecular weathering ratio at the top of the profile is likely associated with surface evaporation (e.g., Retallack, 1997). As such, Category 4 paleosols are inferred to have developed in slightly better-drained environments than the Category 1-3 paleosols and are considered to have formed in transitional environments (i.e., between poorly-drained and well-drained environments) (see Wright et al., 2000). Relative to Category 1-3 paleosols, a higher calcification ratio is inferred to represent a more alkaline watertable (see Ashley and Driese, 2000) and/or drier conditions (as all the carbonate has not been leached out), while a lower leaching ratio is inferred to represent less leaching in Category 4 paleosols (Retallack, 1997).

3.6.5. Category 5 paleosols: Non-gleyed profiles with slickensides

Category 5 paleosols consist of non-gleyed, varicoloured horizons in shades of brown, black, grey, and green (Fig. 3.3, Table 3.1). Horizons are typically thin (9–32 cm), although a thick (~50 cm), basal, gleyed horizon is present in some profiles. Several pedogenic features occur throughout the paleosol profile, including root traces, well-developed slickensides, and common clay-coatings. Iron impregnation of the groundmass varies from weak to moderately strong, often in linear, subparallel zones. Pedogenic features are uncommon in the basal gleyed horizon, although rare clay coatings, faint slickensides, and large depletion redoximorphic features are observed at the top of the horizon. Tongues of the gleyed horizon extend into the overlying sandy horizon. Category 5 paleosols are rare in the HCFm, representing 2.5% of the paleosols (n=2).

Category 5 paleosols are moderately differentiated geochemically, exhibiting slight increases in the salinization, calcification, and clayeness ratios upward through the profile (Fig. 3.3). Similar to Category 4 paleosols, a lower leaching ratio than Category 1-3 paleosols is observed.

3.6.5.1. Interpretation

Category 5 paleosols are interpreted as well-developed paleosols, subject to alternating wet and dry conditions that developed in generally well-drained paleoenvironments. Pedogenic features indicate that the drainage conditions varied throughout the profile. Abundant clay coatings suggest that drainage in the upper part of the profile was unimpeded (see McKeague, 1983). The co-occurrence of clay coatings with slickensides reveals periodic rainfall saturation followed by dry conditions (see Moeyersons et al., 2006; Nordt and Driese, 2009). The presence of a basal gleyed horizon displaying redoximorphic features in some Category 5 paleosols suggests that extended periods of impeded drainage related to a fluctuating watertable occurred at the base of some profiles. Intertonguing of the basal gleyed horizon with the overlying horizon suggests soil movement, likely related to cycles of wet and dry conditions (see Nordt and Driese, 2009), as the watertable fluctuated.

Variation in the molecular weathering ratios of Unit 5 profiles indicates that these profiles are well-developed. Zones with high clayeness ratios correspond to A horizons and are inferred to represent increased weathering at the top of the profile (see Feakes and Retallack, 1988). Similar to Category 4, a lower leaching ratio is inferred to represent less leaching relative to Category 1-3 paleosols; unlike Category 4 paleosols, a lower calcification ratio is inferred to reflect more abundant precipitation resulting in the lack of carbonate accumulation (see MAP calculations below).

3.6.6. Category 6 paleosols: Rooted sandstone

Category 6 paleosols are rooted, fine-grained sandstones that display remnant sedimentary structures, burrows, possible clay coatings, and incipient horizon development. Unlike Category 3 paleosols, Category 6 paleosols lack gleyed subsurface horizons and a surficial coal. These paleosols are rare in the HCFm, representing only 1% of the paleosols (n=1). Geochemical and petrographic analyses were not conducted on these paleosols due to limited pedogenic development.

3.6.6.1. Interpretation

Category 6 paleosols are interpreted as very poorly-developed paleosols, which formed on recently deposited, sandy parent material. The presence of sedimentary structures, the lack of horizon development, and the limited pedogenic features suggest that this paleosol was buried shortly after pedogenesis commenced, halting further soil development.

3.7. Category 7 paleosols: Non- gleyed profiles with carbonate

Category 7 paleosols consist of non-gleyed, olive-green horizons that fine upwards from sandy mudstone to claystone (Fig. 3.3, Table 3.1). Evidence of bioturbation, in the form of small to large root traces and sand- and mud-filled burrows, is visible in these profiles, especially in the uppermost horizons. In thin section, iron coatings in voids and on grains are common in most horizons. Carbonate accumulation is uncommon and occurs in specific horizons, either as sparry in-filling of voids or as small, predominantly sparry accumulation

in the groundmass. Category 7 paleosols are uncommon in the HCFm, representing 5% of the paleosols (n=4).

The geochemical profiles of Category 7 paleosols reveal compositional variation, indicating better horizon differentiation than in previous profiles. A slight increase in the leaching ratio is observed with increasing depth and the calcification ratio displays variation throughout the profile. There is no obvious correlation between the calcification ratio and the occurrence of pedogenic carbonate. Despite the similarly high calcification ratios in all analyzed profiles of this pedotype, carbonate accumulation is only observed in paleosol profiles from Unit 2 and not in those from Unit 1 (Table 3.1). As with Category 4 and 5 paleosols, higher calcification ratios and lower leaching ratios relative to Category 1-3 paleosols are also observed (Fig. 3.3).

3.6.7.1. Interpretation

Category 7 paleosols are interpreted as moderately-developed paleosols that formed in well-drained environments subject to episodic rainfall. The occurrence of ferruginous coatings on grains and in voids, and of sparry carbonate in the upper horizons, indicates that precipitation occasionally saturated these paleosols. Sparry calcite in voids is known to form as a result of short bursts of rainfall during the dry season (Drees and Wilding, 1987). Rainfall transports dissolved carbonate down profile, where it precipitates as water evaporates. Alternating wet and dry conditions result in extended time for carbonate precipitation and the development of sparite (Drees and Wilding, 1987).

The geochemical differentiation of horizons suggests that Category 7 paleosols are well-developed. Again, a higher calcification ratio and a lower leaching ratio are inferred to represent a more alkaline watertable (see Ashley and Driese, 2000) and/or drier conditions and less leaching, respectively, when compared to Category 1-3 paleosols.

3.6.8. Category 8 paleosols: Non- gleyed profiles with weak horizon differentiation

Category 8 paleosols consist of bright, olive-green sandy mudstones that exhibit incipient horizon development (Fig. 3.3, Table 3.1). Macroscopic pedogenic features are

rare in these profiles and restricted to small and medium-sized root traces; the remaining pedogenic features are only observable microscopically. Uncommon, well-developed clay coatings and localized iron coatings on grains and along void surfaces occur in all horizons. Iron impregnation of the groundmass varies from weak to strong. Finally, traces of carbonate accumulation occur in the upper B horizon of one profile. Category 8 paleosols are uncommon in the HCFm, representing 4% of the paleosols (n=3).

Category 8 paleosols do not exhibit geochemical differentiation between horizons except for a slight increase in the salinization ratio towards the top of the profile (Fig. 3.3). As in Categories 4, 5, and 7 paleosols, a higher calcification ratio and lower leaching ratio relative to Category 1-3 paleosols characterize Category 8 paleosols.

3.6.8.1. Interpretation

Category 8 paleosols are interpreted as weakly-developed paleosols that formed in well-drained paleoenvironments subject to periodic saturation due to rainfall. Poor horizon differentiation and limited development of pedogenic features indicate limited pedogenesis. The presence of clay coatings and non-gleyed colours suggest that the paleosol was generally well-drained, but subject to periodic rainfall (see McKeague, 1983; Richardson and Daniels, 1993).

The poorly-developed nature of Category 8 paleosols is underscored geochemically; limited pedogenesis results in little geochemical change down profile (e.g. Feakes and Retallack, 1988; Therrien et al., 2009). The increase in the salinization molecular and weathering ratio at the top of the profile is likely associated with surface evaporation (see Retallack, 1997). Less leaching and higher calcification ratios are consistent with drier conditions and/or a more alkaline watertable relative to Category 1-3 paleosols is inferred.

3.6.9. Category 9 paleosols: Non-gleyed paleosol profiles capped by a thick, surficial coal horizon

Category 9 paleosols consist of alternating, non-gleyed, brown and grey siltstone horizons capped by a 30 cm-thick coal horizon (Fig. 3.3, Table 3.1). Root traces occur

throughout the profile, with the occurrence of burrows restricted to the upper portion of the profile. Clay accumulation occurs as rare to uncommon clay coatings. Ferruginous coatings and hypocoatings are uncommon and occur mostly around root traces and along void surfaces. Tendrils of the surficial horizon are observed extending into the underlying horizon (Fig. 3.3). Whereas most horizons exhibit stipple-speckled to mosaic speckled b-fabrics, the b-fabrics of the uppermost B horizons range from unistriated to reticulate striated and granostriated, some of which may represent slickensides. Category 9 paleosol profiles are rare in HCFm paleosols, representing only 1% of the paleosols (n=1).

Category 9 paleosols are well differentiated geochemically, and show an increase in the calcification and salinization ratios with depth. The leaching molecular ratio generally decreases with depth but increases slightly at a depth of 87 cm (Fig. 3.3). The clayeness ratio does not vary with depth.

3.6.9.1. Interpretation

Category 9 paleosols are interpreted as very well-developed, well-drained organic paleosols based on the development of a thick coal and the absence of non-gleyed subsurface horizons (see Fey, 2010; Driessen and Dudal, 1991). These paleosols were subject to alternating wet and dry conditions related to rainfall, as indicated by the presence of slickensides, ferruginous pedofeatures, and clay coatings (see PiPujol and Buurman, 1994; Nordt and Driese, 2009). The inclusion of material from one horizon into another (i.e., tendrils) also suggest that movement leading to mixing of horizons took place within the soil profile, related either to alternating wet and dry conditions (see Nordt and Driese, 2009) or to plant activity (see Angers and Caron, 1998; Beven and Germann, 1982, Nordt and Driese, 2009).

Variation in the molecular weathering profiles indicates that horizons are differentiated geochemically and the paleosol is well-developed (Feakes and Retallack, 1988). The increase in the leaching molecular ratio at a depth of 87 cm corresponds to a slight increase in dispersed organic matter relative to over and underlying horizons, potentially

representing a buried A horizon. This profile may therefore represent a composite paleosol profile (Kraus, 1999).

3.7. Paleoenvironmental Reconstruction of Horseshoe Canyon Formation

The nine categories of HCFm paleosols represent a continuum of soil drainage conditions from waterlogged to freely-drained paleoenvironments. When the distribution of pedotypes is considered in a stratigraphic context, paleosols reveal that a clear change in soil drainage conditions occurred through the HCFm (Fig. 3.5, Table 3.2):

1) Poorly-drained paleoenvironments characterized by a high but occasionally fluctuating watertable prevailed in Unit 1.

2) Drainage conditions improved slightly through Unit 2 to produce a mixture of poorly-drained and well-drained paleoenvironments.

3) Drainage conditions further improved in Unit 4, resulting in well-drained paleoenvironments.

4) Drainage became impeded in Unit 5, producing poorly-drained paleoenvironments characterized by a high but occasionally fluctuating watertable reminiscent of the conditions observed in Unit 1.

A previous study also documented the paleosols of the upper HCFm. Paleosols preserved in Units 4 and 5, exposed 5km north of Tolman Bridge at Knudsen's Farm were investigated by Forkner (2002) following the same methods used in this study. Consequently, the results of his investigation can be used to complement the current study. To do so, the Knudsen's Farm section was visited briefly in the summer 2010 to convert Forkner's (2002) pedotypes into those used in the present study. Paleosols encountered at Knudsen's Farm were largely equivalent to those found at Tolman Bridge (Table 3.2); however, slight differences in the stratigraphic record present at each locality resulted in the preservation of paleosols at Knudsen's Farm in stratigraphic intervals for which paleosols are absent at Tolman Bridge (e.g., due to erosion by channels). These complementary

pedological records provide a better understanding of the paleoenvironmental changes that occurred through the HCFm.

3.7.1. Unit 1

Unit 1 is characterized by the predominance of hydromorphic paleosols subject to alternating wet and dry conditions and a fluctuating watertable (Categories 1-3) (Fig. 3.5). Pedogenically unaltered mudstone deposits with dispersed organic matter, interpreted as pond deposits, are also present in Unit 1. Hydromorphic paleosols and organic-rich deposits reveal that the landscape was dominated by wetlands and ponds. The three hydromorphic pedotypes may represent slight differences in parent materials, time of formation, and watertable level (e.g., Therrien et al., 2009). The predominance of hydromorphic paleosols in Unit 1 is consistent with previous reconstructions of this unit as a coastal wetland in close proximity to the Bearpaw Sea (e.g., Eberth, 2004; Hamblin, 2004).

Drainage improved occasionally on the coastal plain, at least locally, as indicated by the occurrence of well- drained paleosols at two stratigraphic intervals within Unit 1 (Fig. 3.5): a Category 9 paleosol occurs between Coals 4 and 5 and a Category 7 paleosol occurs between Coals 8 and 9. These paleosols developed during times of improved drainage, possibly related to a significant marine regression (see Chapter 4). While both Category 9 and Category 7 paleosols are well-drained, only the Category 9 paleosol is organic-rich (i.e., possesses a surficial coal horizon; Fig. 3.3, Table 3.1). Differences in the organic matter content of these paleosols may be related to an increase in sediment supply above Coal 7 (see Eberth, 2004). Notably, Category 7 paleosols are also found in Unit 2. The first occurrence of a well-drained Category 7 paleosol stratigraphically high in Unit 1 represents the onset of a change in drainage regime preceding the lithological change at the Unit 1/ Unit 2 contact (Fig. 3.5).

3.7.2. Unit 2

Unit 2 is characterized by a suite of variably-drained pedotypes including hydromorphic paleosols (Categories 2 and 3), moderately-drained paleosols (Category 4), and well-

drained paleosols (Categories 5-7), all subject to alternating wet and dry conditions and a fluctuating watertable. A complex history of drainage and paleoenvironmental changes is preserved in Unit 2. The basal-most paleosol in Unit 2 is hydromorphic (Category 2) which indicates that, although drainage did improve gradually, wetlands persisted across the Unit 1/Unit 2 boundary.

Drainage conditions generally improved higher in Unit 2, as indicated by the presence of well-drained paleosols (Categories 5-7). Improved drainage conditions were short-lived, however, and gradually degraded as indicated by the return of moderately-drained paleosols with low watertable levels (Category 4) followed by the return of hydromorphic paleosols (Category 2). Interestingly, the first appearance of moderately-drained paleosols occurs at different stratigraphic levels at the two localities preserving Unit 2: they appear at approximately 15 m above the base of the unit at the southern locality of Horsethief Canyon and at 20 m above the base of the unit at the northern locality of Morrin Bridge (Fig. 3.6). Drainage conditions continue to worsen up-section towards the Drumheller Marine Tongue (DMT) and become fully impeded in association with Coal 10. Immediately above this coal bed, drainage improved and watertable levels dropped, as indicated by the presence of moderately-drained paleosols (Category 4).

Variation in the timing of changes in drainage conditions observed between the Horsethief Canyon and Morrin Bridge localities may be related to the direction of transgression of the Drumheller Marine Tongue (Fig. 3.6). Based on the geographic distribution of this unit, the Drumheller Marine Tongue is inferred to have transgressed in a northwest direction (see Hamblin, 2004). As the transgression proceeded, more southerly areas would have felt the marine influence (e.g., rise in sea level, occurrence of marine invertebrates) before more northerly areas. As Horsethief Canyon is located approximately 13 km south of Morrin Bridge, this may explain the earlier onset on poorly-drained conditions at this southern locality. Drainage conditions improved slightly directly above the Coal 10 at both localities (Fig. 3.5, 3.6), presumably in response to the DMT regression.

Straight and Eberth (2002) observed a colour change, from red-brown to grey-green, in outcrops of Unit 2 exposed at Horsethief Canyon and Morrin Bridge. They also noted that the transition occurs at a stratigraphically lower elevation at Horsethief Canyon relative to Morrin Bridge. Comparison with the distribution of paleosols reveals that the colour change coincides with transition from well-drained paleosols (Categories 5-7) to hydromorphic paleosols (Categories 2-3) in the sections (Fig 3.6). Thus the colour change reflects the change in paleosol drainage conditions associated with the northward transgression of the DMT.

3.7.3. Unit 3

Because paleosols were not observed in Unit 3, it is impossible to document the nature of the transition between Units 2, 3, and 4.

3.7.4. Unit 4

Unit 4 is characterized by the predominance of weakly-developed and well-drained paleosols (Category 8) as a result of pedogenesis in an unstable landscape subject to frequent modifications. Limited sediment supply and low, but gradually increasing accommodation space and rates of subsidence, inferred to have prevailed during deposition of Unit 4 (Eberth, 2004), could explain the thin nature and immaturity of the paleosols. Under conditions of restricted sediment supply and low rates of subsidence, overbank deposits (where paleosols develop) are subject to frequent reworking by channels (e.g. Blakey and Gubitosa, 1984). Under these circumstances, pedogenesis is time-limited and paleosols are subject to erosion, preventing the development of mature profiles.

The occurrence of a hydromorphic paleosol (Category 2) at the top of Unit 4 (Forkner, 2002) reflects a change in the drainage conditions and rise in watertable level. This paleosol represents the onset of poorly-drained conditions characteristic Unit 5 prior to the Unit 4/Unit 5 lithological contact and demonstrates that the paleoenvironmental changes, associated with the transition between Units 4 and 5, occurred gradually. Evidence supporting the gradual nature of these paleoenvironmental changes is also observed north

of the study area, in Dry Island Buffalo Jump Provincial Park, where an increase in organic-rich facies, similar to those observed in Unit 5, occurs at the top of Unit 4 (Eberth and Currie, 2010).

3.7.5. Unit 5

Unit 5 is characterized by the predominance of hydromorphic paleosols (Categories 1 and 2) associated with Coals 11 and 12, which indicates a return to poorly-drained paleoenvironments characterized by a high watertable. Similar paleoenvironments are observed in Unit 1; however, a series of well-drained paleosols (Categories 5 and 8) occurs between coal beds 11a and 11b (Forkner, 2002), indicating that drainage conditions occasionally improved in Unit 5. The return of poorly-drained paleoenvironments in Unit 5 has been attributed to a number of causes. Hamblin (2004) suggested that two marine transgressions were responsible for the development of coal beds and poor drainage, although no evidence of such events is preserved in the rock record. Conversely, Eberth (2004) argued that sea level change had no influence on the formation of Unit 5 as the sea had receded far to the east at this time. Instead, he inferred that high subsidence rates and increased accommodation space may have resulted poor drainage conditions. The abundance of well-drained paleosols, unlike Unit 1, and their occurrence between related coal seams (e.g., Coal 11A and 11B; Fig. 3.5) argue against a marine influence in this unit. In this case, paleosol hydrology likely represents landscape changes associated with fluvial mechanisms (e.g., avulsion) (Krause and Aslan, 1993).

3.8. Paleoclimatic reconstruction of the Horseshoe Canyon Formation

The geochemical composition of well-drained HCFm paleosols, when considered in a stratigraphic context, provides insight into the climatic conditions (MAT and MAP) that prevailed between 73 and 67 million years ago. The results reveal that mean annual temperature varied between 8.7-10.7^{o}C (±4.4^{o}C) and mean annual precipitation fluctuated between 841-1041 mm/year (±181 mm/yr) in the stratigraphic interval spanning Unit 1 to Unit 4 (no well-drained paleosols were present in Unit 5 in the study area, thus preventing estimation of paleotemperature and paleoprecipitation). A warm and humid climate

prevailed in Unit 1 and across the Unit 1/ Unit 2 boundary. A rapid cooling and aridification event, where MAT dropped by at least 1.3^{o}C and MAP by 57 mm/yr between two consecutive paleosols (but up to 183mm/yr within a short stratigraphic interval of 4 m), occurred 11 m below Coal 10 in Unit 2, prior to the Campanian-Maastrichtian boundary (Fig. 3.5, Table 3.3). The climate remained cool and dry through Unit 4 (Fig. 3.5, Table 3.3).

The results of this study indicate that a cooling and drying event occurred prior to the Campanian-Maastrichtian boundary. These results suggest that cooling occurred earlier than in the United States terrestrial record of climate change for the same time interval; Nordt et al. (2003) reconstructed paleotemperatures based on the isotopic composition of pedogenic carbonate from west Texas and recognized a similar cooling trend following the Campanian-Maastrichtian boundary. This discrepancy could potentially reflect cooling at higher latitudes prior to lower latitudes. Nordt et al. (2003) also inferred a warming event during the early Maastrichtian, but this event could not be confirmed in the HCFm because it is coincident with deposition of Unit 3, in which paleosols were not observed. Conversion of the Nordt et al. (2003) paleotemperature estimates to the paleolatitude of the HCFm (using a latitudinal temperature gradient of 0.4^{o}C/degree reported by these authors) results in slightly cooler temperature estimates than those obtained in this study, but still compatible within the error of estimate (Fig. 3.5). The results of this study also support the cooling trend between the Campanian and Maastrichtian inferred based on leaf physiognomy (Wolfe and Upchurch, 1987). Conversion of paleotemperature estimates based on leaves to the HCFm paleolatitude (using a latitudinal temperature gradient of 0.3^{o}C/degree reported by these authors) results in slightly warmer temperature estimates than those obtained in this study, but still largely compatible within the error of estimate (Fig. 3.5). Notably, however, the two interpretations differ in the rate of change. Whereas HCFm paleosols indicate that climate change was relatively sudden (within 2 m of section in Unit 2), plants suggest that climate change occurred over a longer period of time, reaching the coolest temperature within Unit 4 (Fig. 3.5). The variance between the two methods could either reflect imprecision in the determination of the age of various floral

assemblages (see Wolfe and Upchurch, 1987) or could potentially reflect a lag in plant response to climate change (Davis, 1958; Pennington, 1986; Norris et al., 2003). Such a lag, which can be greater than 85 ka based on the timing of pollen immigration, has also been observed across the Paleocene-Eocene Thermal Maximum (Wing et al., 2003).

3.9. Summary of Paleoenvironmental and Paleoclimatic Changes in HCFm

Warm and humid conditions prevailed for most of Unit 1. Abundant annual precipitation in conjunction with moderate to high accommodation and increasing subsidence (Eberth, 2004) likely contributed to the predominance of hydromorphic paleosols in Unit 1. Rare, organic-rich, well-drained paleosols also occur in Unit 1. Such well-drained, organic-rich soils are found today in environments with abundant and evenly distributed rainfall where the decomposition of organic matter is inhibited by nutrient availability, soil acidity, and wetness (Driessen and Dudal, 1991). These soils are found in areas of Canada and Western Europe (Driessen and Dudal, 1991) and the humid plateaus on the subtropical eastern seaboard of South Africa (Fey, 2010). In particular, the African sites receive 700-950mm of precipitation per year and have a mean annual temperature of 11-16 ^{o} C (Hoffman and Todd, 2000), which is consistent with the predicted ranges of MAP and MAT estimates from Unit 1 (see Table 3.3 and Fig. 3.5).

Contrary to claims of climate change based on lithology (Eberth, 2004; Hamblin, 2004; Brinkman and Eberth, 2006) but in accordance with inferences based on palynology (Srivastava, 1970), wet and warm conditions persisted across the Unit 1/ Unit 2 boundary as evidenced by the presence of a hydromorphic paleosol at the base of Unit 2. Subsequently, drainage conditions improved, even though MAT and MAP estimates remained high. This indicates that the absence of coal beds and the transition to better-drained conditions in Unit 2 are not related to climate change but could be attributed to basinal changes, such as a decrease in accommodation in Unit 2 (Eberth, 2004) or a more upstream position on the coastal plain (Hamblin, 2004). A transition from a warm-humid to a cool-dry climate occurred 12 m above the base of Unit 2. This transition is considered sudden as it occurs between two consecutive paleosols spanning a 2 m stratigraphic

interval. The coolest and driest conditions are reached over a 13 m stratigraphic interval (Fig. 7). The appearance of poorly-drained paleosols, with a watertable that fluctuated in the lower part of the paleosol profile (Category 4), occurred prior to Coal 10 . Category 4 paleosols presumably reflect the rise in watertable associated with the onset of the Drumheller Marine Tongue transgression. Hydromorphic paleosols formed earlier in the south (Horsethief Canyon section) than in the north (Morrin bridge section), reflecting the northward transgression of the DMT (Hamblin, 2004). The highest watertable levels occurred at Coal 10 and better-drained conditions quickly returned in overlying deposits, presumably in direct response to the DMT regression and associated lowering of the watertable.

A cool, dry paleoclimate and well-drained paleoenvironmental conditions persisted through Unit 4. The landscape, however, was subject to frequent reworking, possibly in response to low rates of subsidence (Eberth, 2004), as evidenced by the poorly-developed nature of the paleosols. A slight warming trend may have begun in the upper part of Unit 4, accompanied by a return to poorly-drained paleoenvironments. Poorly-drained conditions prevailed throughout Unit 5, although episodes of well-drained conditions occur. Continued warming and higher precipitation have been inferred through Unit 5, based on leaf physiognomy (Wolfe and Upchurch, 1987) and the abundance of coal and large channel deposits (Eberth, 2004; Brinkman and Eberth 2006). Warm and wet conditions, combined with an increase in subsidence and accommodation space, are likely responsible for the development of hydromorphic paleosols.

3.10. Correspondence between Paleoenvironmental Changes and the Vertebrate Faunal Turnover in the HCFm

A dramatic change in faunal composition occurs within the HCFm. Changes in the HCFm faunal assemblage have been tentatively linked to paleoenvironmental changes associated with the lithological transitions between units, presumably reflecting a drying and cooling event (Eberth et al., 2001). The documented faunal turnover occurs within Unit 2: turtle diversity declines at the Unit 1/Unit 2 contact (Brinkman, 2003; Brinkman and

Eberth, 2006), the disappearance of ceratopsians, of the hadrosaur *Edmontosaurus*, and of the nodosaurid *Edmontonia* occurs at Coal 10, and the appearance of the hadrosaurs *Saurolophus* and *Hypacrosaurus*, and of the ornithopod *Parksosaurus* occurs at the Unit 2/Unit 3 contact (Eberth et al., 2001; see also Russell and Chamney, 1967) (Fig. 3.7). In comparison, a gradual paleoenvironmental transition from poorly-drained to well-drained conditions occurred across the Unit 1/Unit 2 boundary, but paleoclimatic changes occur between 12-14m above the boundary. The discordance between the various phases of paleoenvironmental, paleoclimatic, and faunal changes demonstrates that equating the HCFm faunal turnover with paleoenvironmental changes, as previously suggested, is overly simplistic. While the decrease in turtle diversity may be associated with the transition from poorly-drained to well-drained paleoenvironments across the Unit 1/Unit 2 contact, the two phases of dinosaur faunal turnover postdate both the paleoenvironmental and paleoclimatic changes (Fig. 3.7). It is possible that the lag time separating the paleoenvironmental and paleoclimatic changes from the dinosaur faunal changes reflect the ability of the dinosaur fauna to adapt to changing climatic conditions. The recurrence of poorly-drained paleoenvironments in association with the DTM transgression may have allowed the wetland-loving dinosaur fauna to persist despite the presence of a cooler and drier climate. A threshold may have been reached with the return of well-drained habitats during the regression of the DMT, resulting in the disappearance of ceratopsians, *Edmontosaurus*, *Pachyrhinosaurus*, and *Edmontonia* at or near Coal 10 (Fig 3.7). The apparent faunal gap separating Coal 10 from the Unit 2/ Unit 3 contact may represent a preservation/ sampling artefact or could potentially represent a time lag between the disappearance of the wetland-loving fauna and the immigration of new faunal constituents in the Drumheller Valley. Further paleontological research within that stratigraphic interval is required.

Cooler and drier climatic conditions inferred for Units 3 and 4 allowed for the establishment of a new faunal assemblage. The Unit 4 faunal assemblage is dominated by taxa inferred to have northern affinities, including Holostean A (a bony fish), champsosaurs, *Troodon*, and toothed birds (Larson et al., 2010). The assemblage is also characterized by the absence of faunal indicators for warm climates, such as crocodiles and

albanerpetontids (Larson et al., 2010), as well as a low diversity turtle assemblage (Brinkman and Eberth, 2006). It is possible that these cooler conditions would have favoured the southward migration of taxa living in more northerly latitudes. Although it had been previously suggested that the hadrosaurine *Saurolophus* may have migrated from Asia to North America across the Beringian isthmus during that time, (Russell, 1993), recent phylogenetic analyses suggest that this taxon may have instead originated in North America and migrated to Asia (Bolotsky and Godefoit, 2004; Weishampel, 2004; Bell, in press). *Saurolophus* appears to have evolved and thrived in the cooler, drier climates of the earliest Maastrichtian of North America and spread to Asia during this time.

The return of poorly-drained conditions at the top of Unit 4, recorded at Knudsen's Farm and Dry Island Buffalo Jump, is associated with the establishment of a transitional fauna in a fourth phase of faunal turnover (Fig. 3.7). The faunal assemblage consists of taxa characteristic of Units 3 and 4 as well as *Atrociraptor*, a dromaeosaur previously known from the warm and humid Unit 1 (Larson et al., 2010). The coincidence between hydromorphic paleosols and a mixed fauna at the top of Unit 4 is indicative of the onset of paleoenvironmental changes that lead to the establishment of the poorly-drained paleoenvironments seen in Unit 5. Although the fossil record of Unit 5 is poor, vertebrate remains include one large turtle (*Adocus*), two aquatic vertebrates (one champsosaur and one crocodylian), and one large ceratopsid (*Eotriceratops*) (Eberth et al., 2001; Brinkman and Eberth, 2006; Wu et al., 2007). This fossil assemblage coincides with the warming trend inferred by leaf physiognomy (Wolfe and Upchurch, 1987; Brinkman and Eberth, 2006) and suggests that a return to the warm and humid conditions, characteristics of Unit 1, is associated with the coal-forming paleoenvironments of Unit 5.

3.11. Conclusions

A great diversity of pedotypes has been recognized in the HCFm, ranging from hydromorphic paleosols to well-drained paleosols with clay coatings and slickensides. The stratigraphic distribution of paleosols in the HCFm reveals that paleoenvironmental changes were controlled by the interactions between tectonics, sea level change, and

climate. Unit 1, consisting mainly of hydromorphic (Categories 1-3) paleosols, is the stratigraphically-lowest, coal-bearing interval of the HCFm. It is inferred to have been deposited during a time of moderate to high accommodation in a subsiding basin during a regressive phase of the Bearpaw Sea (Eberth, 2004). The transition to the lithologically-distinct and coal-poor Unit 2 records a gradual change to better-drained paleosols (Categories 5-7), interrupted by a brief return to hydromorphic paleosols (Categories 2 and 4) associated with the DMT transgression. Unit 2 was deposited during a time of reduced accommodation space, subsidence, and sediment supply (Eberth, 2004). Unit 4, devoid of coal, is characterized by poorly-developed, well-drained paleosols that formed under conditions of limited sediment supply and accommodation (Eberth, 2004). The return to hydromorphic paleosols near the top of Unit 4 and in the coal-rich Unit 5 coincides with an increase in subsidence, accommodation space, and sediment supply (Eberth, 2004). Changes in lithology, palynology, and leaf physiognomy have often been inferred to represent climate change in the HCFm. While the study of HCFm paleosols supports the theory of cooling between Unit 1 and Unit 4 (e.g. Wolfe and Upchurch, 1987; Nordt et al., 2003; Eberth 2004), the timing of paleoenvironmental and paleoclimatic changes differs slightly from changes predicted by other methods. First, the transition from warm and humid conditions to cool and dry conditions was inferred to have occurred at the Unit 1/ Unit 2 boundary based on the disappearance of coals (Eberth, 2004), but paleosols in the HCFm indicate that climate change occurred part-way through Unit 2, 12-14 m above the Unit 1/Unit 2 contact. In light of the results presented in this study, the disappearance of coals at the base of Unit 2 may be related to a lowering of the watertable, possibly in response to an extensive regression of the Bearpaw Sea (Hamblin, 2004), and an inferred reduction in sediment supply and accommodation (Eberth, 2004). Second, while paleosols from the HCFm suggest that cooling occurred prior to the Campanian-Maastrichtian boundary, paleosols from Texas (Nordt et al., 2003) indicate that onset of cooling occurred after the boundary. Potentially, this could reflect cooling in northern latitudes prior to lower latitudes. Finally, leaf physiognomy suggests that gradual cooling occurred with the coolest temperatures attained in Unit 4, while paleosols indicate that temperatures dropped relatively rapidly and suddenly within Unit 2. The discordance between climate change and

floral change could potentially be due to a lag time in the response of plants to climate change (Davis, 1958; Pennington, 1986, Wing et al., 2003).

A partial correlation exists between the record of faunal change and of paleoenvironmental and paleoclimatic changes inferred from paleosols. Changes in biodiversity through the HCFm, namely a decline in turtle diversity at the Unit 1/ Unit 2 contact (Brinkman and Eberth, 2006), the disappearance of certain ornithischian dinosaurs near Coal 10, and the appearance of different ornithischian dinosaurs at the Unit 2/ Unit 3 contact (Eberth et al., 2001), do not coincide with the history of climate change recorded by paleosols. Whereas the decline in turtle diversity may have coincided with the transition from poorly-drained to well-drained paleoenvironments, changes in dinosaur faunas may have been delayed by the return of poorly-drained paleoenvironments associated with the DTM transgression. More detailed studies of the first and last occurrences of the dinosaurs involved in the faunal turnover may reveal that certain dinosaurs disappeared earlier in response to these changes while others were able to adapt, temporarily, to the new paleoenvironmental and paleoclimatic conditions. The onset of poorly-drained paleoenvironments near the top of Unit 4 is associated with a mixed vertebrate fauna characterized by animals with both cool-climate and warm-climate affinities. The return of poorly-drained habitats in Unit 5 is associated with the occurrence of taxa previously found in Unit 1, which suggests a return to warm and humid conditions.

TABLE CAPTIONS

Table 3.1: Characteristics of the Horseshoe Canyon Formation pedotypes

Table 3.2: Distribution of pedotypes through the Horseshoe Canyon Formation and inferred paleoenvironmental settings. Pedotypes documented in this study are compared to those observed by Forkner (2002) at Knudsen's Farm. Forkner's (2002) pedotypes and stratigraphic nomenclatures have been converted into the one used in this study.

Table 3.3: Estimates of MAP and MAT based on the geochemical composition of well-drained HCFm paleosols. Asterisk indicates values calculated from equation for poorly-developed paleosols (Sheldon and Tabor, 2009).

FIGURE CAPTIONS

Figure 3.1: Photomicrographs of pedogenic features of the HCFm in cross polarized (XPL), plane polarized (PPL), or normal (NL) light. Photo a) Stipple speckled b-fabric (XPL), b) Mosaic speckled b-fabric (XPL), c) Unistriated b-fabric (XPL), d) Reticulate striated b-fabric (XPL), e) Granostriated b-fabric (XPL), f) Clay coating (XPL), g) Redoximorphic feature (PPL), h) Iron coatings on possible ped surfaces (subangular blocky) (NL), i) Sphaerosiderite (NL), j) Carbonate (XPL).

Figure 3.2: Measured sections of the HCFm correlated to the measured section of Forkner (2002)

Figure 3.3: Molecular weathering ratios, lithology, and horizon identification for the pedotypes of the nine categories of HCFm paleosols. The textural indicator reflects the proportion of fine (clay + silt in grey) to coarse (sand in yellow) grains throughout the profile. Molecular weathering ratios reflect variation in the pedogenic properties throughout the profile (see text for discussion). Horizon division was based on pedogenic features and molecular weathering ratios.

Figure 3.4: Stratigraphic sections below Coal 8 at Horsetheif Canyon demonstrating lateral variation of paleosol profiles. In some instances, horizons pinch out laterally creating false impression of pedogenic development in channel scour (Category 2b profile). These variations can be due to differences in parent material and/ or drainage (as evidenced by presence of clay coatings in Bg1). In other instances, pre-existing topography (e.g. channel scour) can control paleosol development (Category 1 profile).

Figure 3.5: Paleoenvironmental and paleoclimatic changes through the HCFm based on the stratigraphic distribution of pedotypes. Paleosol categories represent poorly-drained (dark grey), moderately-drained (light grey), and well-drained (white) paleoenvironments. MAT and MAP estimates were calculated from the moderately- and well-drained paleosols only. The paleosols observed by Forkner (2002), represented by white squares, were integrated based on their stratigraphic position to complement this study. Paleotemperature and paleoprecipitation estimates (and associated error of

estimate from Sheldon and Tabor (2009) in grey) are based on the geochemical composition of well-drained paleosols. Thin dashed lines represent stratigraphic intervals for which no estimates are available. Paleotemperature estimates are compared to previously published paleotemperature curves, standardized to a paleolatitude of 60°N, and are presented with the climatic divisions of Srivastava (1970), denoted with an asterisk. Presented with ages calculated from the magnetostratigraphy of Lerbekmo and Braman (2002, 2005), based on Gradstein et al. (2004).

Figure 3.6: Correlated sections of Unit 2 showing that the onset of poorly-drained conditions occurs stratigraphically lower at Horsethief Canyon than at Morrin Bridge, inferred to reflect the northward transgression of the Drumheller Marine Tongue. For legend, see Figure 3.2.

Figure 3.7: Comparison of selected faunal constituents with the record of paleoenvironmental and paleoclimatic conditions in the HCFm. Solid circles represent paleosol occurrences reported in this study. Hollow boxes represent paleosol occurrences reported by Forkner (2002). Hollow circles represent the stratigraphic position of a paleosol recorded by Forkner (2002) that coincides with a paleosol of the same category from this study. Cross-hatched boxes represent intervals for which faunal assemblage is unknown. Results reveal that the decline in turtle diversity preceded climatic changes (red line) but coincided with the transition from poorly-drained to well-drained paleoenvironments (green line). In contrast, dinosaur faunal turnover in the lower HCFm occurred after the climatic changes and roughly coincided with the DMT regression (blue line). In the upper HCFm, faunal changes coincide with the return of poorly-drained paleoenvironments (brown line). Faunal distribution from Eberth et al. (2001); Wu et al. (2007); Larson et al. (2010). Turtle diversity from Brinkman and Eberth (2006).

Table 3.1

Category 1: pedotype 102m above base of HCFm; 45.5m above base of Settling Ponds section; 76-120cm thick; mean thickness 71cm

Depth (cm)	Horizon	Lithology	Colour	B-fabric and Illuvial Features	Redoximorphic Features	Notes
0-27	O	Coal	black	None observed	None observed	
27-44	Ag	Mudstone	dark grey (10YR 4/1)	Stipple-speckled b-fabric Uncommon clay coatings in groundmass	None observed	
44-73	Bg	Mudstone	White (5Y 8/1)	Stipple-speckled to mosaic-speckled b-fabric Common clay coatings in groundmass	Uncommon ferruginous redoximorphic features around root traces; weak iron accumulation in groundmass	
73-76	2O	Coal	black	None observed	None observed	
76-109	2ABg	Mudstone	Light grey (10YR 7/1)	Stipple-speckled to unistriated b-fabric Very Common, well- developed clay coatings in groundmass	Rare ferruginous redoximorphic features along root trace	
109-196	2Bg	Mudstone	Grey (10YR 6/1)	Very well developed mosaic-speckled b-fabric Common, well-developed clay coatings in groundmass	None observed	

Category 2a: pedotype 76m above base of HCFm; 28.5m above base of Settling Ponds section ; 83-130cm thick, mean thickness 109.9cm

Depth (cm)	Horizon	Lithology	Colour	B-fabric and Illuvial Features	Redoximorphic Features	Notes
0-15	Ag	Organic-rich mudstone	Greyish brown (10YR 5/2)	Mosaic-speckled to unistriated b-fabric Common, weakly developed clay coatings in groundmass	None observed	Root Traces, Possible slickensides
15-41	Bg1	Mudstone	Light grey (5Y 7/1)	Unistriated to mosaic-speckled b-fabric Common moderately developed clay coatings in groundmass	None observed	Possible slickensides
41-63	Bg2	Mudstone	Light grey	Unistriated to stipple-speckled b-fabric Common moderately developed clay coatings in	None observed	Burrow, Possible

			(5Y 7/1)	groundmass and along root traces		slickensides
63-76	BC	Mudstone	Light brownish grey (2.5Y 6/2)	Stipple-speckled to mosaic speckled b-fabric Uncommon, weakly developed clay coatings in ground mass and along root traces	None observed	Burrow/ Root trace

Category pedotype 2b: 70m above base of HCFm; 26.5m above base of Settling Ponds Section; 40-244cm thick; mean thickness 132.1cm						
Depth (cm)	**Horizon**	**Lithology**	**Colour**	**B-fabric and Illuvial Features**	**Redoximorphic Features**	**Notes**
0-5	A	Mudstone	Very dark grey (2.5Y 3/1)	Well-developed reticulate b-fabric Slickensides		Possible root trace/ burrows
5-21	Bg1	Mudstone	Greenish grey (10GY 5/1)	Well-developed unistriated to reticulate b-fabrics		Root trace
21-67	Bg2	Mudstone	Dark greenish grey (5GY 4/1)	Well-developed reticulate to stipple-speckled b-fabric Uncommon, weakly-developed clay coatings along root traces or ped? surfaces	Uncommon ferruginous redoximorphic features along root traces and ped? surfaces	Root traces
67-90	BC	Siltstone	Greenish grey (10GY 5/1)	Well-developed mosaic-speckled b-fabric Rare granostriation Uncommon, moderately developed clay coatings in groundmass		

Category pedotype 2c : 48m above base of HCFm; 2m above Settling Ponds Section; 31-156cm thick; mean thickness 106.3cm						
Depth (cm)	**Horizon**	**Lithology**	**Colour**	**B-fabric and Illuvial Features**	**Redoximorphic Features**	**Notes**
0-16	ABg	Mudstone	Dark greyish brown (10YR 4/2)	Mosaic speckled to unistriated b-fabric Uncommon, weakly developed clay coatings in groundmass	Rare, weakly developed, ferruginous redoximorphic features	

16-23	Bg	Claystone	Greyish brown (10YR 5/2)	Stipple-speckled to mosaic speckled b-fabric Rare granostriation	Rare, weakly developed, ferruginous redoximorphic features	Root traces
23-31	CBg	Claystone	Dark greyish brown (10YR 4/2)	Unistriated b-fabric Rare granostriation	Rare, weakly developed, ferruginous redoximorphic features	

Category 3: pedotype 45m above base of HCFm; 60m above East Coulee section; 30-244cm thick; mean thickness 91.7cm						
Depth (cm)	**Horizon**	**Lithology**	**Colour**	**B-fabric and Illuvial Features**	**Redoximorphic Features**	**Notes**
0-21	O	Coal	Black	None observed	None observed	
21-37	Ag	Sandstone	White (10YR 8/1)	Stipple-speckled b-fabric Common granostriation Very common, well-developed clay coatings Very common iron coatings on grains, sometimes forming bridges/pendants and link cappings	None observed	
37-53	Bg	Sandstone	White (5Y 8/1)	Unistriated to mosaic-speckled b-fabric Common granostriation Very common, well-developed clay coatings Common iron coatings on grains, sometimes forming bridges/pendants and link cappings	None observed	
53-59	Cg	Sandstone	White (5Y 8/1)	None observed	None observed	

Category 4: pedotype 154m above base of HCFm; 86.5m above base of Horsethief Canyon section; 55-152cm thick; mean thickness 104.4cm						
Depth (cm)	**Horizon**	**Lithology**	**Colour**	**B-fabric and Illuvial Features**	**Redoximorphic Features**	**Notes**
0-26	A	Mudstone with dispersed	Dark olive grey	Stipple speckled to mosaic speckled b-fabric Rare granostriation Uncommon, weakly developed clay coatings in	None observed	Root traces Abundant bioturbation

		organic matter	(5Y 3/2)	groundmass and along root traces Rare iron hypocoatings around root traces Moderate iron impregnation with clouds of weak		
26-49	Bw	Mudstone	Olive grey (5Y 4/2)	Stipple speckled to mosaic speckled b-fabric Uncommon, weakly developed clay coatings in groundmass Large clouds of weak iron impregnation surrounded by rims of moderate impregnation	None observed	
49-74	Bg1	Mudstone	Black (5Y 2.5/1)	Mosaic speckled to unistriated b-fabric Common, weakly developed clay coatings in groundmass	Common ferruginous redoximorphic features	Possible root traces Rare, 20µm sphaerosiderite
74-99	Bg2	Mudstone	Olive grey (5Y 4/2)	Mosaic speckled b-fabric Common, weakly-developed clay coatings in groundmass	Common ferruginous redoximorphic features	Common, 20-30µm sphaerosiderite
99-136	Cg	Mudstone	Black (2.5Y 2.5/1)	Stipple-speckled to mosaic speckled b-fabric Rare granostriation Common, weakly-developed clay coatings in groundmass	Rare ferruginous redoximorphic features	Uncommon, 5-10µm sphaerosiderite

Category 5: pedotype 147m above base of HCFm; 64m above base of Horsethief Canyon section; 54-143cm thick; mean thickness 98.5cm						
Depth (cm)	**Horizon**	**Lithology**	**Colour**	**B-fabric and Illuvial Features**	**Redoximorphic Features**	**Notes**
0-9	A	Mudstone	Dark greyish brown (10YR 4/2)	Mosaic speckled b-fabric Uncommon, weakly developed clay coatings in groundmass Rare iron hypocoatings along root traces Weak to moderate iron impregnation in subparallel, linear zones	None observed	Root traces
9-18	ABss	Mudstone	Light brownish grey (2.5Y 6/2)	Stipple speckled to mosaic speckled b-fabric Uncommon granostriation Uncommon, weakly developed clay coatings in groundmass and along root traces Well-developed slickensides	None observed	Root traces

				Rare iron hypocoatings along root traces Clouds of weak to moderate iron impregnation		
18-30	Btss	Mudstone	Very dark greyish brown (2.5Y 3/2)	Stipple speckled to mosaic speckled b-fabric Rare, well-developed clay coatings in groundmass and along root traces Uncommon iron hypocoatings along root traces Weak iron impregnation with narrow, irregular zones of moderate impregnation	None observed	Root traces
30-54	Bw	Mudstone	Very dark greyish brown (2.5Y 3/2)	Mosaic speckled b-fabric Uncommon, moderately developed clay coatings along root traces Moderate iron impregnation in irregular, elongate zones separating clouds of weakly impregnated goundmass	None observed	

Category 6: pedotype 148m above base of HCFm; 15.5m above base of Morrin Bridge section; 42-43cm thick; mean thickness 42.5cm						
Depth (cm)	**Horizon**	**Lithology**	**Colour**	**B-fabric and Illuvial Features**	**Redoximorphic Features**	Notes
0-43	Bw	Sandy mudstone	Olive grey (5Y 4/2)	possible clay coatings	None observed	

Category 7: pedotype 154m above base of HCFm; 53-177cm thick; 20m above base of Morrin Bridge section; mean thickness 105.8cm						
Depth (cm)	**Horizon**	**Lithology**	**Colour**	**B-fabric and Illuvial Features**	**Redoximorphic Features**	**Notes**
0-21	Bt	Claystone	Olive grey (5Y 4/2)	Stipple speckled to mosaic speckled b-fabric Uncommon granostriation Common, moderately developed clay coatings in groundmass and along ped surfaces Rare iron hypocoatings along voids/ root traces Large clouds of weak iron impregnation with thick rims and clouds of moderate iron impregnation	None observed	Peds subangular, blocky
21-50	Bw1	Mudstone	Olive grey (5Y 4/2)	Mosaic speckled b-fabric Uncommon iron coatings on voids and along	None observed	Uncommon sparry

				voids/ root traces Weak to moderate iron impregnation		carbonate accumulation in voids and sparry to micritic matrix
50-60	Bw2	Mudstone	Dark olive grey (5Y 3/2)	Stipple-speckled to mosaic speckled b-fabric Uncommon, moderately developed clay coatings in groundmass Large clouds of weak iron impregnation with thick rims and clouds of moderate iron impregnation, some surrounding root traces	None observed	Root traces
60-96	Bw3	Mudstone	Olive grey (5Y 4/2)	Stipple-speckled to weakly mosaic speckled b-fabric Uncommon, weakly developed clay coatings Large clouds of weak iron impregnation with moderate accumulation occurring in thick rims and small clouds	None observed	
96-124	Bw4	Sandy Mudstone	Olive grey (5Y 5/2)	Stipple-speckled to weakly mosaic speckled b-fabric Rare granostriation Rare clay coatings Weak iron impregnation	None observed	

Category 8: pedotype 199m above base of HCFm; 19m above base of Tolman Bridge Section; 109-130cm thick; mean thickness 116.3cm						
Depth (cm)	**Horizon**	**Lithology**	**Colour**	**B-fabric and Illuvial Features**	**Redoximorphic Features**	**Notes**
0-62	Bw1	Sandy mudstone	Olive grey (5Y 5/2)	Stipple speckled to mosaic speckled b-fabric Uncommon, well-developed clay coatings Common iron coatings in voids and on grains Weak to strong iron impregnation	None observed	
62-130 (top of horizo	Bw2	Sandy mudstone	Olive grey (5Y 5/2)	Stipple speckled to mosaic speckled b-fabric Uncommon, well-developed clay coatings in voids Uncommon iron coatings in voids and on	None observed	

n)				grains Large clouds of weak iron impregnation with rims of moderate		

Category 9: pedotype 56m above base of HCFm; 10m above base of Settling Ponds Section; 200cm thick						
Depth (cm)	**Horizon**	**Lithology**	**Colour**	**B-fabric and Illuvial Features**	**Redoximorphic Features**	**Notes**
0-30	O	Coal	Black	None observed	None observed	
30-55	A	Siltstone	Light brownish grey (10YR 6/2)	Mosaic speckled to unistriated b-fabric Uncommon iron coatings on grains and hypocoatings along possible root traces Weak to moderate iron impregnation	None observed	Possible burrow, root traces
52-77	Bw1	Siltstone	Greyish brown (10YR 5/2)	Well-developed unistriated to faint reticulate b-fabric Granostriation Slickensides Rare clay coatings around root traces Weak to moderate iron impregnation	None observed	Root traces
77-95	Bw2	Siltstone	Greyish brown (10YR 5/2)	Stipple-speckled to mosaic-speckled b-fabric Rare clay coatings Common granostriation Uncommon iron coatings on grains and hypocoatings along root traces and/ or Weak to moderate iron impregnation	None observed	Burrow
95-130	Bw3	Mudstone	Light brownish grey (10YR 6/2)	Stipple-speckled b-fabric Weak to moderate iron impregnation	None observed	Root traces
130--200	Bw4	Siltstone	Light brownish grey (2.5Y 6/2)	Very well developed mosaic-speckled b-fabric Rare clay coatings around root traces Weakly impregnated with a few, isolated clouds of moderate impregnation	None observed	Root traces

Table 3.2

Unit	Pedotypes (this study)	Paleo-environments (this study)	Stratigraphic section	Pedotypes observed (Forkner, 2002)	Paleo-environments (Forkner, 2002)
5	2	Wetlands	Tolman Bridge	1, 2, 5, 8	Wetlands and well-drained habitats
4	8	Well-drained habitats (rapidly-changing)	Tolman Bridge	2, 8	Well-drained habitats (rapidly-changing) and rare wetlands
3	None observed	n/a	Morrin Bridge, Tolman Bridge	Not studied	n/a
2	2, 3, 4, 5, 6, 7	Wetlands, wetlands with low watertable, and well-drained habitats	Horsethief Canyon Morrin Bridge	Not studied	n/a
1	1, 2, 3, 7, 9	Wetlands and rare well-drained habitats	East Coulee, Hoodoos, Settling Ponds, Ski Hill, Kirkpatrick, Horsethief Canyon	Not studied	n/a

Table 3.3

Unit	Well-drained paleosol category investigated	Stratigraphic Position from base of HCFm (m)	MAT (^{o}C)	MAP (mm/year)
5	None observed	n/a	n/a	n/a
4	8 8 8	217 215 200	9.9* 10.7* 10.0*	888 905 841
3	None observed	n/a	n/a	n/a
2	4 (not reported in Fig. 3.7, 3.5) 4	179	9.3	876

	7 4 4 7 5 5	177 166 162 160 158 156 155	8.7 9.3 8.8 9.4 10.7 10.6 9.9	865 858 886 858 915 1041 921
1	7 9	120 60	10.7 10.5	976 968
Standard error of estimate:			4.4/ 0.6*	181

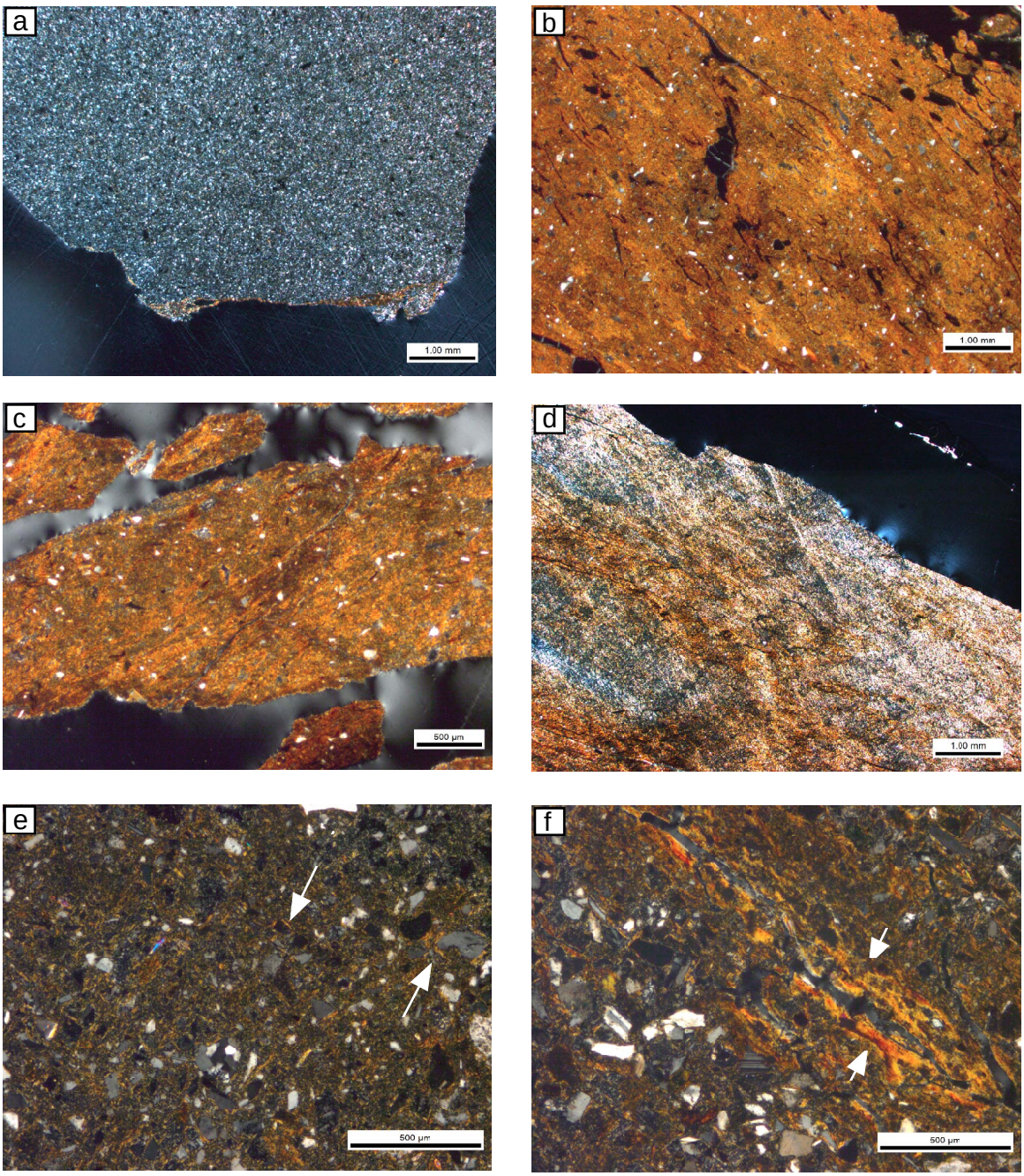

Figure 3.1, p. 1 of 2

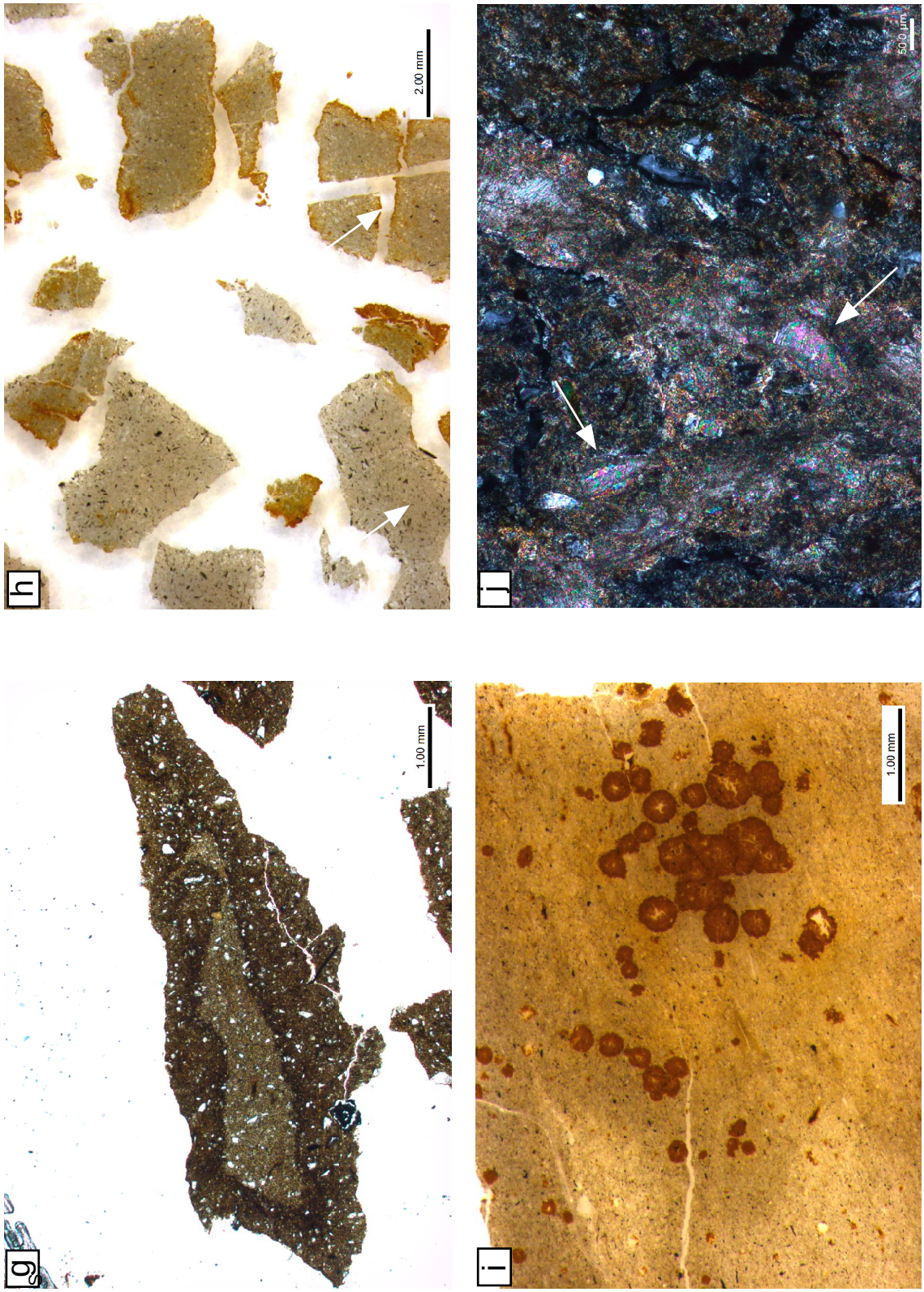

Figure 3.1, p. 2 of 2

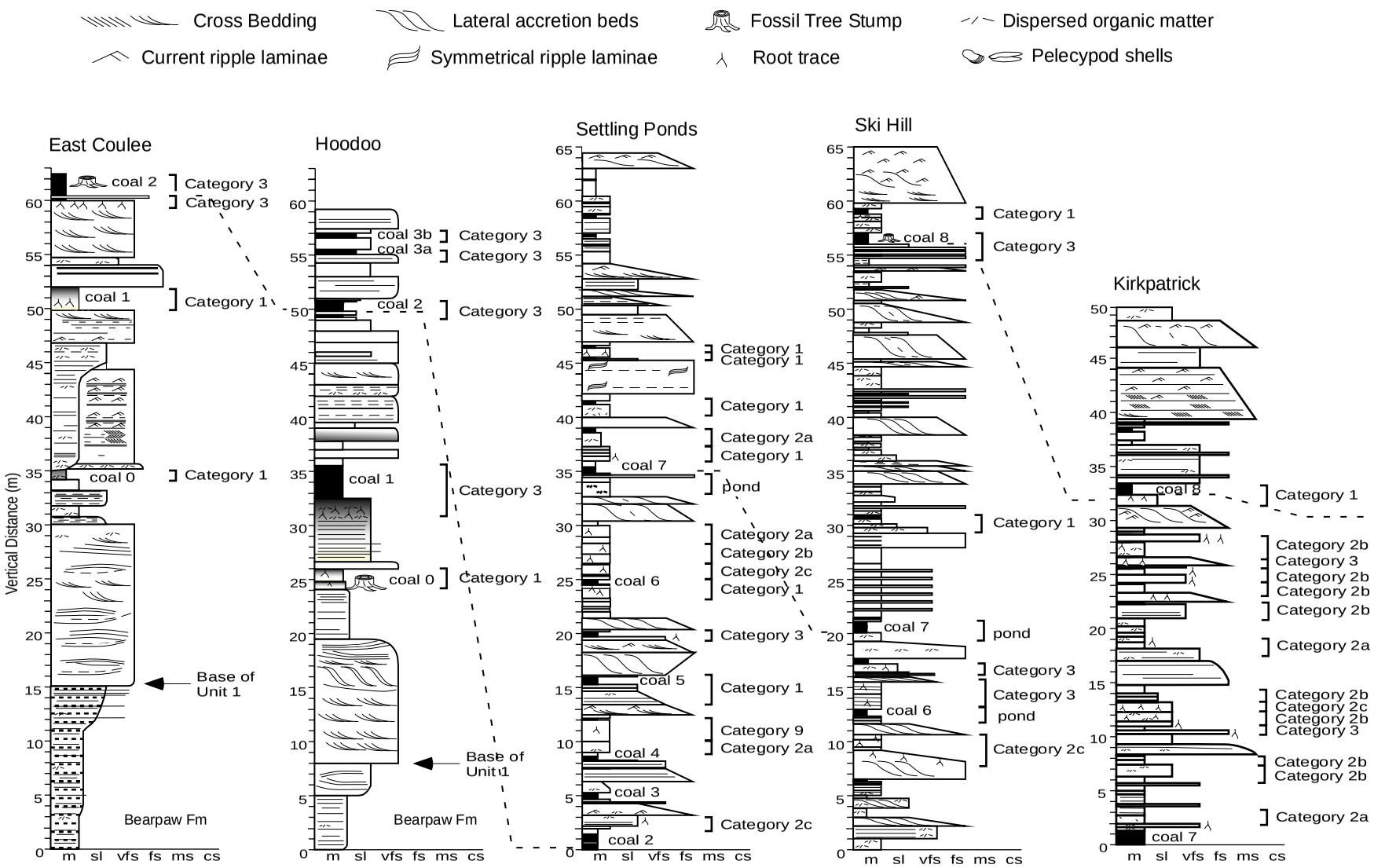

Figure 3.2 p.1 of 2

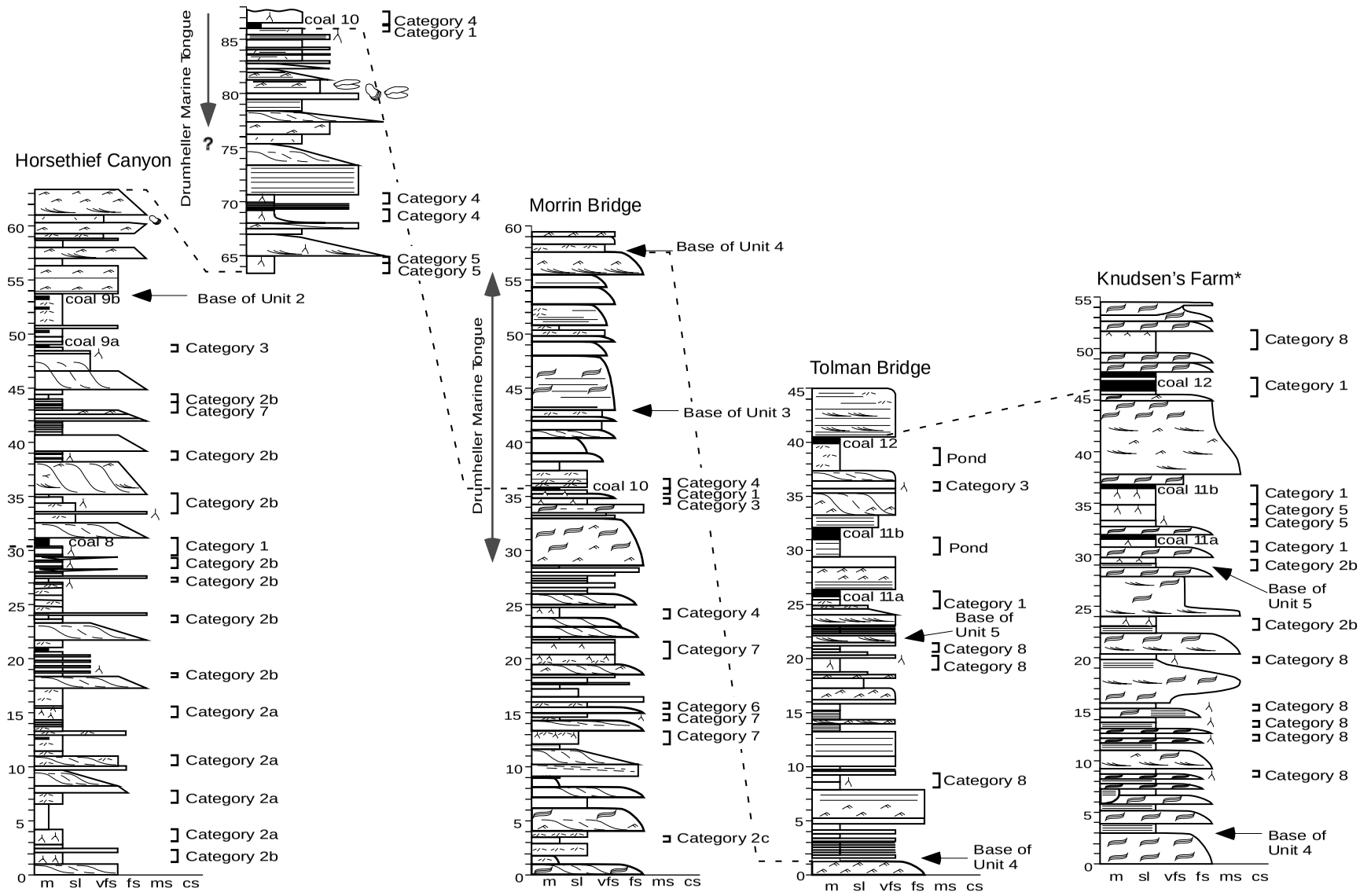

Figure 3.2 p.2 of 2

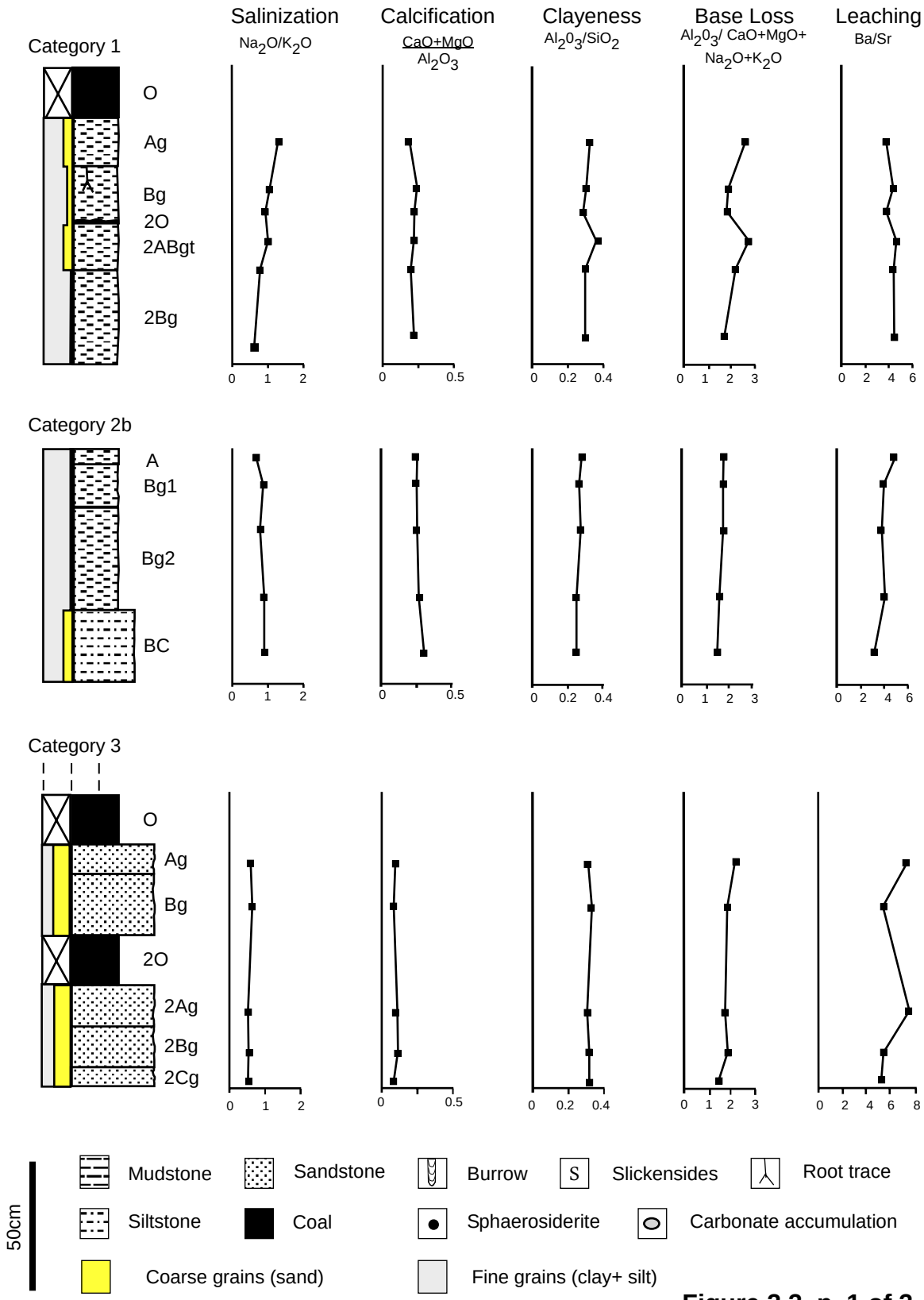

Figure 3.3, p. 1 of 3

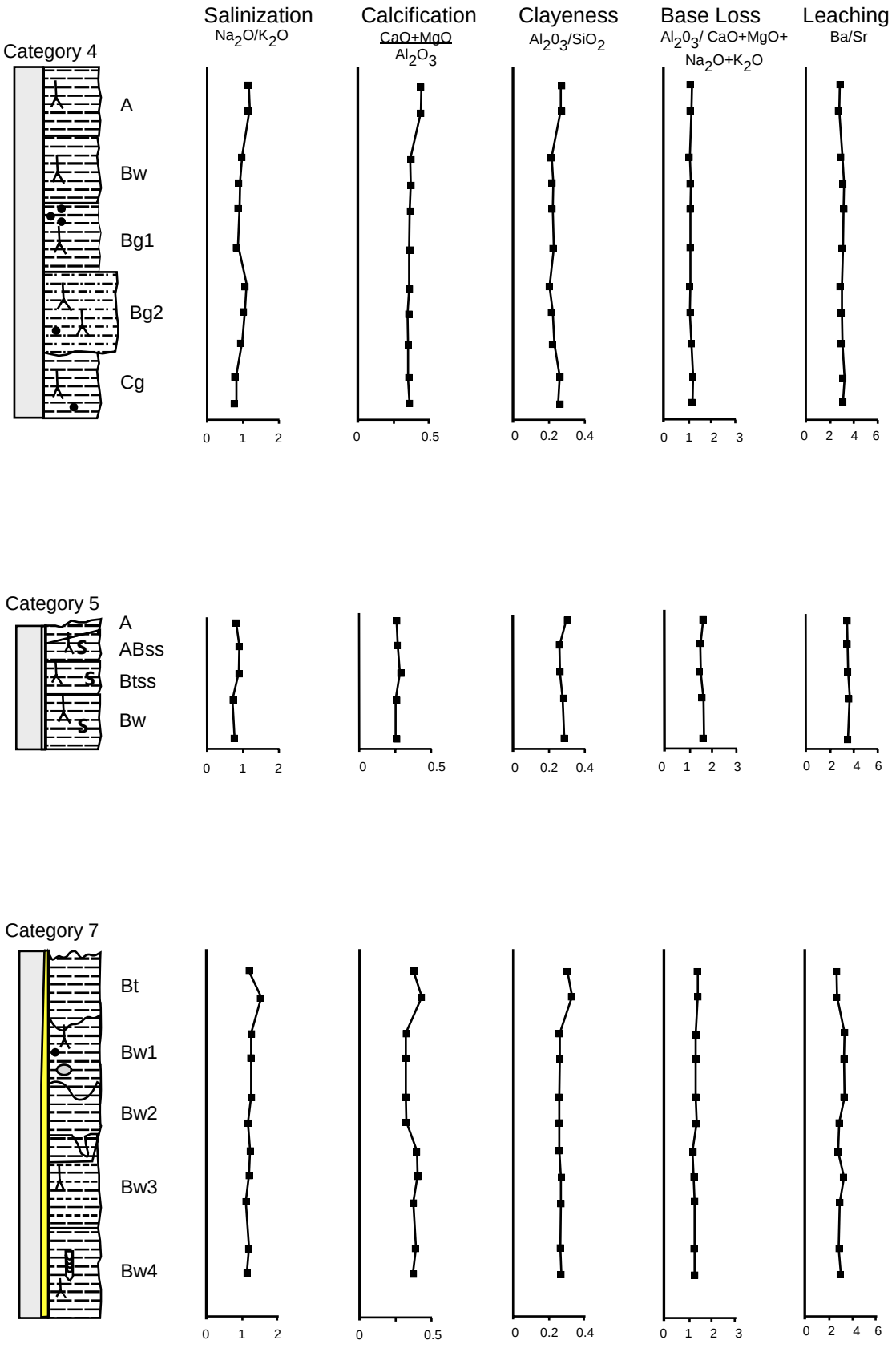

Figure 3.3, p. 2 of 3

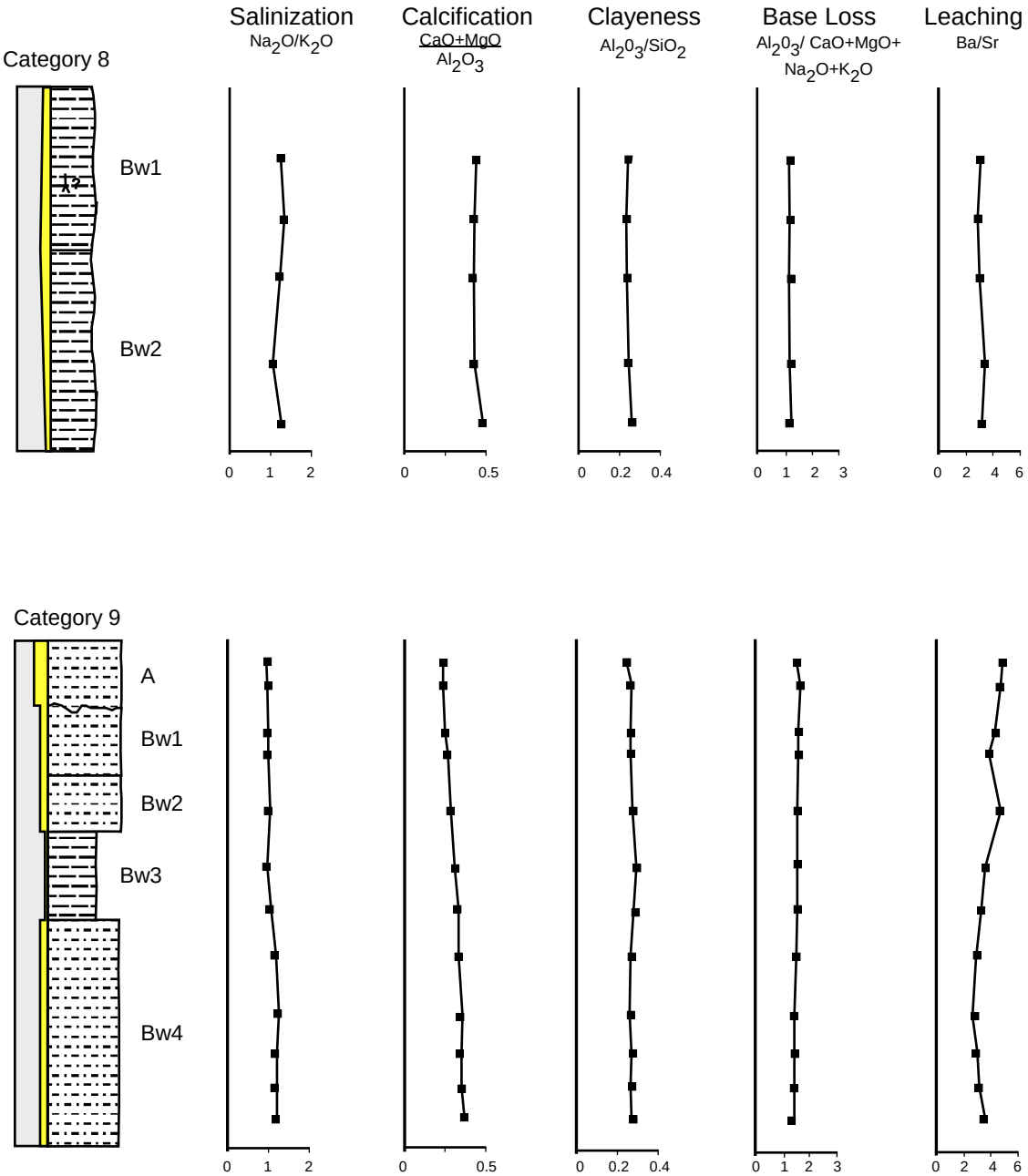

Figure 3.3, p. 3 of 3

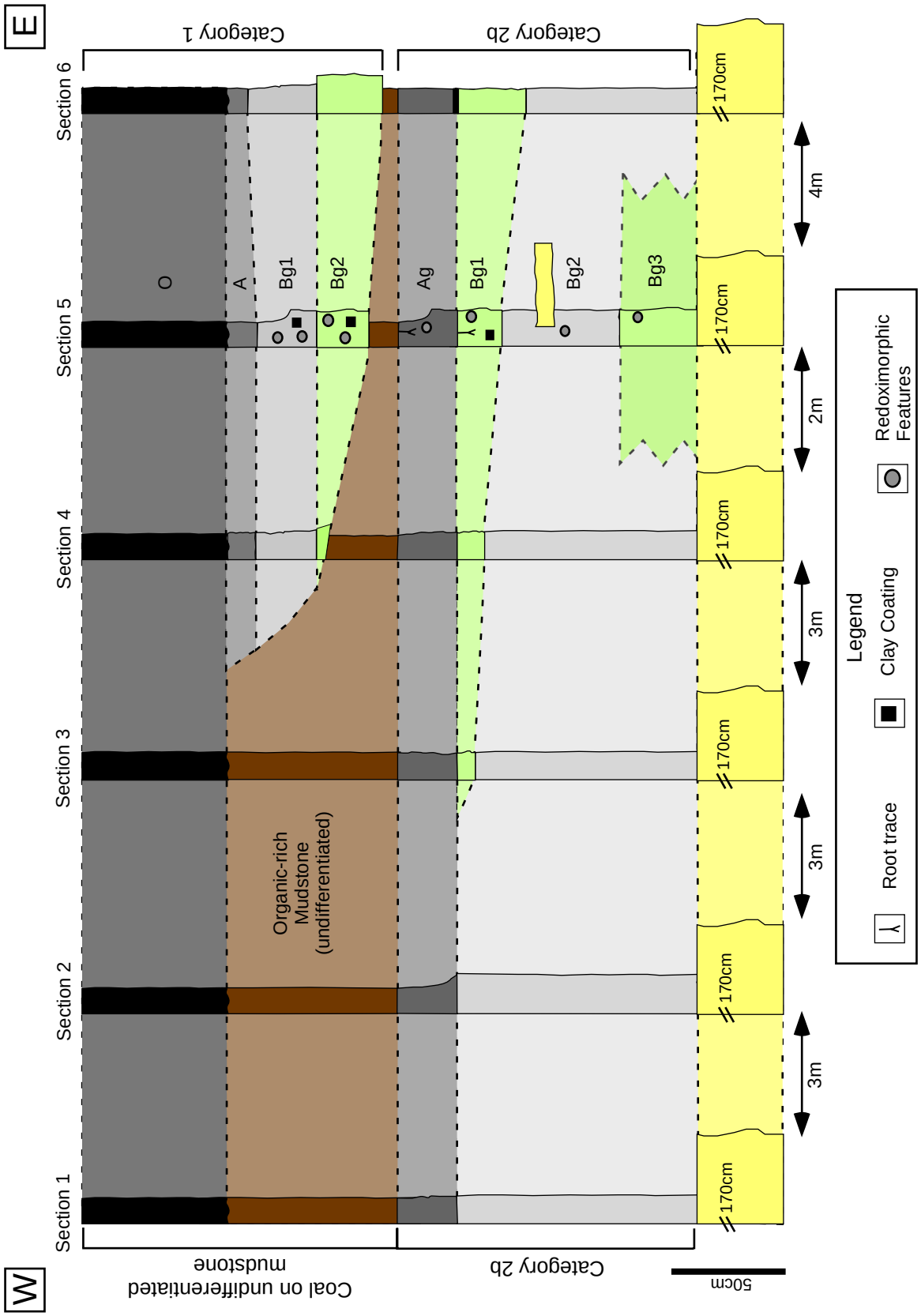
W
E
Section 1
Section 2
Section 3
Section 4
Section 5
Section 6
Coal on undifferentiated mudstone
Category 2b
Category 1
Category 2b
Organic-rich Mudstone (undifferentiated)
O
A
Bg1
Bg2
Ag
Bg1
Bg2
Bg3
170cm
3m
4m
2m
50cm
Legend
Root trace
Clay Coating
Redoximorphic Features

Figure 3.4

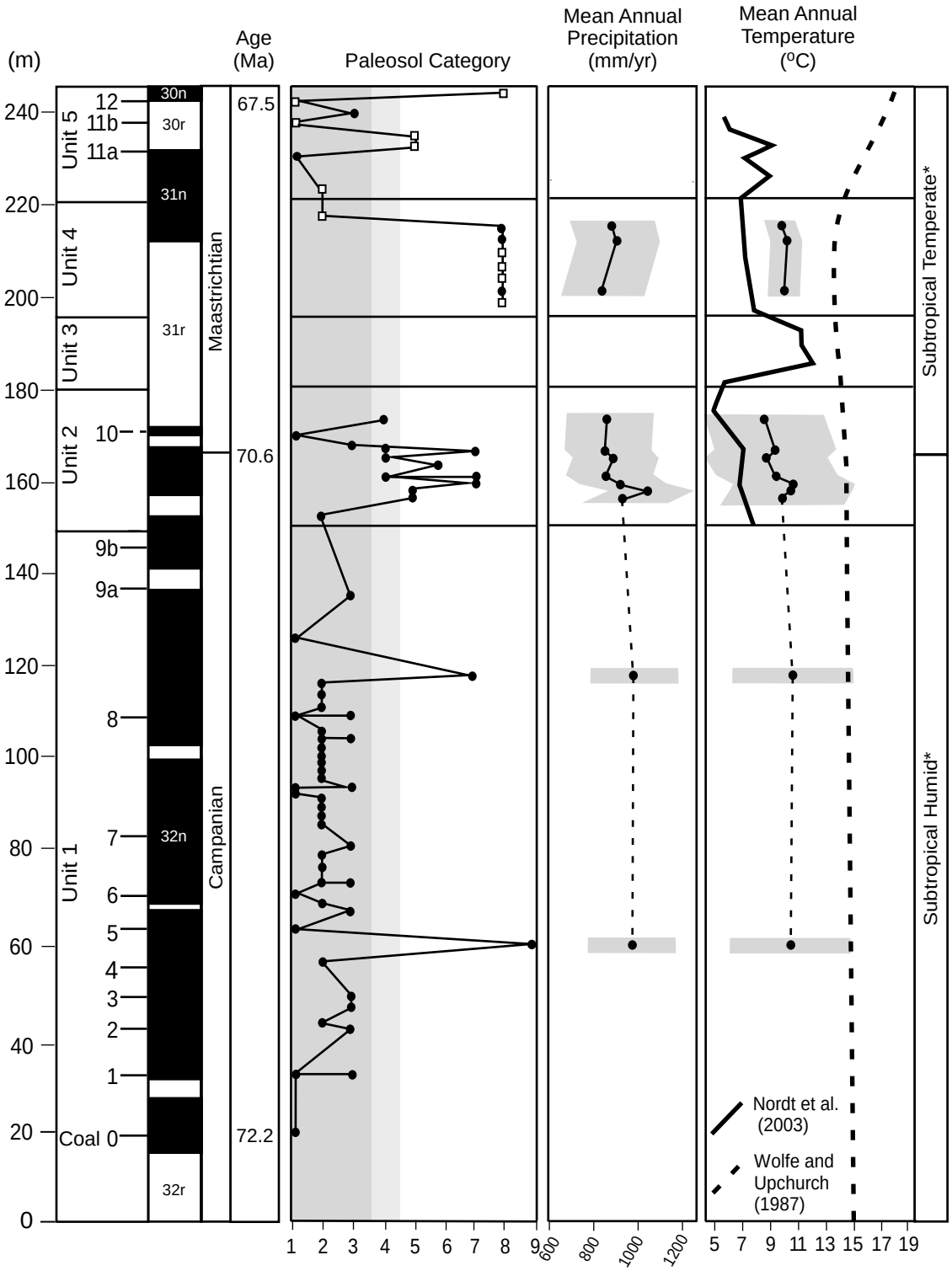
(m)
Age (Ma)
Paleosol Category
Mean Annual Precipitation (mm/yr)
Mean Annual Temperature (°C)
Unit 5
Unit 4
Unit 3
Unit 2
Unit 1
Maastrichtian
Campanian
30n
30r
31n
31r
32n
32r
67.5
70.6
72.2
Coal 0
Subtropical Temperate*
Subtropical Humid*
Nordt et al. (2003)
Wolfe and Upchurch (1987)

Figure 3.5

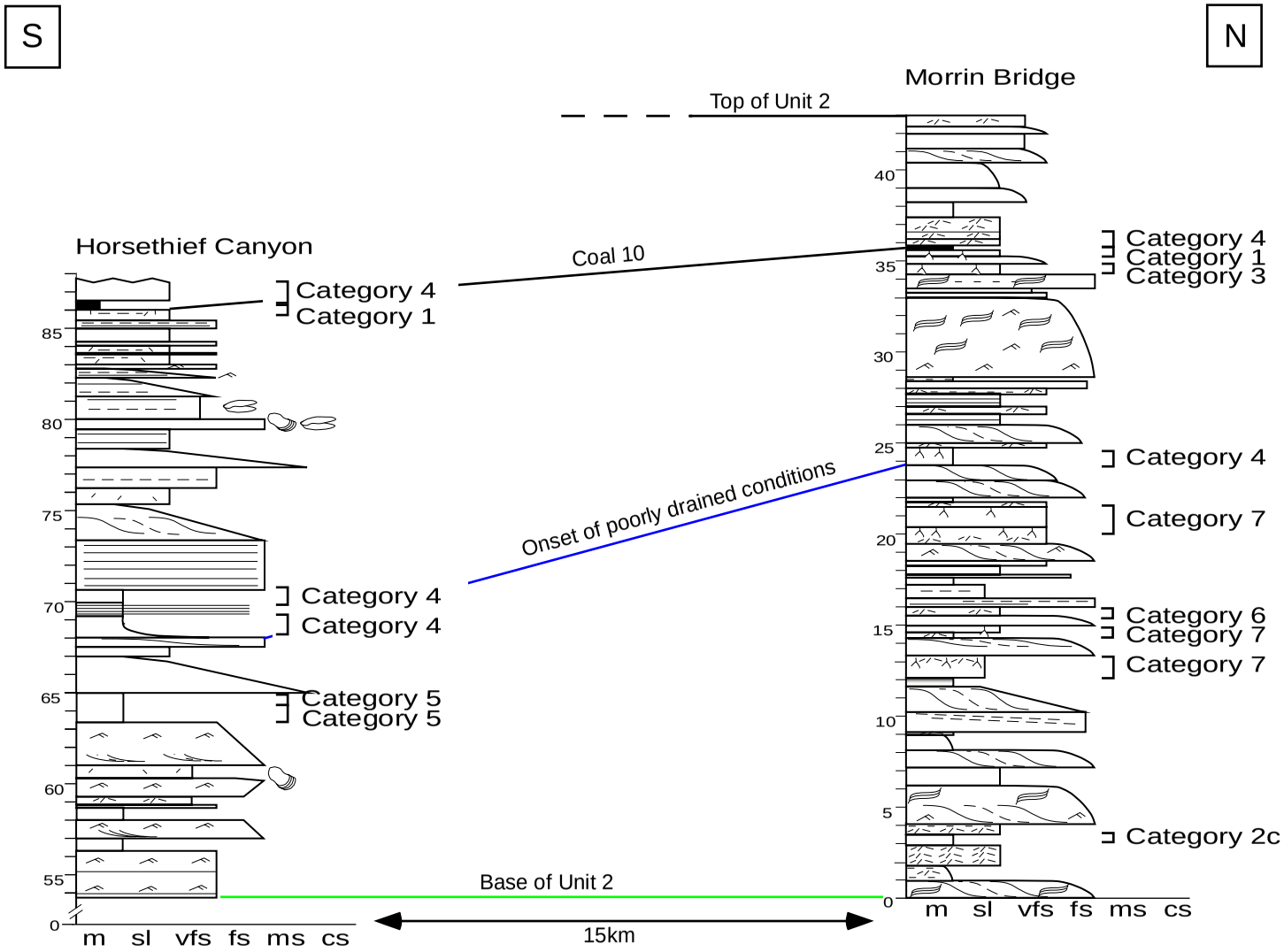
S
N
Morrin Bridge
Top of Unit 2
Horsethief Canyon
Coal 10
Category 4
Category 1
Category 3
Category 4
Category 1
Category 4
Onset of poorly drained conditions
Category 7
Category 4
Category 4
Category 6
Category 7
Category 7
Category 5
Category 5
Category 2c
Base of Unit 2
15km
m sl vfs fs ms cs
m sl vfs fs ms cs
0
5
10
15
20
25
30
35
40
55
60
65
70
75
80
85

Figure 3.6

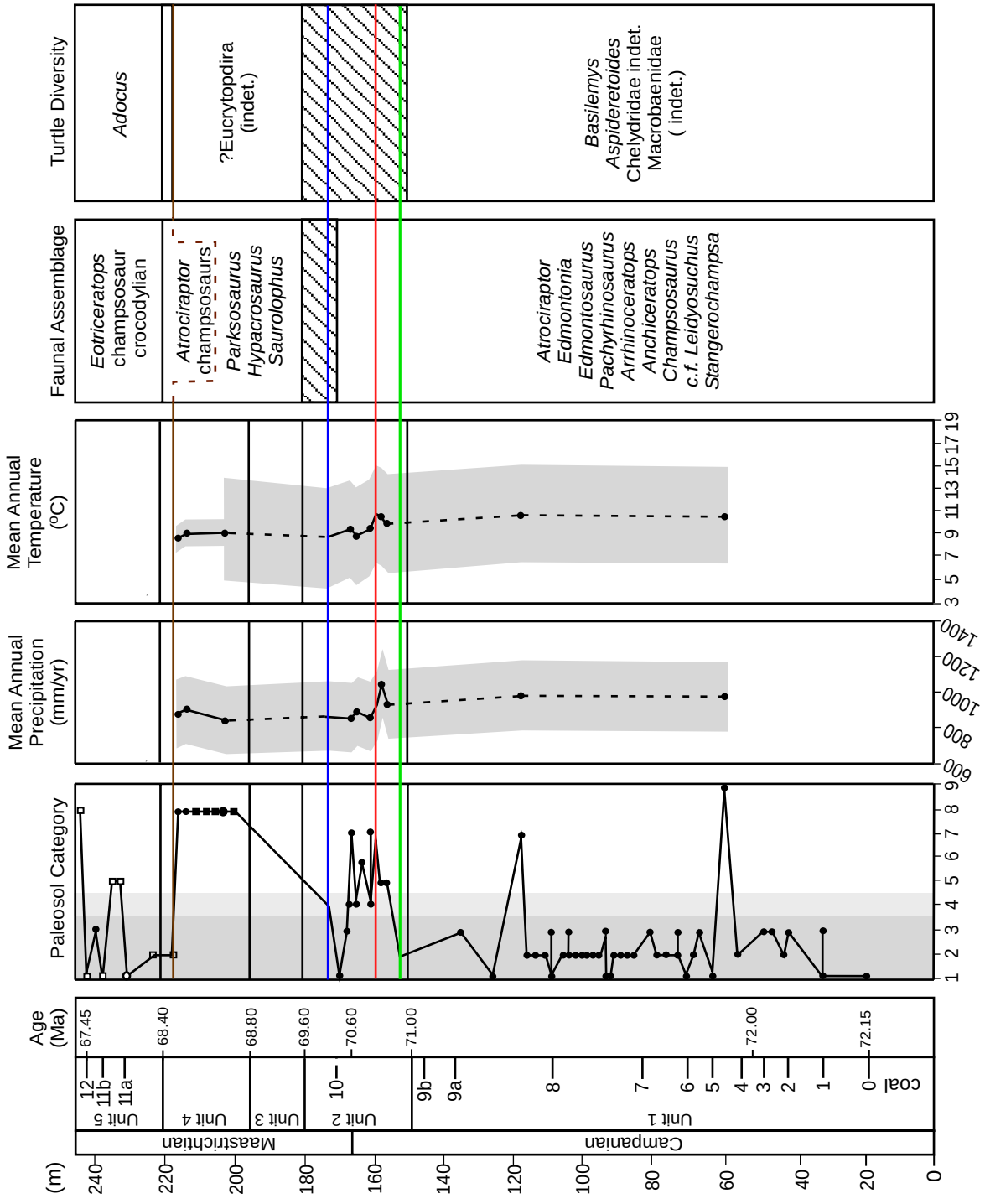
Turtle Diversity
Adocus
?Eucrytopdira (indet.)
Basilemys
Aspideretoides
Chelydridae indet.
Macrobaenidae (indet.)
Faunal Assemblage
Eotriceratops
champsosaur
crocodylian
Atrociraptor
champsosaurs
Parksosaurus
Hypacrosaurus
Saurolophus
Atrociraptor
Edmontonia
Edmontosaurus
Pachyrhinosaurus
Arrhinoceratops
Anchiceratops
Champsosaurus
c.f. Leidyosuchus
Stangerochampsa
Mean Annual Temperature (°C)
Mean Annual Precipitation (mm/yr)
Paleosol Category
Age (Ma)
67.45
68.40
68.80
69.60
70.60
71.00
72.00
72.15
Unit 5
Unit 4
Unit 3
Unit 2
Unit 1
coal
Maastrichtian
Campanian
(m)

Figure 3.7

Chapter Four: Testing the Utility of Paleosols as Sequence Stratigraphic Markers in the Horseshoe Canyon Formation

4.1. Abstract

The marginal marine to non-marine sediments of the Upper Cretaceous Horseshoe Canyon Formation preserve abundant paleosols, with a developmental history thought to have been influenced, at least in part, by sea-level fluctuations. Although several stratigraphic and sedimentologic studies have been undertaken in the HCFm, no attempt has been made to incorporate paleosols into sequence stratigraphic analyses. Because paleosols are considered important sequence stratigraphic markers, they are incorporated here into pre-established sequence stratigraphic interpretations of the HCFm based on the identification of sequence-bounding surfaces, facies distribution, and stratigraphic architecture. Comparisons between the paleosols and the various sequence stratigraphic interpretations are made to determine if correlations exist between sea level change and the degree of development and hydrology of paleosols in the HCFm. The results reveal that, similar to other methods, HCFm paleosols record 4th order transgressive-regressive cycles superimposed onto an overall 3rd order regressive cycle. The ability of HCFm paleosols to resolve T-R cycles depends on a) the inferred distance to the sea and b) the magnitude of the relative change in sea-level.

4.2. Introduction

Studies of sequence stratigraphy in marginal marine and coastal plain deposits commonly utilize the base of incised channels as sequence stratigraphic markers (e.g. Shanley and McCabe, 1994). Recently, paleosols have been incorporated into terrestrial sequence stratigraphic models as interfluve paleosols, inferred to be temporally-equivalent to the base of incised channels, may represent sequence boundaries (e.g., Shanley and McCabe, 1994; Tandon and Gibling, 1994; Aitken and Flint, 1996; Wright, 1996; Currie, 1997; Kraus, 1999; McCarthy et al., 1999; McCarthy, 2002; McCarthy and Plint, 1998, 1999; Atchley et al., 2004; Bennett et al., 2006). While sequence-bounding paleosols may be unusually thick and well-structured, these paleosols have similar features to those of other interfluve paleosols and, consequently, require detailed stratigraphic analyses in order

to be recognized as sequence boundaries (McCarthy and Plint, 1998). The degree of development and hydrology of interfluve paleosols, however, is believed to be correlated to various systems tracts associated with sea level change, with deviations from the pattern inferred to represent catenary relationships (Wright and Marriott, 1993; McCarthy and Plint, 2003).

Major fluctuations in sea level are inferred to have dramatic impacts on the landscape of the coastal plain. The development of extensive coal seams has been interpreted as the landward expression of elevated sea level (Hamilton and Tadros, 1994; Catuneanu and Sweet, 1999; Catuneanu et al., 1999, 2000), which causes watertable levels to rise (Catuneanu et al., 2000) and hydromorphic paleosols to form (e.g. McCarthy and Plint, 2003). Whereas hydromorphic paleosols are associated with times of elevated sea-level, low sea-level is associated with subaerial exposure and erosion (Catuneanu et al., 2000) and the formation of well-developed and well-drained paleosols (Currie, 1997; McCarthy and Plint, 1998). Based on their study of the early Upper Cretaceous Dunvegan Formation, McCarthy and Plint (2003: fig. 20) developed a three-phase model that correlates the degree of development and hydrology of interfluve paleosols to the various systems tracts associated with 4th order sea level change:

1. An aggradational phase characterized by normal alluvial sedimentation during the transgressive through highstand systems tracts. Poorly-drained, coastal depositional setting subject to frequent flooding prevail, resulting in the formation of thick, cumulic, hydromorphic soils with organic-rich surficial deposits in response to a high watertable.
2. A phase of non-deposition or degradation characterized by valley incision due to the lowering of base level during the falling stage through lowstand systems tract. While ground drainage improves towards the margins of incised valleys, areas located far from the valley margin remain poorly-drained. During this phase, soils that developed during Phase 1 become thicker and better developed, and those adjacent to incised valley walls exhibit improved drainage.

3. An aggradational phase characterized by valley-filling, rising watertable levels and flooding during the transgressive systems tract. Flooding results in renewed sedimentation that is focused along the margins of the valleys, producing poorly-drained, cumulic soils with organic-rich surface horizons. Sediment supply may be restricted to areas of the interfluve far from a valley margin, leading to the development of thick coal horizons on pre-existing hydromorphic soils.

Based on theoretical principles, Wright and Marriott (1993: fig. 1) developed a four-phase model of paleosol development in relation to 3rd order changes in sea level and accommodation:

1. A lowstand phase dominated by coarser-grained channel deposits. Low gradients may result in braided channel deposits with restricted aerial extent. Well-developed and well-drained soils develop on terrace surfaces.

2. An early transgressive phase associated with a slow rate of creation of accommodation space and the development of multi-storey sandstone bodies. Floodplain deposits may be subject to reworking. Hydromorphic soils develop in response to rising base-level.

3. A late transgressive phase is associated with increased accommodation rates and the preservation of floodplain deposits with well-separated channel deposits. Weakly developed and well-drained soils develop in response to rapid vertical accretion. More mature soils may develop on the floodplain in the latest stages, but are rarely preserved due to the reduced rate of creation of accommodation space.

4. A highstand phase characterized by reduced accommodation and floodplain accretion, resulting in increased reworking of floodplain sediments and density of channel deposits. Soils are not commonly preserved in this phase.

The two models predict similar responses to lowstands and transgressions but differ in the predicted responses to late transgressive phases and highstands. Study of paleosols that formed in a coastal setting has the potential to shed light on the validity of these models.

Exposed in the Red Deer River Valley in south-central Alberta, the Upper Cretaceous Horseshoe Canyon Formation (HCFm) records the overall and final regression of the Bearpaw Sea, punctuated by episodes of marine transgression (Straight and Eberth, 2002; Eberth, 2004; Hamblin, 2004). To date, no attempt has been made to incorporate paleosols into sequence stratigraphic models for the HCFm. The study of paleosols preserved within the HCFm provides a unique opportunity to study the effects of base-level change on a terrestrial paleoenvironmental record spanning approximately six million years. The degree of development and hydrology of paleosols are compared to previous sequence stratigraphic models to determine if paleosols record a similar history of changes in sea level through the HCFm.

4.3. Geological Setting

The upper Campanian-lower Maastrichtian HCFm is approximately 250-275 metres thick in the Drumheller area (Eberth, 2004) and consists of interbedded sandstones, siltstones, shales, and coals (Eberth, 2004; Hamblin, 2004). Deposited in a coastal to alluvial plain setting on the western edge of the epeiric Bearpaw Sea, the HCFm consists of marginal marine to non-marine sediments. Major lithological changes occurring throughout the HCFm are inferred to reflect tectonic, marine and climatic controls on deposition. Lithologic boundaries are the basis for subdivision of the HCFm into the five, informal sub-units (Fig. 1.3) outlined below (Eberth, 2004).

4.3.1. Unit 1

Unit 1 is 150-160 m thick and consists of shoreface sandstones, isolated to stacked lenticular channel-fills, overbank deposits, and abundant coal beds (Eberth, 2004) numbered successively from 0-9 (Gibson, 1977). A coastal to alluvial depositional setting is inferred for Unit 1 (Shepheard and Hills, 1970; McCabe et al., 1989; Rahmani, 1988; Lavigne, 1999; Eberth, 2004; Hamblin, 2004; Lerbekmo and Braman, 2005), with the lower-most section recording the marine to non-marine transition as the Bearpaw Sea regressed (Eberth, 2004). Based on sequence stratigraphic models, Hamblin (2004) inferred that each coal bed is overlain by a marine flooding surface; dinoflagellates, however, are only documented from the deposits immediately overlying coals 0-3, suggesting that

marine flooding surfaces only overlie these coal beds (Braman, pers com, 2010). Lithologic features suggest that sedimentation occurred during a period of moderate-to-high accommodation and dominantly vertical aggradation below Coal 7. In contrast, sediment supply (and possibly subsidence) is inferred to have increased above Coal 7 (Eberth, 2004).

4.3.2. Unit 2

Unit 2 is approximately 30 m thick and consists of overbank mudstones interbedded with laterally-extensive sandstones. Compared to Unit 1, Unit 2 exhibits thinner beds, smaller paleochannels, rare organic horizons, and common ripple-laminated sandstones (Eberth, 2004, Hamblin, 2004). These features suggest that sediment supply, accommodation space, and rates of subsidence decreased relative to Unit 1 (Eberth, 2004). Unit 2 is also subject to a major marine transgression from the south (Catuneanu and Sweet, 1999; Hamblin, 2004), known as the Drumheller Marine Tongue (DMT). The transgression is associated with the occurrence of a single coal bed (Coal 10) and of brackish-water pelecypods in the middle of the unit.

4.3.3. Unit 3

Unit 3 is approximately 10-20 m thick and consists mainly of laterally extensive, light brown, fine-grained, stacked channels and shoreline sandstones (Eberth, 2004). Finer-grained deposits, interpreted as lacustrine and paludal facies, are uncommon and coal beds are absent (Eberth, 2004). Based on the stratigraphic architecture, Unit 3 is inferred to have been deposited during a time of decreased accommodation coincident with a marine highstand (Straight and Eberth, 2002; Eberth, 2004).

4.3.4. Unit 4

Unit 4 is approximately 25m thick and consists of subequal proportions of overbank mudstones and fine-grained sandstones (Eberth, 2004). Unit 4 channel deposits are single-storied and well separated by overbank deposits, suggesting deposition during a period characterized by greater accommodation, low depositional gradients, and reduced sediment supply (Eberth, 2004). The change in stratigraphic architecture from Unit 3 to Unit 4 may

have been induced by an orogenic pulse to the west, as suggested by the presence of coarse-grained volcanic ash deposits and well-separated fluvial sandstones (Eberth, 2010).

4.3.5. Unit 5

Unit 5 is approximately 20 m thick and consists of overbank mudstones interbedded with laterally-extensive sandstone bodies and at least two coal beds (Coal 11 and Coal 12) (Hamblin, 2004; Eberth, 2004). Thick, stacked paleochannel deposits consisting of fine- to medium-grained sandstone (Hamblin, 2004; Eberth, 2004) and occasional extra-formational pebbles (Eberth, 2004) are present in this unit. The increase in grain size relative to Unit 4, the abundance of alluvial sediments, and the presence of extra-formational pebbles suggests that Unit 5 formed during a period of increased sediment supply and accommodation that was likely tectonically-driven by foredeep rebound in proximal portions of the basin (Catuneanu et al., 2000; Eberth, 2004; see also Eberth and Hamblin, 1993). The genesis of coal beds within Unit 5 has been subject to debate: whereas Hamblin (2004) suggested that coal formation was related to sea level rise, Eberth (2004) suggested that it was related to an increase in basin subsidence.

4.4. Previous sequence stratigraphic models for the HCFm

Sequence stratigraphic investigations on HCFm deposits have focused mainly on the recognition of sequence bounding surfaces, stratigraphic architecture, and facies distribution within the formation (see Catuneanu and Sweet, 1999; Catuneanu et al., 1999, 2000; Straight and Eberth, 2002; Eberth, 2004; Hamblin, 2004). The Bearpaw-Horseshoe Canyon succession is generally inferred to represent a third-order (1-10 Ma) regressive cycle that is overprinted by a series of fourth-order (0.1-1 Ma: Hamblin, 2004; Catuneanu et al., 2000) or fifth-order (0.01-0.1 Ma: Hamblin, 2004) transgressive-regressive (T-R) cycles. These fourth and fifth-order cycles, ranging between 10-30 m in thickness, have been inferred based on unconformity-bound, fining-upward packages in outcrop (Straight and Eberth, 2002) or on flooding surface-bound, coarsening-upward packages in well-logs (Hamblin, 2004).

Straight and Eberth (2002) recognized a series of ten fining-upward, unconformity-bound packages of rock, inferred to represent approximately 4th and 5th order T-R cycles within a grand (3rd order) cycle, up to the base of Unit 4 (Fig. 4.1). The base of each T-R cycle, representing a lowstand, is defined in outcrop as a basal scour resulting from channel incision. An internal surface, defined by localized erosion, a facies change, and slight coarsening upward, marks the highstand and divides each package into a thicker transgressive system tract and a thinner regressive system tract.

Based on well-log data, Hamblin (2004) recognized several, 5th order T-R cycles superimposed onto 4th order cycles in the HCFm. Five 4th order T-R cycles were observed within a 3rd order regressive cycle (Fig. 4.1). The T-R cycle boundaries are generally placed at the top of coal horizons, inferred to correspond to marine flooding surfaces traceable to the base of transgressive marine shale tongues. Similar interpretations have also been made for the base of Unit 1 by Rahmani (1983), Saunders (1989), Ainsworth (1994), and Lavigne (1999) based on outcrop data.

4.5. Materials and Methods

To determine if previously-proposed terrestrial sequence stratigraphic models for the HCFm coincide with the degree of development and hydrology of paleosols, the stratigraphic distribution of paleosols within the formation was compared to the record of sea-level change. Eight localities spanning the entire stratigraphic interval of the HCFm were visited within the Red Deer River Valley, Alberta (Fig. 2.1). The stratigraphic position of paleosols preserved within overbank deposits was documented based on the HCFm stratigraphic scheme of Eberth (2004) (Fig. 1.3).

Seventy-eight paleosol profiles were identified in exposures of the HCFm from south-central Alberta in the summer of 2010 based on the presence of pedogenic features, including horizons, root traces, clay coatings, and slickensides. These paleosols were studied for the purpose of paleoenvironmental and paleoclimatic reconstruction (see Chapter 3). Nine pedotypes (Categories 1-9 paleosols) were recognized based on field observations, petrographic study, and geochemical analyses. The pedotypes are inferred to

represent groups of paleosols that formed under similar paleoenvironmental and paleoclimatic conditions (see Retallack, 1994). Detailed descriptions of the collection and analyses of these pedotypes, along with descriptions of the profiles, can be found in Chapter 3. The paleosols recognized by Forkner (2002) within Units 4 and 5 were incorporated into this study. Brief descriptions (using the terminology of Bullock et al. [1985]) and the inferred paleoenvironmental reconstructions are presented below.

4.5.1. Category 1 paleosols: Gleyed profile capped by coal horizon

Category 1 paleosols consist of coal-capped, gleyed profiles that possess clay coatings and ferruginous redoximorphic features around root traces. These paleosols are interpreted as well-developed, hydromophic paleosols that formed in poorly-drained environments subject to periodic drying and aeration along pores (e.g., Daniels et al., 1971; Retallack, 1988; Brewer, 1960; McKeague, 1983; PiPujol and Buurman, 1994; Wright et al., 2000).

4.5.2. Category 2 paleosols: Gleyed profiles capped by a thin, organic-rich surficial horizon

Category 2 paleosol consist of gleyed profiles overlain by an organic-rich A horizon and possess small clay coatings and ferruginous redoximorphic features in voids, along root traces, and along ped surfaces. These paleosols are interpreted as moderately-developed, hydromorphic paleosols that developed in poorly-drained environments with a high, but fluctuating, watertable resulting in periods of drying and aeration along pores (e.g., Daniels et al., 1971; Retallack, 1988; Brewer, 1960; McKeague, 1983; PiPujol and Buurman, 1994; Wright et al., 2000)

4.5.3. Category 3 paleosols: Pedogenically-modified sandstone overlain by coal horizon

Category 3 paleosols consist of coal-capped, low-chroma sandstones that display remnant sedimentary structures and abundant clay coatings and iron coatings on grains. These paleosols are interpreted as weakly-developed, hydromorphic paleosols that developed on channel or crevasse splay deposits. Although gleyed colours and extensive coal development are suggest poorly-drained environments, abundant clay and iron coatings indicate that drainage improved periodically during the formation of Category 3

paleosols (e.g. Brewer, 1960; Pipujol and Buurman, 1994; McKeague, 1983; Wright et al., 2000).

4.5.4. Category 4 paleosols: Profiles with gleyed basal horizons and non-gleyed upper horizons

Category 4 paleosols consist of gleyed lower horizons that contain coccoid siderite and non-gleyed upper horizons that display depletion redoximorphic features and clay coatings. These paleosols are capped by an organic-rich A horizon. Category 4 paleosols are interpreted as moderately-developed paleosols that formed in moderately-drained environments with a low watertable that fluctuated occasionally into the upper part of the profile (e.g., Daniels et al., 1971; Driese et al., 2010; McKeague, 1983; Wright et al., 2000).

4.5.5. Category 5 paleosols: Non-gleyed profiles with slickensides

Category 5 paleosols generally consist of non-gleyed, varicoloured horizons, although the profile may preserve a basal, gleyed horizon. The non-gleyed horizons display abundant clay coatings and slickensides. Category 5 paleosols are interpreted as well-developed paleosols that formed in generally well-drained environments subject to wet and dry conditions related to precipitation (see McKeague, 1983; Driese et al., 2010; Moeyersons et al., 2006; Nordt and Driese, 2009). In some paleosols, the watertable rose to the bottom of the profile, resulting in the formation of a gleyed basal horizon.

4.5.6. Category 6 paleosols: Rooted sandstone

Category 6 paleosols consist of rooted, fine-grained sandstone deposits displaying faint sedimentary structures, incipient horizon development, and small clay coatings. Category 6 paleosols are therefore interpreted as very weakly-developed, well-drained paleosols.

4.5.7. Category 7 paleosols: Non-gleyed profiles with carbonate

Category 7 paleosols consist of non-gleyed horizons that display iron coatings on grains and along voids and microscopic pedogenic carbonate accumulation. Category 7 profiles are interpreted as moderately developed paleosols that formed in well-drained, drier environments subject to periodic bursts of precipitation (see Drees and Wilding, 1987).

4.5.8. Category 8 paleosols: Non-gleyed profiles with weak horizon differentiation

Category 8 paleosols consist of non-gleyed horizons that display limited pedogenic features, including microscopic clay coatings and iron coatings on grains and along voids. Category 8 paleosols are interpreted as weakly-developed, moderately-drained paleosols subject to alternating wet and dry conditions (see McKeague, 1983; Feakes and Retallack, 1988; Richardson and Daniels, 1993).

4.5.9. Category 9 paleosols: Non-gleyed profiles capped by a thick, surficial coal

Category 9 paleosols consist of coal-capped, non-gleyed horizons that display slickensides, ferruginous pedofeatures, and clay coatings. These paleosols are interpreted as very well-developed, organic paleosols that formed in well-drained environments subject to alternating wet and dry conditions in response to rainfall (see Fey, 2010; Driessen and Dudal, 1991; PiPujol and Buurman, 1994; Nordt and Driese, 2009).

4.6. Results

The stratigraphic distribution and location of paleosols within the HCFm are outlined in Table 3.2 and Figures 3.2 and 4.1. Whereas Category 1-3 paleosols represent poorly-drained paleoenvironments, Category 4 paleosols represent transitional paleoenvironments, and Category 5-9 paleosols represent well-drained paleoenvironments. The distribution of paleosols indicates that:

1. Unit 1 is dominated by well-developed, hydromorphic paleosols indicative of poorly-drained paleoenvironments characterized by a high and stable watertable. The occurrence of only two well-drained paleosols in this unit indicates that drainage rarely improved on the floodplain.

2. Unit 2 consists of alternating stratigraphic intervals dominated, in turn, by well-developed hydromorphic and well-drained paleosols. This pattern indicates that poorly-drained and well-drained paleoenvironments alternated within an overall trend of improving drainage conditions.

3. Unit 4 is dominated by poorly-developed, well-drained paleosols with a single occurrence of a hydromorphic paleosol at the top of the unit. Although well-drained conditions persisted from Unit 2 to Unit 4, poorly-drained conditions returned near the end of Unit 4.

4. Unit 5 consists of stratigraphic intervals dominated, in turn, by well-developed hydromorphic and well-drained paleosols, indicating that poorly-drained paleoenvironments alternated with well-drained paleoenvironments.

Despite the presence of several T-R cycles in Unit 1, paleosols are dominantly hydromorphic (Category 1-3). While Hamblin (2004) inferred that hydromorphic paleosols capped by a coal bed (Category 1) were associated with marine transgressions, the marine highstands of Straight and Eberth (2002) do not always coincide with a coal. Two occurrences of well-drained paleosols, between Coals 4 and 5 and between Coals 8 and 9, coincide closely with inferred periods of base level fall or lowstand by both Straight and Eberth (2002) and Hamblin (2004). Numerous other regressive and lowstand phases recognized by these authors, however, coincide with hydromorphic paleosols.

Paleosols preserved in Unit 2, exposed at Morrin Bridge and Horsethief Canyon, vary from waterlogged (Categories 2 and 3), to moderately-drained (Category 4), to well-drained (Categories 5-7) paleosols. A hydromorphic paleosol is found at the base of Unit 2, which coincides roughly with a lowstand recognized by Straight and Eberth (2002) and, potentially, an inferred flooding surface recognized by Hamblin (2004) (Fig 4.1). Unfortunately, the exact stratigraphic position of this flooding surface could not be determined because it does not correlate to a known coal or marker bed. Stratigraphically higher paleosols are predominantly well-drained and occur within a single T-R cycle according to both Straight and Eberth (2002) and Hamblin (2004). Drainage worsens as Coal 10 is approached, coinciding with the late phase of a marine transgression recognized by Hamblin (2004) and, in contrast, with a lowstand of Straight and Eberth (2002). The maximum transgression of the DMT is marked by the occurrence of a hydromorphic paleosol associated with Coal 10 (Category 1). This paleosol corresponds to a flooding surface of Hamblin (2004) and to the middle interval of a T-R cycle of Straight and Eberth

(2002). Drainage conditions improved immediately above Coal 10, coinciding with the late stage of the "H" T-R cycle of Straight and Eberth (2002) and a marine regression of Hamblin (2004).

Study of the relationship between paleosols and T-R cycles in the upper HCFm was complicated due to the paucity of paleosols in some stratigraphic intervals (i.e., Unit 3) and the lack of sequence stratigraphic models in others (i.e., Units 4 and 5). Paleosols were not preserved in Unit 3, preventing comparison with reported T-R cycles. Unit 4 is characterized by a series of poorly-developed, well-drained paleosols that formed during a 4th order regression recognized by Hamblin (2004). The occurrence of one well-drained paleosol in Unit 4 coincides with a 5th order flooding surface inferred by Hamblin (2004) (Fig. 4.1). A hydromorphic paleosol occurring at the top of Unit 4 may be associated with another 5th order flooding surface inferred by Hamblin (2004). Unit 5 paleosols are predominantly poorly-drained and organic-rich (Categories 1-3). The hydromorphic paleosols associated with Coals 11 and 12 correspond to Hamblin's (2004) inferred flooding surfaces, but well-drained paleosols (Categories 5 and 8) occur between two coal beds associated with the Coal 11 swarm and above Coal 12 (Fig. 4.1).

4.7. Discussion

The distribution of pedotypes in the HCFm reflects the record of sea level change up to the base of Unit 5, with the best resolution occurring in well-drained units. The distribution of pedotypes through each of the five units is discussed below.

4.7.1. Unit 1

Paleosols in Unit 1 are dominantly hydromorphic (Categories 1-3) and generally do not reflect T-R cycles, remaining waterlogged despite small-scale fluctuations in sea level. Whereas Category 1 paleosols have a coal horizon and are better developed than Category 2 paleosols, both categories exhibit pedogenic features suggestive of periods of improved drainage (e.g. clay and iron coatings) (see Wright et al., 2000). Although the occurrence of Category 1 paleosols and their associated coal beds (Coals 0 through 9) has been inferred to coincide with marine transgressions and flooding surfaces (Fig. 4.1; see Hamblin, 2004),

Straight and Eberth (2002) did not find evidence of marine transgressions associated with every coal bed. Furthermore, the presence of dinoflagellates in deposits immediately overlying Coals 0-3, but their absence in deposits overlying stratigraphically-higher coal beds, suggests that coal seam development in the HCFm may not have always been associated with marine transgressions. Transgressive events, therefore, do not appear to be a factor responsible for the preferential formation of Category 1 paleosols relative to Category 2 paleosols. The development of a thick coal horizon in Category 1 paleosols may be, in some cases, associated with pedogenesis in an area of restricted sediment supply, as per phase 3 of the McCarthy and Plint (2003) model. Ergo, landscape position may control the development of Category 1 versus Category 2 paleosols. Time of development may also determine the type of paleosol that will form, as the thick coal deposits of Category 1 paleosols may represent more mature profiles than Category 2 paleosols.

Although Unit 1 paleosols are predominantly hydromorphic, two instances of improved drainage are observed. The first instance, a single Category 9 paleosol interpreted as a freely drained, organic-rich soil, occurs between Coal 4 and Coal 5 (Fig. X). This paleosol records a period of improved drainage that occurred during a marine regressive phase recognized by both Straight and Eberth (2002) and Hamblin (2004). The second instance, a single Category 5 paleosol interpreted as a well-drained soil lacking an organic-rich surficial horizon, occurs above Coal 8 (Fig. 4.1). The absence of a surficial coal horizon in the Category 5 paleosol may reflect an increase in sediment supply inferred to have taken place above Coal 7 (Eberth, 2004). This paleosol records a period of improved drainage that occurred during a lowstand or early transgressive phase (Straight and Eberth, 2002) or during a marine regression (Hamblin, 2004). Although the occurrence of these well-drained paleosols are consistent with phase 2 of McCarthy and Plint's (2003) model and phase 1 of Wright and Marriott's (1993) model, they are not associated with incised valleys or coarser-grained deposits. Because the remaining paleosols of Unit 1 are poorly-drained, likely in response to the close proximity of the Bearpaw Sea, the well-drained paleosols must correspond with major marine regressions that resulted in a dramatically lower watertable. The first occurrence of a Category 5 paleosol late in Unit 1 represents the onset

of a trend towards improved drainage conditions that is recorded in the upper HCFm, presumably reflecting the extensive regression of the Bearpaw Sea.

4.7.2. Unit 2

The hydromorphic paleosol (Category 2) found at the base of Unit 2 reflects the gradual transition between the poorly-drained Unit 1 and the better-drained Unit 2. Although this paleosol occurs near one of Hamblin's (2004) flooding surfaces, no coal bed or direct evidence of marine transgression is observable within that stratigraphic interval. The presence of this paleosol cannot be easily explained in the context of a close association with one Straight and Eberth's (2002) lowstands (Fig. 4.1) unless the reason for a high watertable is not related sea level fluctuations. As stated above, there is little direct evidence for the association of marine transgressions with hydromorphic paleosols above Coal 3. Thus, it is likely that the transition between Unit 1 and Unit 2 may reflect basinal changes rather than a drop in sea level.

Drainage conditions improved from the basal hydromorphic paleosol of Unit 2 upwards, although the two localities investigated (Morrin Bridge and Horsethief Canyon) differ in the details of the transition. Well-drained paleosols occur stratigraphically above the hydromorphic paleosol at both localities, consistent with the 4th order regression of the Upper Bearpaw Tongue (Fig. 4.1; Hamblin, 2004). These paleosols do not record any of the smaller-scale, 5th order fluctuations inferred by Hamblin (2004) nor any base level changes associated with the "G" T-R cycle of Straight and Eberth (2002).

The return of moderately-drained paleosols (Category 4) preceding the hydromorphic paleosol associated with Coal 10 (Category 1) is interpreted to represent the initial rise of the watertable in response to the DMT transgression. Interestingly, the return of moderately-drained paleosols occurs earlier at the southern Horsethief Canyon section (15 m above base of Unit 2) than at the northern Morrin Bridge section (20 m above base of Unit 2) (Fig. 4.1). The earlier occurrence of impeded drainage in the southerly section is interpreted to reflect the transgression of the DMT from the south (Catuneanu and Sweet, 1999; Hamblin, 2004). Moderately-drained paleosols are overlain by hydromorphic

paleosols associated with Coal 10, which, in turn, are immediately overlain by moderately-drained paleosols. Consequently, the paleosols associated with Coal 10 are interpreted to represent the highest watertable level attained in Unit 2 and, therefore, the maximum transgression of the DMT. The return of moderately-drained paleosols immediately above Coal 10, indicative of a lowering of the watertable, is inferred to represent improved drainage conditions as the DMT regressed. The succession of paleosols across Coal 10 correspond well with the highstand and flooding surface of Hamblin (2004) but appears to occur near one of Straight and Eberth's (2002) lowstands (between cycles "G" and "H"; Fig. 4.1). In this instance, the paleosol record appears to be more congruent with Hamblin's model than Straight and Eberth's.

A colour change, from red-brown to grey-green, in the exposures of Unit 2 noted by Straight and Eberth (2002) coincides with the transition in drainage conditions inferred from paleosols within the DMT: the colour change reflects the transition from well-drained paleosols (Category 5-7) to hydromorphic paleosols (Category 1-4). Straight and Eberth (2002:fig. 4) noted that the colour change occurred stratigraphically lower at Horsethief Canyon compared to Morrin Bridge, presumably reflecting the earlier appearance of moderately-drained paleosols at Horsethief Canyon than at Morrin Bridge. This interpretation further supports the hypothesis of transgression of the DMT from the south, as suggested by Catuneanu and Sweet (1999) and Hamblin (2004).

4.7.3 Unit 3

The stratigraphic architecture of Unit 3, consisting of stacked sandstone bodies, suggests that the unit was deposited during a marine highstand in a period of low subsidence and low accommodation (Eberth, 2004). Under these conditions, pre-existing sediments are cannibalized and reworked (e.g., Blakey and Gubitosa, 1984), greatly reducing the formation and preservation potential of paleosols (Wright and Marriott, 1993). No paleosols were observed in Unit 3 which, according to Wright and Marriott (1993), is indicative of a marine highstand. Straight and Eberth (2002), however, recognized at least two cycles of sea-level rise and fall cycles within Unit 3, suggesting that Unit 3 may represent a more complex and long-lived history than is suggested by a single highstand.

4.7.4. Unit 4

Unit 4 paleosols are weakly-developed, well-drained paleosols (Category 8). The development of these paleosols is consistent with a reduced sediment supply, a low rate of subsidence, and the continued regression of the Bearpaw Sea (see Eberth, 2004), which resulted in a low watertable. Under these conditions, fluvial deposits were subject to constant reworking (e.g., Blakey and Gubitosa, 1984) and paleosol development and preservation was limited. The presence of a hydromorphic paleosol (Category 2) at the top of Unit 4 (Forkner, 2002) indicates a rise in watertable level and the onset of poor drainage conditions preceding the Unit 4/Unit 5 lithological contact. This hydromorphic paleosol corresponds with the onset of a 4th order marine transgression inferred by Hamblin (2004). Despite the suggestion by Hamblin (2004) that a series of 5th order T-R cycles can be observed in the subsurface, paleosols in Unit 4 do not preserve any evidence of marine incursion. The occurrence of a hydromorphic soil at the top of Unit 4 is more likely related to basinal changes, such as an increase in rate of subsidence through Unit 5 (see Eberth, 2004), which could have resulted in a higher watertable.

4.7.5. Unit 5

Hydromorphic paleosols (Category 1-3) are prevalent in Unit 5. These paleosols are associated with Coals 11 and 12 and represent a return to Unit 1-type poorly-drained paleoenvironments characterized by a high watertable. However, well-drained paleosols (Category 5) occur between Coal 11a and 11b, as well as above Coal 12. Hamblin (2004) attributed the formation of Coals 11 and 12 to two, distinct marine transgressions, which produced coastal settings, although no sedimentological evidence for these transgressions is preserved. The presence of well-drained paleosols between Coals 11a and 11b is inconsistent with Hamblin's model as a major marine regression would have needed to take place between closely-related coal beds of the same swarm in order to lower watertable levels sufficiently to improve soil drainage. Alternatively, Eberth (2004) argued that sea level change had no influence on the formation of Unit 5 as the sea had receded far to the east by this time. Instead, he inferred that Unit 5 was characterized by increased subsidence and greater accommodation space, potentially resulting in longer residency time of

sediment and a higher watertable, leading to the formation of well-developed, poorly-drained paleosols as seen in Unit 1. Thus, contrary to the depositional settings of Unit 1 and those proposed by Hamblin (2004), Eberth (2004) concluded that the sediments of Unit 5 were deposited in an alluvial setting rather than a coastal setting. This difference in depositional environments could explain the occurrence of well-drained paleosols in the stratigraphic interval separating Coal 11a and Coal 11b (see Forkner, 2002): whereas proximity to the shoreline in Unit 1 may have resulted in a high watertable regardless of changes in the fluvial system (i.e., avulsions and relative proximity to the channels), thus preventing the development of well-drained paleosols, changes in the fluvial system in Unit 5 may have had a greater impact on the local drainage conditions and development of paleosols due to the great distance from the shoreline. Indeed, pedological studies in alluvial settings have postulated that river avulsion can produce dramatic changes in soil drainage conditions, whereas landscapes situated proximal to channels are better drained than distant floodplains located far from the channels (e.g., Kraus and Aslan, 1993).

4.8. Comparison between the stratigraphic distribution of HCFm paleosols to sequence stratigraphic records of the HCFm and models of paleosol response to sea level change

Based on hydrologic and developmental criteria, paleosols preserved in the continental strata of the HCFm are inferred to resolve:

a) The 3rd order regression of the Bearpaw Sea, from Unit 1 to Unit 5, represented by generally improved drainage up-section.
b) The 4th order transgressive-regressive cycle associated with the Drumheller Marine Tongue. The hydromorphic paleosol associated with Coal 10 represents the highest water table levels attained during the DMT transgression and, therefore, the terrestrial equivalent of the marine flooding surface or a highstand. The well-drained paleosols in Unit 4 represent a 4th order regressive phase.
c) Two major 5th order regressions in Unit 1 based on two occurrences of well-drained paleosols.

These results are consistent, in part, with cycles of the multi-phase sequence-stratigraphic paleosol models of both McCarthy and Plint (2003) and Wright and Marriott (1993):

1. The appearance of hydromorphic paleosols associated with the DMT T-R cycle coincides with phase 1 (transgression/ highstand) of McCarthy and Plint (2003).

2. The occurrence of hydromorphic paleosols with thick coal horizons (Category 1) in Unit 1 coincides with phase 3 (marine transgression) of McCarthy and Plint (2003) up to the stratigraphic level of Coal 3. Above Coal 3 however, thick coal horizons may not always be associated with marine transgressions as suggested by: 1) the presence of coal horizons associated with well-drained paleosols inferred to have developed during a regression, and 2) the presence of Category 1 paleosols with coal beds that do not coincide with marine transgressions as inferred by either Straight and Eberth (2002) or Hamblin (2004),

3. The two occurrences of well-drained paleosols in Unit 1 coincide with the lowstand phases of the models of paleosol response to sea level change (phase 2 of McCarthy and Plint [2003] and phase 1 of Wright and Marriott [1993]).

The results of this study correspond closely to the model of McCarthy and Plint (2003) but less so with the model of Wright and Marriott (1993). The differing degree of congruence is presumably related to the scale of the models: whereas Wright and Marriott's (1993) model is based on 3rd order T-R cycles, McCarthy and Plint's (2003) model is based on 4th order T-R cycles. Although the HCFm records the overall 3rd order regression of the Bearpaw Sea, the stratigraphic record preserved within it reflects predominantly 4th and 5th order T-R cycles.

The distribution of paleosols within the HCFm is consistent with parts of Hamblin's (2004) model, but contradicts others. The studies are consistent in that:

a. Well-drained paleosols in Unit 1 coincide with two 5th order regressive phases (between Coals 4 and 5 and between Coals 8 and 9) recognized by Hamblin (2004).

b. The occurrence of stacked, well-drained paleosols low in Unit 2 and in Unit 4 coincide with the 4th order regression of Hamblin's Upper Bearpaw and Tolman tongues, respectively.

c. The sequence of moderately-drained and hydromorphic paleosols associated with Coal 10 reflect the 4th order T-R cycle of the DMT.

However, the results of this study are inconsistent with the model of Hamblin (2004) in that:

1. Not every coal bed in the HCFm is associated with a marine flooding surface. In fact, marine influence is only documented up to the level of Coal 3 (Braman, pers com, 2010) and certain coal beds are associated with well-drained paleosols. The latter suggests that a high watertable, presumably as a result of marine transgression, is not always required for coal development.

2. Although the presence of a hydromorphic paleosol at the top of Unit 4 coincides with a 5th order flooding surface inferred by Hamblin (2004), the occurrence of this paleosol is not thought to be related to sea-level change, but to basinal and fluvial changes that occur in Unit 5. The occurrence of well-drained paleosols in Unit 5, between related coal seams (i.e. the Coal 11 swarm: Forkner, 2002), supports the argument that the development of these paleosols is not controlled by sea-level changes but, presumably, to changes in the fluvial system.

The distribution of paleosols within the HCFm also supports parts of Straight and Eberth's (2002) model. These studies are consistent in that the occurrence of well-drained paleosols between Coals 4 and 5 and between Coals 8 and 9 correspond with a regressive phase and a lowstand, respectively, recognized by Straight and Eberth (2002). The results of this study, however, are inconsistent with Straight and Eberth's (2002) conclusions in

that the paleosols at the stratigraphic level of Coal 10 argue for the presence of a marine highstand, a stage not recognized by Straight and Eberth (2002). The moderately-drained paleosol overlying Coal 10 and its associated hydromorphic paleosol (Category 1) suggests that the maximum transgression of the DMT approximately coincides with Coal 10. The DMT subsequently regressed, resulting in paleosols with improved drainage directly above Coal 10.

4.9. Conclusions

The hydrology and degree of development of HCFm paleosols can be used to track major changes in sea level, but small-scale fluctuations are more difficult to detect. During times of elevated sea level, such as in Unit 1 and the Drumheller Marine Tongue, watertable levels are high and hydromorphic paleosols (Categories 1-3) develop. Conversely, when sea-level is low, watertable levels are low and well-drained paleosols (Categories 5-9) develop. Transitional moderately-drained paleosols (Category 4) can develop during transgressive or regressive phases, as observed in association with the DMT.

The ability of paleosols to resolve small-scale sea level fluctuations depends on 1) the relative distance to the sea and 2) the magnitude of sea-level change. In Unit 1, despite the occurrence of numerous 4th order and 5th order fluctuations in sea-level, nearly all paleosols are hydromorphic. Except for major marine regressions (i.e., between Coals 4 and 5 and Coals 8 and 9), the effects of sea-level change are not recorded in paleosols that developed on the coastal plain due to the perpetually high watertable levels. HCFm paleosols provide the best resolution of sea level changes in Unit 2, where the predominant paleosols are well-drained. In this case, the 4th order T-R cycle of the DMT is denoted by the vertical succession from moderately-drained paleosols (Category 4) to hydromorphic paleosols (Category 1) and back to moderately-drained paleosols (Category 4), a paleosol sequence consistent with phase 2 of McCarthy and Plint's (2003) model. Further up-section, the ability to resolve base level changes diminishes as the Bearpaw Sea had retreated far to the east by this time: paleosols are not preserved in Unit 3 and weakly-developed, well-drained paleosols (Category 8) are preserved in Unit 4, recording no evidence of 5th order T-R

cycles. Finally, at the top of Unit 4 and throughout Unit 5, variations in paleosol hydrology do not coincide with inferred T-R cycles, but are thought to be related to the shifting fluvial system during a phase of increased subsidence.

FIGURE CAPTIONS

Figure 4.1: Distribution of pedotypes in relation to the inferred records of sea level change. Paleosol categories represent poorly-drained (dark grey), transitional (light grey), and well-drained (white) paleoenvironments. Hollow boxes represent paleosol occurrences of Forkner (2002), integrated based on their stratigraphic position to complement this study. Hollow circles represent the stratigraphic position of a paleosol recorded by Forkner (2002) that coincides with a paleosol of the same category from this study. LST= lowstand system tract; HST= highstand system tract. Dashed lines represent flooding surfaces inferred by Hamblin (2004). Question marks represent uncertainty of stratigraphic position of Hamblin's (2004) flooding surfaces because they do not correlate to a known coal or marker bed.

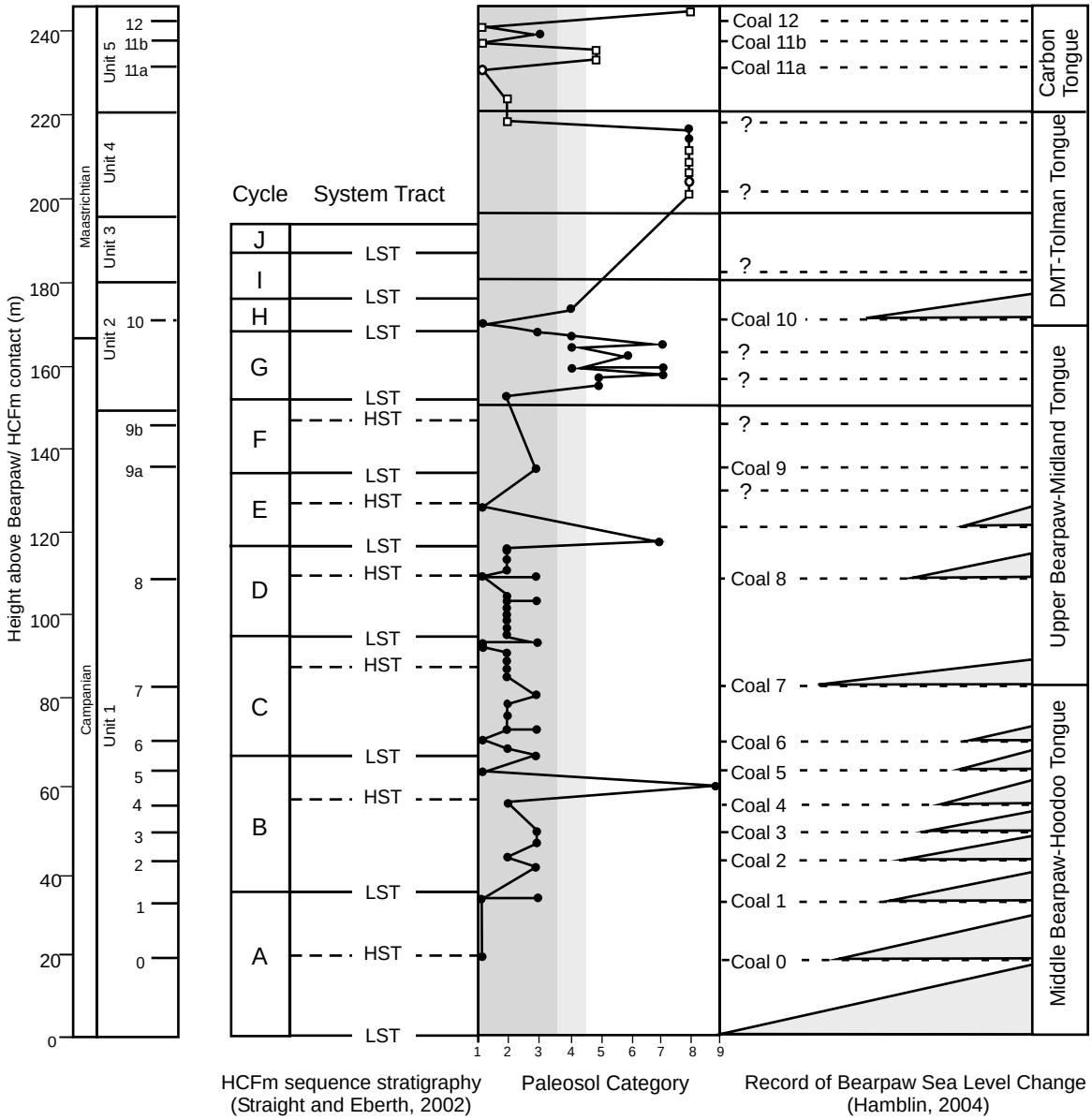
Height above Bearpaw/ HCFm contact (m)
Maastrichtian
Campanian
Unit 5
Unit 4
Unit 3
Unit 2
Unit 1
Cycle
System Tract
J
I
H
G
F
E
D
C
B
A
LST
HST
Coal 12
Coal 11b
Coal 11a
Coal 10
Coal 9
Coal 8
Coal 7
Coal 6
Coal 5
Coal 4
Coal 3
Coal 2
Coal 1
Coal 0
Carbon Tongue
DMT-Tolman Tongue
Upper Bearpaw-Midland Tongue
Middle Bearpaw-Hoodoo Tongue
HCFm sequence stratigraphy
(Straight and Eberth, 2002)
Paleosol Category
Record of Bearpaw Sea Level Change
(Hamblin, 2004)

Figure 4.1

Chapter Five: Conclusion

A great diversity of paleosols has been observed in the HCFm, ranging from well-drained to poorly-drained and from weakly-developed to well-developed. Because the formation of paleosols is influenced by interactions between tectonics, climate, and sea level change, the hydrology and degree of development of paleosols from each of the five units of the HCFm can be used to reconstruct the paleoenvironments and paleoclimates that existed during the Upper Cretaceous.

1. The paleoenvironments of the HCFm are generally inferred to have been poorly-drained throughout the deposition of Unit 1. This is presumably due to the close proximity of the Bearpaw Sea at this time (Eberth, 2004; Hamblin, 2004). A warm and humid paleoclimate is inferred throughout Unit 1.

2. Although poorly-drained paleoenvironments persist across the Unit 1/ Unit 2 boundary, well-drained environments appear slightly higher in section. Improved drainage conditions in Unit 2 are attributed to a marine regression (see Hamblin, 2004). The subsequent DMT transgression caused poorly-drained paleosols to reappear near the stratigraphic level of Coal 10. A period of rapid cooling and drying occurs in Unit 2, prior to the DMT transgression, but does not correspond to a change in paleosols. The development of paleosols in Unit 2 is thought to be related more to sea level changes than to climate or tectonics.

3. Paleosols are not documented in Unit 3, preventing reconstructions of the environments and climates that existed at this time.

4. Well-drained, poorly-developed paleosols are documented from Unit 4. The development of Unit 4 paleosols is thought to be more influenced by tectonics, mainly low accommodation (Eberth, 2004), than by climate or sea-level changes. Unit 4 was deposited during a cool, dry period.

5. Well-drained and poorly-drained paleosols are documented from Unit 5. Because the Bearpaw Sea is thought to have regressed far to the east by this time, the

development of paleosols in this unit is thought to be related to the shifting fluvial environment coincident with an increase in subsidence (see Eberth, 2004). Based on sedimentologic and fossil evidence, a return to warm, humid environments is inferred for Unit 5 (Eberth, 2004; Brinkman and Eberth, 2006).

Environmental and climatic changes inferred from paleosols throughout the HCFm coincide with episodes of faunal change. The faunal turnover in vertebrate species of the HCFm occurs in five phases:

1. A decline in turtle diversity at the Unit 1/ Unit 2 contact (Brinkman and Eberth, 2006).

2. The disappearance of certain ornithischian dinosaurs near Coal 10 (Eberth et al., 2001).

3. The appearance of different ornithischian dinosaurs at the Unit 2/ Unit 3 contact (Eberth et al., 2001).

4. The appearance of a transitional fauna including *Atrociraptor* at the top of Unit 4 (Larson et al., 2010).

5. The return of a ceratopsian, a crocodilian, a champsosaur, and *Adocus* at the Unit 4/ Unit 5 contact (Eberth et al., 2001; Brinkman and Eberth, 2006; Wu et al., 2007).

The first three phases of the faunal turnover do not coincide with the history of climate change recorded by paleosols, but with paleoenvironmental changes. The decline in turtle diversity seems to have coincided with the transition from poorly-drained to well-drained paleoenvironments at the Unit 1/ Unit 2 boundary. The disappearance of some ornithischian dinosaurs in Unit 2 is associated with the appearance of well-drained environments; the disappearance may have occurred earlier in Unit 2 had poorly-drained paleoenvironments not returned briefly in association with the DTM transgression. More detailed studies of the first and last occurrences of the dinosaurs involved in the faunal turnover may reveal that certain dinosaurs disappeared earlier in response to these changes while others were able to

adapt, temporarily, to the new paleoenvironmental and paleoclimatic conditions. The appearance of different ornithischian dinosaurs at the Unit 2/ Unit 3 boundary is likely associated with the establishment of well-drained paleoenvironments. The final phase of the faunal turnover is associated with the return of poorly-drained paleoenvironments near the top of Unit 4 and prevalence throughout Unit 5. A mixed vertebrate fauna, characterized by animals with both cool-climate and warm-climate affinities, is established at the top of Unit 4. By Unit 5, poorly-drained habitats are associated with the occurrence of taxa previously found in Unit 1, which suggests a return to warm and humid conditions. Both paleoenvironmental and paleoclimatic changes are inferred to be responsible for this final phase of the faunal turnover.

The hydrology and degree of development of HCFm paleosols can also be used to track major changes in sea level. Hydromorphic paleosols develop during times of elevated sea level (i.e., Unit 1 and the maximum transgression of the DMT) when watertable levels are high (see Catuneanu et al., 2000). Conversely, well-drained paleosols develop when watertable levels are low and sea-level is low (i.e. the base of Unit 2) (see Catuneanu, 2000). Transitional, moderately-drained paleosols can develop during transgressive or regressive phases (i.e., in association with the DMT) when watertable levels are intermediate or fluctuating.

The ability of paleosols to resolve sea level fluctuations depends on the relative distance to the sea and the magnitude of sea-level change. Despite the occurrence of numerous fluctuations in sea-level throughout Unit 1, nearly all paleosols are hydromorphic. Except for major marine regressions (i.e., between Coals 4 and 5 and Coals 8 and 9), the effects of sea-level change are not recorded in Unit 1, presumably due to the close proximity of the Bearpaw Sea leading to perpetually high watertable levels. The best resolution of sea level changes in the HCFm occurs in Unit 2, where paleosols are predominantly well-drained. In this case, the T-R cycle of the DMT is denoted by the vertical succession from moderately-drained paleosols to hydromorphic paleosols associated with Coal 10, and back to moderately-drained paleosols. Paleosols are not recorded in Unit 3 and, further up-section, the ability to resolve sea-level fluctuations diminishes as the Bearpaw Sea is inferred to

have regressed far to the east by this time. Weakly-developed, well-drained paleosols are preserved in Unit 4, recording no evidence of T-R cycles. At the top of Unit 4 and throughout Unit 5, variations in paleosol hydrology do not coincide with inferred T-R cycles, but are thought to be related to the shifting fluvial system during a phase of increased subsidence.

REFERENCES

Ainsworth, R.B., 1994. Marginal marine sedimentology and high resolution sequence analysis: Bearpaw-Horseshoe Canyon transition, Drumheller, Alberta, Canada. Bulletin of Canadian petroleum geology 42: 26-54.

Aitken, J.F. and Flint, S.S., 1995. The application of high-resolution sequence stratigraphy to fluvial systems: a case study from the Upper Carboniferous Breathitt Group, eastern Kentucky, USA. Sedimentology 42: 3-30.

Aitken, J.F. and Flint, S.S., 1996. Variable expressions of interfluvial sequence boundaries in the Breathitt Group (Pennsylvanian), eastern Kentucky, USA. In: J.A. Howell and J.F. Aitken (Editors), High Resolution Sequence Stratigraphy: Innovations and Applications. Geological Society Special Publications 104, London, pp. 193-206.

Allan, J.A. and Sanderson, J.O.G., 1945. Geology of the Red Deer and Rosebud Sheets, Alberta. Alberta Research Council Report 13, 109 pp.

Amiot, R., Lecuyer, C., Buffetaut, E., Fluteau, F., Legendre, S. and Martineau, F., 2004. Latitudinal temperature gradient during the Cretaceous upper Campanian-middle Maastrichtian: $d^{18}0$ record of continental vertebrates. Earth and planetary science letters 226: 255-272.

Angers, D. and Caron, J., 1998. Plant-induced changes in soil structure: processes and feedbacks. Biogeochemistry 42: 55-72.

Ashley, G.M. and Driese, S.G., 2000. Paleopedology and paleohydrology of a volcaniclastic paleosol interval: implications for early Pleistocene stratigraphy and paleoclimate record, Olduvai Gorge, Tanzania. Journal of sedimentary research 70: 1065-1080.

Atchley, S., Nordt, L.C. and Dworkin, S., 2004. Eustatic control on alluvial sequence stratigraphy: a possible example from the Cretaceous-Tertiary transition of the Tornillo Basin, Big Bend National Park, West Texas, U.S.A. Journal of sedimentary research 74: 391-404.

Bailey, H.P. and Sinnott, E.W., 1915. A botanical index of Cretaceous and Tertiary climates. Science 41: 831-834.

Bell, P.R., 2011. Cranial osteology and ontogeny of *Saurolophus angustirostris* from the Late Cretaceous of Mongolia with comments on *Saurolophus osborni* from Canada. Acta palaeontologica polonica (in press).

Bennett, G.L., Weissmann, G.S., Baker, G.S. and Hyndman, D.V., 2006. Regional-scale assessment of a sequence-bounding paleosol on fluvial fans using ground-penetrating radar, eastern San Joaquin Valley, California. Geological society of America bulletin 118: 724-732.

Beven, K. and Germann, P., 1982. Macropores and water flow in soils. Water resources research 18: 1311-1325.

Birkeland, P.W., 1999. Soils and Geomorphology, 3rd edition. Oxford University Press, Oxford.

Blakey, R. and Gubitosa, R., 1984. Controls of sandstone body geometry and architecture in the Chinle Formation (Upper Triassic), Colorado Plateau. Sedimentary geology 38: 51-86.

Blodgett, R.H., 1988. Calcareous paleosols in the Triassic Dolores Formation, southwestern Colorado. In: J. Reinhardt and W.R. Sigleo (Editors), Paleosols and Weathering Through Geologic Time: Principles and Applications. Geological Society of America Special Paper 216, pp. 103-121.

Blodgett, R.H., Crabaugh, J.P. and McBride, E.F., 1993. The color of red beds- a geologic perspective. In: J.M. Bigham and E.J. Ciolkosz (Editors), Soil Color. Soil Science of America Special Publication 31, pp. 127-159.

Blum, M.D. and Tornqvist, T.E., 2000. Fluvial responses to climate and sea-level change: a review and look forward. Sedimentology 47: 2-48.

Boggs, S., 2006. Principles of Sedimentology and Stratigraphy, 4th edition. Pearson Prentice Hall, Upper Saddle River, New Jersey, 662 pp.

Bolotsky, Y. and Godefroit, P., 2004. A new hadrosaurine dinosaur from the Late Cretaceous of Far Eastern Russia. Journal of vertebrate paleontology 24: 351-365.

Brewer, R., 1960. Cutans: their definition, recognition, and interpretation. Journal of soil science 11: 280-292.

Brinkman, D.B., 2003. A review of nonmarine turtles from the Late Cretaceous of Alberta. Canadian journal of earth sciences 40: 557-571.

Brinkman, D.B. and Eberth, D.A., 2006. Turtles of the Horseshoe Canyon and Scollard formations: further evidence fo a biotic response to Late Cretaceous climate change. Fossil turtle research 1: 11-18.

Bullock, P., Federoff, N., Jongerius, A., Stoops, G. and Tursina, T., 1985. Handbook for Soil Thin Section Description. Waine Research Publications, Albrighton, England.

Cant, D., 1989. Lower Zuni sequence: Middle Jurassic to Cretaceous In: B.D. Ricketts (Editor), Western Canada Sedimentary Basin: A Case History. Canadian Society of Petroleum Geologists, Calgary, pp. 251-267.

Cant, D. and Stockmal, G., 1989. The Alberta foreland basin: relationship between stratigraphy and Cordilleran terrane-accretion events. Canadian journal of earth sciences 26: 1964-1975.

Catuneanu, O. and Sweet, A.R., 1999. Maastrichtian-Paleocene foreland-basin stratigraphies, western Canada: a reciprocal sequence architecture. Canadian journal of earth sciences 36: 685-703.

Catuneanu, O., Sweet, A.R. and Miall, A.D., 1999. Concept and styles of reciprocal stratigraphies: Western Canada foreland system. Terra nova 11: 1-8.

Catuneanu, O., Sweet, A.R. and Miall, A.D., 2000. Reciprocal stratigraphy of the Campanian-Paleocene Western Interior of North America. Sedimentary geology 134: 235-255.

Chadwick, O.A., Brimhall, G.H. and Hendricks, D.M., 1990. From a black to a gray box: a mass balance interpretation of pedogenesis. Geomorphology 3: 369-390.

Currie, B.S., 1997. Sequence stratigraphy of nonmarine Jurassic-Cretaceous rocks, central Cordilleran foreland-basin system. Geological society of America bulletin 109: 1206-1222.

Dahms, D.E., 1998. Soil taxonomy and paleoenvironmental reconstruction: a critical commentary. Quaternary international 51/52: 58-60.

Dahms, D.E. and Holiday, V.T., 1998. Soil taxonomy and paleoenvironmental reconstruction: a critical commentary. Quaternary international 51/52: 109-114.

Daniels, R.B., Gamble, E.E. and Nelson, L.A., 1971. Relations between soil morphology and water-table levels on a dissected North Carolina coastal plain. Soil science society of America journal 35: 781-784.

Davis, M.B., 1958. Three pollen diagrams from central Massachusetts. American journal of science 256: 540-570.

Dawson, F.M., Evans, C.G., Marsh, R. and Richardson, R., 1994. Uppermost Cretaceous and Tertiary strata of the Western Canada Sedimentary Basin. In: G.D. Mossop and I. Shetsen (Editors), Geological Atlas of the Western Canada Sedimentary Basin. Canadian Society of Petroleum Geologists and Alberta Research Council, Special Report 4

Dobos, R.R., Ciolkosz, E.J. and Waltman, W.J., 1990. The effect of organic carbon, temperature, time, and redox conditions on soil color. Soil science 150: 506-512.

Drees, L.R. and Wilding, L.P., 1987. Micromorphic record and interpretations of carbonate forms in the rolling plains of Texas. Geoderma 40: 157-175.

Driese, S.G., Ludvigson, G.A., Roberts, J.A., Fowle, D.A., Gonzalez, L.A., Smith, J.J., Vulava, V.M. and McKay, L.D., 2010. Micromorphology and stable-isotope geochemistry of historical pedogenic siderite formed in PAH-contaminated alluvial clay soils, Tennessee, U.S.A. Journal of sedimentary research 80: 943-954.

Driese, S.G., Medaris, G., Ren, M., Runkel, A. and Langford, R., 2007. Differentiating pedogenesis from diagenesis in early terrestrial paleoweathering surfaces formed on granitic composition parent materials. Journal of geology 115: 387-406.

Driese, S.G., Mora, C.I., Stiles, C.A. and Joeckel, R.M.N., L.C., 2000. Mass-balance reconstruction of a modern Vertisol: implications for interpreting the geochemistry and burial alteration of paleo-Vertisols. Geoderma 95: 179-204.

Driese, S.G., Nordt, L.C., Lynn, W.C., Stiles, C.A., Mora, C.I. and Wilding, L.P., 2005. Distinguishing climate in the soil record using chemical trends in a Vertisol climosequence from the Texas coast prairie, and application to interpreting Paleozoic paleosols in the Appalachian Basin, U.S.A. Journal of sedimentary research 75: 339-349.

Driessen, P.M. and Dudal, R., 1991. The Major Soils of the World. Lecture Notes on their Geography, Formation, Properties and Use. Agricultural University Wageningen, The Netherlands, and Katholieke Universiteit Leuven, Belgium, 151-159 pp.

Eberth, D.A., 2004. A revised stratigraphy for the Edmonton Group (Upper Cretaceous) and its potential sandstone reservoirs. ICE 2004 field trip No. 7 guidebook, CSPG-CHOA-CWLS Joint Conference, Calgary, Alberta, pp. 1-45.

Eberth, D.A., 2010. A revised stratigraphic architecture and history for the Horseshoe Canyon Formation (Upper Cretaceous), southern Alberta plains, AAPG International Conference and Exhibition Calgary, Canada, pp. 1-4.

Eberth, D.A. and Currie, P., 2010. Stratigraphy, sedimentology, and taphonomy of the *Albertosaurus* bonebed (upper Horseshoe Canyon Formation, Maastrichtian), southern Alberta, Canada. Canadian journal of earth sciences 47: 1119-1143.

Eberth, D.A., Currie, P.J., Brinkman, D.B., Ryan, M.J., Braman, D.R., Gardner, J.D., Lam, V.D., Spivak, D.N. and Newman, A.G., 2001. Alberta's dinosaurs and other fossil vertebrates: Judith River and Edmonton groups (Campanian-Maastrichtian). In: C.L. Hills (Editor), Mesozoic and Cenozoic Paleontology in the Western Plains and Rocky

Mountains: Guidebook for the Field Trips, Society of Vertebrate Paleontology, 61st Annual Meeting. Museum of the Rockies Occasional Paper No.3, Bozeman, Montana, pp. 49-75.

Eberth, D.A. and Hamblin, A.P., 1993. Tectonic, stratigraphic, and sedimentologic significance of a regional discontinuity in the upper Judith River Group (Belly River wedge) of southern Alberta, Saskatchewan, and Northern Montana. Canadian journal of earth sciences 30: 174-200.

Fastovsky, D.E. and McSweeney, K., 1987. Paleosols spanning the Cretaceous-Paleogene transition, eastern Montana and western North Dakota. Geological society of America bulletin 99: 66-77.

Fastovsky, D.E. and Weishampel, D.B., 2005. The Evolution and Extinction of Dinosaurs. Cambridge University Press, Cambridge, 485 pp.

Feakes, C.R. and Retallack, G., 1988. Recognition and chemical characterization of fossil soils developed on alluvium: a Late Ordovician example In: J. Reinhardt and W.R. Sigleo (Editors), Paleosols and Weathering Through Geologic Time: Principles and Applications. Geological Society of America Special Paper, Boulder, Colorado, pp. 35-48.

Fey, M., 2010. Soils of South Africa. Cambridge University Press, Cambridge, 287 pp.

Forkner, R.M., 2002. Paleoenvironmental variability across the Cretaceous-Tertiary boundary in the Alberta Foreland Basin, as interpreted from fluvial deposits and paleosols, Red Deer River Valley, Alberta, Canada, Unpublished M.Sc. thesis, Baylor University, Waco, Texas, 121 pp.

Frey, R.W. and Pemberton, S.G., 1990. Bioturbate texture or ichnofabric? Palaios 5: 385-386.

Furnival, G.M., 1950. Cypress Lake map-area, Saskatchewan, Geologcial Survey of Canada, Memoir 242.

Gibson, D.W., 1977. Upper Cretaceous and Tertiary Coal-Bearing Strata in the Drumheller-Ardley Region, Red Deer River Valley, Alberta. Geological Survey of Canada Paper 76-35, 41 pp.

Goudie, A.S., 1973. Duricrusts in Tropical and Subtropical Landscapes. Oxford Clarendon Press, United Kingdom.

Goudie, A.S., 1983. Calcrete. In: A.S. Goudie and K. Pye (Editors), Chemical Sediments and Geomorphology-Precipitates and Residua in the Near-Surface Environment. Academic Press, Orlando, pp. 93-131.

Hamilton, D.S. and Tadros, N.Z., 1994. Utility of coal seams as genetic stratigraphic sequence boundaries in nonmarine basins; an example from the Gunnedah Basin, Australia. AAPG Bulletin 78: 267-286.

He, S., Kyser, T.K., Caldwell, W.G.E., 2005. Paleoenvironment of the western interior seaway inferred from 18O and 13C values of molluscs from the Cretaceous Bearpaw marine cyclothem. Palaeogeography, Palaeoclimatology, Palaeoecology 217: 67-85.

Hoffman, T. and Todd, S., 2000. A national review of land degredation in South Africa: the influence of biophysical and socioeconomic factors. Journal of southern African studies 26: 17-36.

Irish, E.J.W., 1970. The Edmonton Group of south-central Alberta. Bulletin of Canadian petroleum geology 18: 125-155.

Jaques, F.M.B., Su, T., Spicer, R., Xing, Y., Huang, Y., Wang, W. and Zhou, Z., 2011. Leaf physiognomy and climate: are monsoon systems different? Global and planetary change 76: 56-62.

Jerzykiewicz, T., 1992. Controls on the distribution of coal in the Campanian to Paleocene post-Wapiabi strata of the Rocky Mountain Foothills, Canada. Geological society of America special paper 267: 139-150.

Jerzykiewicz, T. and Sweet, A.R., 1988. Sedimentological and palynological evidence of regional climatic changes in the Campanian to Paleocene sediments of the Rocky Mountain Foothills, Canada. Sedimentary geology 59: 29-76.

Kamola, D.L. and Van Wagoner, J.C., 1995. Stratigraphy and facies architecture of parasequences with examples from the Spring Canyon Member, Blackhawk Formation, Utah. AAPG memoir 64: 27-54.

Khidir, A. and Catuneanu, O., 2009. Basin-scale distribution of authigenic clay minerals in the late Maastrichtian-early Paleocene fluvial strata of the Alberta foredeep: implications for burial depth. Bulletin of Canadian petroleum geology 57: 251-274.

Kraus, M.J., 1999. Paleosols in clastic sedimentary rocks: their geologic applications. Earth-science reviews 47: 387-406.

Kraus, M.J. and Aslan, A., 1993. Eocene hydromorphic paleosols: significance for interpreting ancient floodplain processes. Journal of sedimentary petrology 63: 453-463.

Kraus, M.J. and Brown, T.M., 1986. Paleosols and time resolution in alluvial stratigraphy. In: P.V. Wright (Editor), Paleosols: Their Recognition and Interpretation. Princeton University Press, Princeton, N.J., pp. 180-207.

Larson, D.W., Brinkman, D.B. and Bell, P.R., 2010. Faunal assemblages from the upper Horseshoe Canyon Formation, an early Maastrichtian cool-climate assemblage from Alberta, with special reference to the *Albertosaurus sarcophagus* bonebed. Canadian journal of earth sciences 47: 1159-1181.

Lavigne, J., 1999. Aspects of marginal marine sedimentology, stratigraphy, and ichnology of the Upper Cretaceous Horseshoe Canyon Formation, Drumheller, Alberta., Unpublished M.Sc. thesis, University of Alberta, Edmonton, 146 pp.

Leckie, D.A. and Smith, D.G., 1992. Regional setting, evolution, and depositional cycles of the Western Canada Sedimentary Basin. In: R.W. Macqueen and D.A. Leckie (Editors), Foreland Basins and Fold Belts. AAPG Memoir 55, pp. 9-46.

Lerbekmo, J.F., 2002. The Dorothy bentonite: an extraordinary case of secondary thickening in a late Campanian volcanic ash in central Alberta. Canadian journal of earth sciences 39: 1745-1754.

Lerbekmo, J.F. and Braman, D.R., 2002. Magnetostratigraphic and biostratigraphic correlation of late Campanian and Maastrichtian marine and continental strata from the Red Deer Valley to the Cypress Hills, Alberta, Canada. Canadian journal of earth sciences 39: 539-557.

Lerbekmo, J.F. and Braman, D.R., 2005. Magnetostratigraphic and palynostratigraphic correlation of the late Campanian to early Maastrichtian strata of the Bearpaw and Horseshoe Canyon formations between CPOG Strathmore corehole and the Red Deer Valley section, Alberta, Canada. Bulletin of Canadian petroleum geology 53: 154-164.

Longrich, N. and Currie, P., 2009. *Albertonykus borealis*, a new alvarezsaur (Dinosauria: Theropoda) from the early Maastrichtian of Alberta, Canada: implications for the systematics and ecology of the Alvarezsauridae. Cretaceous research 30: 239-252.

Ludvigson, G.A., Gonzalez, L.A., Metzger, R.A., Witzke, B.J., Brenner, R.L., Murillo, A.P. and White, T.S., 1998. Meteoric sphaerosiderite lines and their use for paleohydrology and paleoclimatology. Geology 26: 1039-1042.

Mack, G.H., James, C.W. and Monger, C., 1993. Classification of Paleosols. Geological society of America bulletin 105: 129-136.

McCabe, P.J., Strobl, R.S., Macdonald, D.E., Nurkowski, J. and Bosman, A., 1989. Coal Resource Evaluation of the Horseshoe Canyon Formation and Laterally Equivalent Strata, to a Depth of 400m, in the Alberta Plain Area. Alberta Research Council Open File Report 1989-7, 87 pp.

McCarthy, P.J., Faccini, U. and Plint, A.G., 1999. Evolution of an ancient coastal plain: palaeosols, interfluves and alluvial architecture in a sequence stratigraphic framework, Cenomanian Dunvegan Formation, NE British Columbia. Sedimentary geology 46: 861-891.

McCarthy, P.J. and Plint, A.G., 1998. Recognition of interfluve sequence boundaries: integrating paleopedology and sequence stratigraphy. Geology 26: 387-390.

McCarthy, P.J. and Plint, A.G., 1999. Floodplain palaeosols of the Cenomanian Dunvegan Formation, Alberta and British Columbia, Canada: micromorphology, pedogenic processes and palaeoenvironmental implications. Geological society special publications 163: 289-310.

McCarthy, P.J. and Plint, A.G., 2003. Spatial variability of paleosols across Cretaceous interfluves in the Dunvegan Formation, NE British Columbia, Canada: palaeohydrological, palaeogeomorphological and stratigraphic implications. Sedimentology 50: 1187-1220.

McKeague, J.A., 1983. Clay skins and the argillic horizon. In: P. Bullock and C.P. Murphy (Editors), Soil Micromorphology, Soil Genesis. AB Academic Berkhamsted, pp. 367-388.

MCrea, R.T., Lockley, M.G. and Meyer, C.A., 2001. Global distribution of putported ankylosaur track occurences. In: K. Carpenter (Editor), The Armored Dinosaurs. Indiana University Press, Bloomington, pp. 413-454.

McSweeney, K. and Fastovsky, D.E., 1990. Recognition and interpretation of cemented subsurface horizons in sandy paleosols of Cretaceous- Paleocene age, eastern Montana In: L.A. Douglas (Editor), Soil Micromorphology: A Basic Science. Elsevier, Amsterdam, pp. 683-688.

Moeyersons, J., Nyssen, J., Poesen, J., Deckers, J. and Haile, M., 2006. On the origin of rock fragment mulches on Vertisols: a case study from the Ethiopian highlands. Geomorphology 76: 411-429.

Munsell, 2005. Munsell Soil Colour Charts: Matte Collection. Macbeth Division of Kollmorgen Corp., Baltimore.

Nadon, G., 1988. Tectonic Controls on Sedimentation within a Foreland Basin: the Bearpaw, Blood Reserve and St. Mary River Formations, southwestern Alberta. Canadian Society of Petroleum Geologists Field Trip Guidebook, 85 pp.

Newbrey, M., Murray, A., Brinkman, D.B., WIlson, M. and Newman, A., 2010. A new articulated freshwater fish (Clupeomorpha, Ellimmichthyiformes) from the Horseshoe Canyon Formation, Maastrichtian, of Alberta, Canada. Canadian journal of earth sciences 47: 1183-1196.

Nordt, L.C., Atchley, S. and Dworkin, S., 2002. Paleosol barometer indicates extreme fluctuations in atmospheric CO_2 across the Cretaceous-Tertiary boundary. Geology 30: 703-706.

Nordt, L.C., Atchley, S. and Dworkin, S., 2003. Terrestrial evidence for two greenhouse events in the latest Cretaceous. GSA today 13: 4-9.

Nordt, L.C. and Driese, S.G., 2009. Hydropedological model of vertisol formation along the Gulf Coast Prarie land resource area of Texas. Hydrology and earth system sciences 13: 2039-2053.

Nordt, L.C. and Driese, S.G., 2010. New weathering index improves paleorainfall estimates from vertisols. Geological society of America bulletin 38: 407-410.

Nurkowski, J., 1980. Geology and coal resources of the upper part of the Horseshoe Canyon Formation, Red Deer area, Alberta. Alberta research council open file report 80-10: 1-27.

Nurkowski, J., 1984. Coal quality, coal rank variation and its relation to reconstructed overburden, Upper Cretaceous and Tertiary plains coals, Alberta, Canada. The American association of petroleum geologists bulletin 68: 285-295.

Nurkowski, J. and Rahmani, R.A., 1984. An Upper Cretaceous fluvio-lacustrine coal-bearing sequence, Red Deer area, Alberta, Canada. In: R.A. Rahmani and R.M. Flores (Editors), Sedimentology of Coals and Coal-Bearing Sequences. International Society of Sedimentologists Special Publication 7. Blackwell Publishing Oxford, UK, pp. 163-176.

Ower, J.R., 1960. The Edmonton Formation. Journal of the Alberta society of petroleum geologists 8: 309-323.

Pennington, W., 1986. Lags in adjustment of vegetation to climate caused by the pace of soil development: Evidence from Britain. Vegetation 67: 105-118.

Pimentel, D., Houser, J., Preiss, E., White, O., Fang, H., Mesnick, L., Barsky, T., Taraiche, S., Schreck, J. and Alpert, S., 1996. Water resources: agriculture, the environment, and society. Bioscience 47: 97-106.

PiPujol, M.D. and Buurman, P., 1994. The distinction between ground-water gley and surface-water gley phenomena in Tertiary paleosols of the Ebro Basin, NE Spain. Palaeogeography, palaeoclimatology, palaeoecology 110: 103-113.

PiPujol, M.D. and Buurman, P., 1997. Dynamics of iron and calcium carbonate redistribution and paleohydrology in middle Eocene alluvial paleosols of the southeast Ebro Basin margin (Catalonia, northeast Spain). Palaeogeography, palaeoclimatology, palaeoecology 134: 87-107.

Rahmani, R.A., 1983. Facies relationships and paleoenvironments of a Late Cretaceous tide-dominated delta, Drumheller, Alberta. Canadian Conference on the Mesozoic of Middle North America, Field Trip Guidebook No. 2, 36 pp.

Rahmani, R.A., 1988. Estuarine tidal channel and nearshore sedimentation of a Late Cretaceous epicontinental sea, Drumheller, Alberta, Canada. In: P.L. de Boer and A. van Gelder (Editors), Tide-Influenced Sedimentary Environments and Facies. Reidel Publishing Company, pp. 433-471.

Reeves, C.C.J., 1976. Caliche: Origin, Classification, Morphology, and Uses. Estacado Books, Texas.

Retallack, G., 1988. Field recognition of paleosols In: J. Reinhardt and W.R. Sigleo (Editors), Paleosols and Weathering Through Geologic Time: Principles and Applications. Geological Society of America Special Paper 216, Boulder, Colorado, pp. 1-20.

Retallack, G., 1991a. Miocene Paleosols and Ape Habitats of Pakistan and Kenya. Oxford University Press, New York, 346 pp.

Retallack, G., 1991b. Untangling the effects of burial alteration and ancient soil formation. Annual review of earth planetary science 19: 183-206.

Retallack, G., 1994. A pedotype approach to latest Cretaceous and earliest Tertiary paleosols in eastern Montana. Geological society of America bulletin 106: 1377-1397.

Retallack, G., 1997. A Colour Guide to Paleosols. John Wiley and Sons, New York, 175 pp.

Retallack, G., 2001. Soils of the Past: an Introduction to Paleopedology. Blackwell Science, Oxford.

Richardson, J.L. and Daniels, L.B., 1993. Stratigraphic and hydraulic influences on soil color development. In: J.M. Bigham and E.J. Ciolkosz (Editors), Soil Color. Soil Science Society of America, San Antonio, Texas, pp. 109-125.

Russell, D.A., 1993. The role of Central Asia in dinosaurian biogeography. Canadian journal of earth sciences 30: 2002-2012.

Russell, D.A. and Chamney, P.T., 1967. Notes on the biostratigraphy of dinosaurian and microfossil faunas in the Edmonton Formation (Cretaceous), Alberta. National museum of Canada natural history papers 35: 1-22.

Russell, D.A. and Manabe, M., 2002. Synopsis of the Hell Creek Formation (uppermost Cretaceous) dinosaur assemblage. In: J.H. Hartman, K.R. Johnson and D.J. Nichols (Editors), The Hell Creek Formation and the Cretaceous-Tertiary Boundary in the Northern Great Plains: An Integrated Continental Record of the End of the Cretaceous Geological Society of America Special Paper 361, Boulder, Colorado, pp. 169-176.

Saunders, T.D.A., 1989. Trace fossils and sedimentology of a Late Cretaceous progradation barrier island sequence: Bearpaw-Horseshoe Canyon Formation transition, Dorothy, Alberta, Unpublished M.Sc. thesis, University of Alberta, Edmonton, Alberta.

Schwertmann, U., 1993. Relations between iron oxides, soil color and soil formation. In: J.M. Bigham and E.J. Ciolkosz (Editors), Soil Color. SSSA Special Publication 31, San Antonia, Texas, pp. 51-69.

Shanley, K.W. and McCabe, P.J., 1991. Predicting facies architecture through sequence stratigraphy: an example from the Kaiparowits Plateau, Utah. Geology 19: 742-745.

Shanley, K.W. and McCabe, P.J., 1994. Perspectives on the sequence stratigraphy of continental strata. American association of petroleum geologists bulletin 78: 544-568.

Sheldon, N.D., 2006. Quaternary Glacial-Interglacial cycles in Hawaii. Journal of geology 114: 367-376.

Sheldon, N.D., Retallack, G. and Tanaka, S., 2002. Geochemical climofunctions from North American soils and application to paleosols across the Eocene-Oligocene boundary in Oregon. Journal of geology 110: 687-696.

Sheldon, N.D. and Tabor, N.J., 2009. Quantitative paleoenvironmental and paleoclimatic reconstruction using paleosols. Earth-science reviews 95: 1-52.

Shepheard, W.W. and Hills, L.V., 1970. Depositional environments, Bearpaw-Horseshoe Canyon (Upper Cretaceous) transition zone, Drumheller 'badlands", Alberta. Bulletin of Canadian petroleum geology 18: 166-215.

Smart, P., 1970. Residual shear strength, Proceedings of the American society of civil engineers, soil mechanics and foundations Division 96, pp. 2181-2183.

Smith, A.G., Hurley, A.M. and Briden, J.C., 1981. Phanerozoic Paleocontinental Maps. Cambridge University Press, Melbourne, Australia.

Spicer, R., Valdes, P.J., Spicer, T.E.V., Craggs, H.J., Srivastava, G., Mehrotra, R.C. and Yang, J., 2009. New developments in CLAMP: calibration using global gridded meteorological data. Palaeogeography, palaeoclimatology, palaeoecology 283: 91-98.

Spicer, R.A., Herman, A.B. and Kennedy, E.M., 2004. The foliar physiognomic record of climatic conditions during dormancy: CLAMP and the cold month mean temperature. Journal of geology 112: 685-702.

Srivastava, S.K., 1968. Angiospermic microflora of the Edmonton Formation, Alberta, unpublished Ph.D. dissertation, University of Alberta, 343 pp.

Srivastava, S.K., 1970. Pollen biostratigraphy and paleoecology of the Edmonton Formation (Maastrichtian), Alberta, Canada. Palaeogeography, palaeoclimatology, palaeoecology 7: 221-276.

Stott, D.F., 1984. Cretaceous sequences of the foothills of the Canadian Rocky Mountains. Canadian society of petroleum geologists memoir 9: 85-107.

Straight, W.H. and Eberth, D.A., 2002. Testing the utility of vertebrate remains in recognizing patterns in fluvial deposits: an example from the lower Horseshoe Canyon Formation, Alberta. PALAIOS 17: 472-490.

Tandon, S.K. and Gibling, M.R., 1994. Calcrete and coal in Late Carboniferous cyclothems of Nova Scotia, Canada; climate and sea-level changes linked. Geology 22: 775-758.

Therrien, F., 2005. Palaeoenvironments of the latest Cretaceous (Maastrichtian) dinosaurs of Romania: insights from fluvial deposits and paleosols of the Transylvanian and Haţeg basins. Palaeogeography, palaeoclimatology, palaeoecology 218: 15-56.

Therrien, F., Zelenitsky, D.K. and Weishampel, D.B., 2009. Palaeoenvironmental reconstruction of the Late Cretaceous Sânpetru Formation (Haţeg Basin, Romania) using paleosols and implications for the "disappearance" of dinosaurs. Palaeogeography, palaeoclimatology, palaeoecology 272: 37-52.

Torrent, J., Schwertmann, U. and Schultze, D.G., 1980. Iron oxide mineralogy of some soils of two river terrace sequences in Spain. Geoderma 23: 191-208.

Upchurch, G. and Wolfe, J.A., 1993. Cretaceous vegetation of the Western Interior and adjacent regions of North America. In: W.G.E. Cladwell and E.G. Kauffman (Editors), The Evolution of the Western Interior Basin. Geological Society of Canada Special Paper 39, pp. 243-281.

Vepraskas, M.J., 1992. Redoximorphic features for identifying aquic conditions. North Carolina agricultural research services technical bulletin 301: 1-33.

Vepraskas, M.J. and Caldwell, P.V., 2008. Interpreting morphological features in wetland soils with a hydrologic model. Catena 73: 153-165.

Vepraskas, M.J., Richardson, J.L. and Tandarich, J.P., 2006. Dynamics of redoximorphic feature formation under controlled ponding in a created riverine wetland. Wetlands 26: 486-496.

Vepraskas, M.J., Wilding, L.P. and Drees, L.R., 1993. Aquic conditions for soil taxonomy: concepts, soil morphology and micromorphology. Developments in soil science 22: 117-131.

Webb, L.J., 1959. A physiognomic classification of Australian rain forests. Journal of ecology: 551-570.

Weishampel, D.B., Dodson, P. and Osmolska, H. (Editors), 2004. The Dinosauria, 2nd edition. University of California Press, Berkeley

Wing, S., Harrington, G., Brown, G. and Koch, P., 2003. Floral change during the initial Eocene thermal maximum in the Powder River Basin, Wyoming. In: S.L. Wing, P.D. Gingerich, B. Schmits and E. Thomas (Editors), Causes and Consequences of Globally Warm Climates in the Early Paleogene. Geological Society of America Special Paper 369, Boulder, Colorado, pp. 425-440.

Wolfe, J.A., 1979. Temperature parameters of humid to mesic forests of eastern Asia and relation to forests of other regions of the Northern Hemisphere and Australia. U.S. geological survey professional paper 1106: 1-37.

Wolfe, J.A. and Upchurch, G.R., 1987. North American nonmarine climates and vegetation during the Late Cretaceous. Palaeogeography, palaeoclimatology, palaeoecology 61: 33-77.

Wright, P.V., 1996. The use of palaeosols in sequence stratigraphy of peritidal carbonates. Geological Society Special Publications, London.

Wright, P.V. and Marriott, S.B., 1993. The sequence stratigraphy of fluvial depositional systems: the role of floodplain sediment storage. Sedimentary geology 86: 203-210.

Wright, P.V., Taylor, K.G. and Beck, V.H., 2000. The paleohydrology of Lower Cretaceous seasonal wetlands, Isle of Wight, southern England. Journal of sedimentary research 70: 619-632.

Wu, X., Brinkman, D.B., Eberth, D.A. and Braman, D.R., 2007. A new ceratopsid dinosaur (Ornithischia) from the uppermost Horseshoe Canyon Formation (upper Maastrichtian), Alberta, Canada. Canadian journal of earth sciences 44: 1243-1265.

Yaalon, D.H. and Kalmar, D., 1978. Dynamics of cracking & swelling clay soils: displacement of skeletal grains, optimum depth of slickensides and rate of intra-pedonic turbation. Earth surface processes 3: 31-42.

Appendix A: Geochemical Data

Category	Horizon	Sample ID	SiO2 %	Al2O3 %	Fe2O3 %	MgO %	CaO %	Na2O %	K2O %	TiO2 %	P2O5 %	MnO %	Cr2O3 %	LOI %	Sum %	Nb ppm	Zr ppm	Y ppm	Sr ppm	Rb ppm	Ba ppm
1	Ag	Coulee 11	68.7	15.7	2.7	0.96	0.48	2.03	3.91	0.62	0.01	<0.01	0.01	4.5	99.8	13	175	19	193	114	820
	Bg1	Coulee 10	68.1	15.5	2.79	0.99	0.54	2.1	3.8	0.62	0.02	<0.01	0.02	4.6	99.2	13	183	22	203	113	820
	Bg2	Coulee 9	68.9	15.4	2.89	1.06	0.67	2.3	3.5	0.62	0.02	<0.01	0.01	4.15	99.6	14	188	24	228	108	970
1	Ag	Coal 1-4	65.6	15.4	2.94	1.34	0.6	1.97	1.91	0.63	0.01	<0.01	0.03	8.2	98.8	12	212	20	261	77	1070
	BAg	Coal 1-3	68.4	15.2	3	1.32	0.85	2.23	1.93	0.54	0.02	<0.01	0.02	5.25	99	14	175	24	281	74	940
	Bg	Coal 1-2	68.4	15.1	3.17	1.28	0.92	2.26	1.92	0.5	0.02	<0.01	0.02	5.3	99.1	15	164	24	286	75	910
	C	Coal 1-1	68.7	15.3	3.23	1.35	1.18	2.37	2.01	0.49	0.03	<0.01	0.02	4.8	99.7	14	155	24	304	73	960
1	Ag	SET5-11	66	17.5	3.69	1.08	0.82	1.95	1.79	0.7	0.02	<0.01	<0.01	5.7	99.4	17	147	25	201	95	830
	Ag	SET5-10	65.9	17.3	3.62	1.05	0.81	2.04	1.89	0.69	0.02	<0.01	<0.01	5.2	98.6	15	149	24	206	96	670
	Ag	SET5-9	66.3	17.2	3.72	1.05	0.88	2.13	1.91	0.69	0.02	<0.01	<0.01	5.05	99.1	16	164	26	218	97	880
	Bg1	SET5-8	70.3	15.7	3.03	1.1	1.1	2.52	1.83	0.61	0.04	<0.01	<0.01	3.25	99.7	13	164	28	263	81	740
	Bg1	SET5-7	70.7	15.1	2.91	1.07	1.2	2.56	1.8	0.58	0.05	<0.01	<0.01	3	99.2	12	165	27	268	75	750
	Bg1	SET5-6	69.4	15.5	3.39	1.12	1.12	2.48	1.91	0.62	0.06	<0.01	<0.01	3.3	99	14	164	28	252	85	750
	Bg2	SET5-5	70.2	15.4	3.08	1.1	1.2	2.54	1.91	0.6	0.05	<0.01	<0.01	3.2	99.4	14	171	28	260	80	700
	Bg2	SET5-4	70.7	15	2.83	1.12	1.18	2.47	1.84	0.6	0.05	<0.01	<0.01	2.95	98.9	15	170	28	259	81	750
	Bg2	SET5-3	70.3	15	3.03	1.09	1.25	2.5	1.87	0.6	0.05	<0.01	<0.01	3.3	99.2	13	174	29	258	83	720
	BC	SET5-2	70.5	14.8	2.63	1.04	1.22	2.47	1.86	0.59	0.05	<0.01	<0.01	3.7	99	14	177	27	281	71	820
	C	SET5-1	73.1	14.1	1.82	0.91	1.47	2.72	1.72	0.45	0.04	<0.01	<0.01	3.05	99.5	13	178	23	317	57	920
1	Ag	SET9-2	68.5	15.4	3.06	1.15	1.07	1.94	1.46	0.63	0.03	<0.01	<0.01	6	99.4	16	173	25	231	78	950
	Bg	SET9-1	66.4	15	5.16	1.14	1.14	1.95	1.25	0.59	0.04	0.1	<0.01	6.4	99.2	16	174	30	233	69	640
1	Ag	SET11-6	65	18.7	3.03	0.88	0.64	1.57	1.23	0.8	0.01	<0.01	0.01	7.7	99.6	15	169	21	154	72	560
	Bg	SET11-5	67.3	18.1	2.95	1.13	0.75	2.05	2.04	0.71	0.02	<0.01	0.01	4.4	99.6	15	163	19	193	84	830
	Bg	SET11-4	68	17.1	2.74	0.99	0.7	1.98	2.18	0.7	0.02	<0.01	<0.01	4.25	98.8	14	172	23	184	87	670
	2ABg	SET11-3	59.7	19.7	3.67	1.04	0.9	1.25	1.24	0.96	0.05	<0.01	0.02	10.2	98.8	17	160	67	174	78	790
	2ABg	SET11-2	66.7	17.9	3.13	1.06	0.52	1.53	1.97	0.83	0.02	<0.01	0.01	5.1	98.9	18	144	27	138	107	580
	2Bg	SET11-1	64.9	17.3	2.89	1	0.66	1.76	2.93	0.75	0.02	<0.01	0.02	7.1	99.4	14	146	35	174	124	760
1	Ag	HT 4.15	69.8	13.8	2.46	0.76	0.68	2.05	1.91	0.67	0.02	< 0.01	< 0.01	7.64	99.8	10	142	14	177	80	783
	Bg1	HT 4.14	69.9	13.9	2.57	0.78	0.74	2.03	1.93	0.67	0.02	< 0.01	0.01	7.67	100.3	10	143	14	182	85	760
	Bg1	HT 4.13	70.1	14	2.58	0.77	0.73	2.07	1.99	0.68	0.02	0.01	0.02	6.73	99.7	11	146	14	181	90	703
	Bg2	HT 4.12	67.3	15.5	3.53	0.87	0.73	2.12	2.2	0.7	0.02	< 0.01	< 0.01	7	100	10	137	16	191	107	708

Appendix A: Geochemical Data

Category	Horizon	Sample ID	SiO2 %	Al2O3 %	Fe2O3 %	MgO %	CaO %	Na2O %	K2O %	TiO2 %	P2O5 %	MnO %	Cr2O3 %	LOI %	Sum %	Nb ppm	Zr ppm	Y ppm	Sr ppm	Rb ppm	Ba ppm
	Bg2	HT 4.11	64.7	16.1	4.83	1.13	0.62	1.91	2.55	0.72	0.03	0.01	0.01	7.37	100	11	122	17	175	126	714
2a	Ag	SET7-12	66.1	16.8	3.53	0.89	0.87	2.06	2.47	0.71	0.02	<0.01	0.01	5.5	99.2	17	204	28	211	121	890
	Bg1	SET7-11	68.8	16.1	3.38	0.91	0.96	2.3	2.36	0.65	0.03	<0.01	<0.01	3.35	98.9	16	178	34	242	104	790
	Bg2	SET7-10	67.8	16.5	3.26	1.06	0.87	2.1	2.74	0.68	0.05	<0.01	<0.01	4.1	99.3	14	166	26	214	104	770
	BC	SET7-9	66.3	16.5	3.15	1.06	0.86	2.05	2.8	0.69	0.07	<0.01	<0.01	4.9	98.5	15	170	28	214	104	820
2a	Ag	HT 1.42	66.7	15.6	3.06	1.15	0.74	2.18	1.79	0.67	0.02	0.02	0.01	7.58	99.5	12	159	17	178	86	660
	Bg1	HT 1.41	65.9	15.6	3.13	1.14	0.7	2.15	1.77	0.67	0.02	0.02	0.01	8.12	99.3	12	169	19	184	85	652
	Bg2	HT 1.40	66.1	16.1	3.36	1.16	0.72	2.15	1.87	0.69	0.02	0.02	0.01	7.85	100.1	12	159	21	176	98	632
	Bg2	HT 1.39	65.6	15.8	3.53	1.19	0.76	2.17	1.84	0.65	0.03	0.04	0.02	7.77	99.5	12	159	22	190	95	657
	Bg3	HT 1.38	65.8	15.9	3.47	1.16	0.79	2.19	1.68	0.64	0.02	0.03	0.01	8.07	99.7	14	180	22	183	84	578
	Bg3	HT 1.37	67.7	15.6	2.92	1.12	0.78	2.28	1.66	0.6	0.02	0.01	0.02	6.96	99.7	13	184	21	197	73	694
2b	Bg	SET2-8	67.4	16	3.33	1.42	1.21	2.41	2.04	0.66	0.08	0.01	0.01	4	98.8	15	185	25	257	90	820
	2Bg1	SET2-7	66.9	16.9	3.1	1.66	1.04	2.28	2	0.69	0.11	0.01	0.01	4.25	99.1	15	166	24	227	82	750
	2Bg1	SET2-6	67.2	16.2	2.9	1.63	1.41	2.2	2	0.67	0.15	0.04	<0.01	4.25	98.9	16	158	26	234	81	760
	2Bg2	SET2-5	67.2	16.1	3.3	1.67	1.22	2.1	1.96	0.67	0.19	0.02	0.01	4.6	99.2	13	152	24	219	78	830
	2Bg3	SET2-4	66.6	16.6	3.55	1.57	0.89	2.12	2.02	0.68	0.07	<0.01	<0.01	4.65	98.9	17	231	24	210	92	690
	2Bg3	SET2-3	67.9	15.8	3.55	1.51	0.88	2.03	1.91	0.64	0.06	<0.01	0.01	4.25	98.7	14	141	24	192	93	680
	2Bg3	SET2-2	67.4	15.8	3.35	1.57	0.8	1.85	1.93	0.63	0.06	<0.01	<0.01	4.95	98.5	15	124	23	202	91	850
	2Bg3	SET2-1	66.9	16.2	3.28	1.6	0.86	1.93	1.92	0.66	0.09	<0.01	0.01	4.85	98.5	15	130	27	195	85	700
2b	bh	SET7-8	65.7	17.4	4.1	1.04	0.61	1.95	2.28	0.76	0.02	<0.01	0.01	4.5	98.5	18	163	31	178	116	720
	Ag	SET7-7	66.2	17.4	3.4	1.1	0.58	1.84	2.77	0.76	0.02	<0.01	0.05	4.8	99.1	17	142	22	173	126	810
	Bg1	SET7-6	68	16.6	3.38	0.95	0.71	2.09	2.34	0.75	0.02	<0.01	0.01	4.15	99.1	16	160	27	204	110	780
	Bg2	SET7-5	66	17	3.73	1.03	0.7	2	2.43	0.77	0.03	<0.01	0.01	5	98.8	16	161	28	197	122	720
	Bg2	SET7-4	68	15.8	3.29	0.98	0.83	2.17	2.41	0.71	0.04	<0.01	<0.01	3.95	98.3	15	161	32	223	107	870
	CBg	SET7-3	68.6	15.9	3.12	1.02	1.05	2.24	2.42	0.7	0.06	<0.01	<0.01	4.3	99.5	14	163	26	240	95	730
	bh	SET7-2	64.4	17.8	4.15	1.08	0.76	1.93	2.02	0.77	0.02	<0.01	0.01	5.9	98.9	17	171	31	196	123	800
	OA	SET7-1	63.6	16.6	3.65	1	0.87	1.98	1.89	0.73	0.02	<0.01	0.01	8.45	99	16	188	29	215	110	820
2b	bh	HT 4.10	63.7	15.3	2.89	0.88	0.7	1.86	2.12	0.67	0.03	0.01	0.01	11.4	99.6	10	155	32	195	108	949
	Ag	HT 4.9	65.4	16	3.01	0.95	0.64	1.88	2.28	0.71	0.02	< 0.01	< 0.01	8.63	99.6	11	130	22	181	114	748
	Ag	HT 4.8	64.9	16	3.14	0.91	0.65	1.98	2.36	0.72	0.02	0.01	0.02	8.59	99.3	11	135	25	174	116	725

Appendix A: Geochemical Data

Category	Horizon	Sample ID	SiO2 %	Al2O3 %	Fe2O3 %	MgO %	CaO %	Na2O %	K2O %	TiO2 %	P2O5 %	MnO %	Cr2O3 %	LOI %	Sum %	Nb ppm	Zr ppm	Y ppm	Sr ppm	Rb ppm	Ba ppm
	Bg1	HT 4.7	63.3	16.8	4.55	1.23	0.66	2.02	2.51	0.73	0.03	0.02	0.02	7.5	99.4	10	129	28	195	117	764
	Bg1	HT 4.6	62.8	17.2	4.18	1.24	0.71	2.06	2.57	0.75	0.04	0.01	0.02	7.87	99.5	10	129	26	188	114	982
	Bg2	HT 4.5	63.6	16.7	3.68	1.19	0.73	2.04	2.63	0.73	0.04	0.01	0.01	8.31	99.6	10	130	27	210	116	980
	Bg2	HT 4.4	62.5	16.8	3.62	1.22	0.71	1.89	2.71	0.73	0.06	0.02	0.02	9.57	99.8	10	142	27	179	119	834
	Bg2	HT 4.3	61.2	16.8	3.63	1.14	0.67	1.82	2.64	0.71	0.04	0.01	0.02	10.7	99.5	11	145	29	181	126	860
	Bg3	HT 4.2	64.3	17.2	3.37	0.97	0.68	1.91	2.51	0.72	0.03	0.01	0.01	8.53	100.3	12	136	27	193	117	817
	Bg3	HT 4.1	64.3	17	3.21	0.89	0.72	2.09	2.76	0.7	0.03	0.01	0.02	7.94	99.7	12	153	25	190	115	732
2c	bh	SET-6	65.7	16.9	2.89	1.57	0.91	2.38	2.15	0.76	0.09	<0.01	0.02	5.7	99.3	15	159	29	258	86	1060
	ABg	SET-5	66.6	16.7	2.87	1.55	0.89	2.4	2.12	0.74	0.1	<0.01	0.02	4.55	98.7	15	168	28	243	87	870
	Bg	SET-4	65.4	17.2	3.12	1.64	0.73	2.31	2.28	0.79	0.09	<0.01	0.02	5.05	98.8	16	155	31	201	97	730
	CBg	SET-3	66.3	17.3	3.1	1.6	0.71	2.32	2.3	0.77	0.09	0.01	0.01	4.55	99.2	15	154	30	207	96	800
	C	SET-2	69.5	15.3	2.43	1.22	0.88	2.52	1.81	0.61	0.05	<0.01	0.02	4.75	99.2	12	221	27	255	69	800
	p	SET-1	69	15	2.32	1.25	0.72	2.49	1.8	0.61	0.05	<0.01	<0.01	5.8	99.3	14	191	26	344	67	840
3	Ag	Tree 3	74.8	13.3	1.37	0.59	0.3	1.67	3.22	0.26	<0.01	<0.01	0.02	2.85	98.6	8	75	10	175	76	1280
	Bg	Tree 2	74.2	14.5	1.43	0.65	0.36	1.7	3.06	0.27	<0.01	<0.01	0.02	3.4	99.8	10	81	11	193	78	1010
	C	Tree 1	78	11.7	1.14	0.54	0.32	1.84	3.38	0.26	<0.01	<0.01	0.02	2.2	99.6	11	80	10	214	83	1080
3	Ag	Tree 5	76.7	12.7	1.01	0.49	0.36	1.27	2.13	0.32	<0.01	<0.01	0.02	4.05	99.3	8	139	6	158	49	1130
	Bg	Tree 4	79.6	11.8	0.75	0.51	0.39	1.49	2.35	0.2	<0.01	<0.01	0.01	2.8	100	7	82	7	183	51	970
3	A	SET4-3	68.3	16.3	2.7	0.92	1.17	2.47	1.84	0.62	0.01	<0.01	<0.01	4.1	98.6	15	181	21	278	78	1050
	Bg1	SET4-2	68	16.6	3.21	1.02	1.23	2.46	1.89	0.65	0.02	<0.01	<0.01	4	99.3	17	180	26	284	89	1060
	Bg2	SET4-1	67.7	16.4	3.36	1.03	1.26	2.45	1.95	0.65	0.03	<0.01	<0.01	4	99.1	16	180	25	258	97	840
4	A	HT 27B	62.9	16.1	4.7	1.81	1.57	2.25	1.87	0.58	0.12	< 0.01	0.01	8.08	100	11	178	25	331	80	1021
	A	HT 26B	62.5	16.1	4.67	1.81	1.62	2.29	1.9	0.6	0.13	0.02	0.01	8.01	99.7	12	179	25	298	79	878
	Bw	HT 25B	69	13.6	4.12	1.22	1.27	2.25	2.21	0.64	0.11	0.13	0.01	5.41	99.9	11	154	24	243	102	778
	Bw	HT 24B	67.4	14	4.44	1.31	1.21	2.18	2.33	0.68	0.1	0.05	0.01	5.89	99.6	12	151	24	229	109	767
	Bg1	HT 23B	67.4	13.8	4.52	1.28	1.21	2.17	2.39	0.66	0.11	0.19	< 0.01	6.04	99.8	11	150	24	227	109	773
	Bg1	HT 22B	66.8	14.3	4.61	1.34	1.2	2.19	2.49	0.69	0.1	0.03	0.02	6.46	100.3	11	156	24	227	113	764
	Bg2	HT 21B	70.7	13.4	3.27	1.1	1.28	2.42	2.12	0.6	0.09	0.04	< 0.01	5.23	100.2	9	148	22	243	83	757
	Bg2	HT 20B	68.2	13.8	4.02	1.17	1.23	2.33	2.18	0.65	0.09	0.12	0.02	6.31	100.2	10	155	24	235	94	748

Appendix A: Geochemical Data

Category	Horizon	Sample ID	SiO2 %	Al2O3 %	Fe2O3 %	MgO %	CaO %	Na2O %	K2O %	TiO2 %	P2O5 %	MnO %	Cr2O3 %	LOI %	Sum %	Nb ppm	Zr ppm	Y ppm	Sr ppm	Rb ppm	Ba ppm
	Bg2	HT 19B	67.7	14.1	4.3	1.2	1.19	2.27	2.27	0.67	0.08	0.03	0.01	6.49	100.3	11	156	26	234	103	758
	Cg	HT 18B	61.6	15.2	5.62	1.46	1.11	1.95	2.35	0.74	0.07	0.06	0.01	9.88	100.1	12	157	22	212	126	714
	Cg	HT 17B	61.3	15.1	5.39	1.44	1.18	1.96	2.38	0.72	0.07	0.04	< 0.01	10.5	100.1	11	154	23	224	122	756
4	Bw	HT37B	63.4	15.3	5.64	1.54	1.58	2.47	2.3	0.66	0.16	0.06	0.01	6.81	99.9	---	---	---	---	---	---
4	Bw	HT44B	65.2	15.2	5.16	1.21	1.26	2.48	2.66	0.67	0.09	< 0.01	0.02	6.14	100.1	---	---	---	---	---	---
4	Bw	M2.76B	66.5	14.7	4.09	1.34	1.24	2.33	2.72	0.67	0.12	0.04	0.01	5.83	99.6	---	---	---	---	---	---
5	AB	HT 11B	53.3	12.8	3.28	0.92	1.16	1.88	1.98	0.55	0.02	< 0.01	0.01	24	99.9	11	242	26	245	82	711
	Bt	HT 10B	67.5	15.7	3.7	1	0.92	2.31	2.23	0.68	0.02	< 0.01	0.01	6.7	100.7	10	162	22	240	100	719
	Bt	HT 9B	66.2	15.5	3.82	1.04	0.89	2.24	2.28	0.68	0.02	< 0.01	0.02	7.22	100	11	157	23	239	104	681
	Bw1	HT 8B	67.9	14.6	3.37	0.84	1.03	2.3	2.36	0.57	0.02	< 0.01	0.03	7.06	100.1	10	189	19	255	92	749
	Bw1	HT 7B	69.8	13.9	3.07	0.81	1.12	2.47	2.33	0.53	0.02	0.01	0.01	5.9	100	9	192	19	266	86	803
	Bw2	HT 6B	70.1	14	3.14	0.89	1.15	2.54	2.18	0.54	0.04	< 0.01	0.03	5.73	100.3	9	189	20	270	84	752
	Bw2	HT 5B	68.9	14.2	3.34	1	1.21	2.48	2.08	0.56	0.05	< 0.01	< 0.01	6.13	99.9	9	183	20	271	84	717
	Bt2	HT 4B	64.3	16.1	4.91	1.21	1.04	2.26	1.87	0.67	0.02	0.01	0.01	8.04	100.5	12	170	15	232	94	627
	Bt2	HT 3B	63.8	16.3	5.19	1.32	1	2.32	1.81	0.66	0.02	< 0.01	< 0.01	8.14	100.6	11	164	15	234	89	530
	Bt2	HT 2B	62.2	16.3	5.55	1.54	0.99	2.23	1.85	0.69	0.02	< 0.01	0.02	8.41	99.8	12	160	19	246	96	630
	Bt2	HT 1B	62.4	16.7	5.14	1.43	1.44	2.39	1.65	0.63	0.02	< 0.01	< 0.01	8.04	99.9	11	173	24	299	88	594
5	A	HT 16B	61.3	17	4.79	1.37	0.73	1.95	2.45	0.63	0.02	0.01	0.02	9.62	99.9	11	151	22	181	124	607
	ABss	HT 15B	65	15.6	3.99	1.16	0.82	2.14	2.42	0.72	0.02	< 0.01	0.01	7.86	99.8	11	155	23	214	117	713
	Btss	HT 14B	64.6	15.6	4.52	1.31	0.8	2.1	2.39	0.73	0.05	< 0.01	< 0.01	7.47	99.7	11	144	23	202	110	689
	Bw	HT 13B	62.7	16.3	4.72	1.4	0.61	1.83	2.51	0.71	0.03	< 0.01	0.01	8.98	99.8	11	135	20	170	125	600
	Bw	HT 12B	62.6	16.6	4.67	1.39	0.62	1.85	2.47	0.73	0.03	< 0.01	< 0.01	8.98	99.9	11	137	20	175	125	603
7	A	HT 8.12	63.9	15.3	3.34	1.57	0.83	1.85	2.6	0.65	0.09	0.02	0.01	9.54	99.7	10	122	20	189	102	804
	A	HT 8.11	58.6	15.5	3.32	1.41	1.07	1.99	2.64	0.61	0.08	0.02	< 0.01	14.3	99.6	11	174	18	243	105	787
	Bw	HT 8.10	62.9	17.3	3.96	1.31	0.88	2.12	2.15	0.72	0.02	0.01	0.02	8.67	100.1	11	152	17	234	110	764
	Bw	HT 8.9	62.5	17.5	4.18	1.32	1.01	2.16	2.08	0.71	0.02	< 0.01	0.01	8.85	100.4	11	156	18	243	109	636
	CB	HT 8.8	65.7	16.1	3.79	1.29	1.17	2.46	2.17	0.64	0.03	0.03	0.03	6.46	99.9	9	166	22	278	91	687
7	A	M 2.12B	67.2	15.1	3.82	1.32	1.06	2.34	1.69	0.6	0.02	< 0.01	0.01	6.49	99.7	13	193	19	242	91	769
	Bw1	M 2.11B	66.9	15.3	4.42	1.3	1.25	2.46	1.85	0.52	0.03	< 0.01	0.02	5.51	99.7	13	196	30	270	88	913

Appendix A: Geochemical Data

Category	Horizon	Sample ID	SiO2 %	Al2O3 %	Fe2O3 %	MgO %	CaO %	Na2O %	K2O %	TiO2 %	P2O5 %	MnO %	Cr2O3 %	LOI %	Sum %	Nb ppm	Zr ppm	Y ppm	Sr ppm	Rb ppm	Ba ppm
	Bw1	M 2.10B	66.9	15.6	4.39	1.4	1.44	2.46	1.84	0.54	0.05	< 0.01	< 0.01	5.47	100.2	13	195	33	272	88	716
	Bw2	M 2.9B	66	15.8	4.76	1.55	1.37	2.33	1.83	0.56	0.08	< 0.01	0.01	5.76	100.1	13	188	36	255	95	714
	Bw2	M 2.7B	65.9	16.3	4.68	1.66	1.23	2.29	1.68	0.56	0.07	< 0.01	< 0.01	5.94	100.4	13	192	29	245	87	656
	Bw2	M 2.6B	65.2	16.2	4.78	1.65	1.39	2.29	1.66	0.55	0.07	< 0.01	0.01	6.11	100	13	200	30	251	87	705
	Bw3	M 2.5B	64.7	16.2	4.75	1.61	1.48	2.24	1.66	0.56	0.06	0.02	0.01	6.58	99.9	14	207	29	253	87	752
	Bw3	M 2.4B	64.4	16.2	4.64	1.6	1.4	2.25	1.67	0.56	0.07	0.01	< 0.01	6.75	99.6	13	210	29	260	87	825
	Bw3	M 2.3B	64.5	16.1	4.67	1.61	1.17	2.16	1.81	0.6	0.07	0.01	< 0.01	6.72	99.5	12	181	28	246	93	897
	Bw3	M 2.2B	63.9	16.1	4.6	1.62	1.14	2.15	1.8	0.58	0.07	0.01	0.01	7.37	99.5	12	181	26	252	88	917
7	Bt	M 2.39B	63.9	16.4	4.94	1.54	1.4	2.47	2.05	0.61	0.08	0.02	0.01	6.41	99.9	12	174	23	315	105	787
	Bt	M 2.38B	61.3	17.2	5.3	1.8	1.68	2.38	1.57	0.54	0.1	0.02	< 0.01	8.08	99.9	10	173	21	275	83	706
	Bw1	M 2.37B	68.5	14.7	4.03	1.02	1.29	2.58	2.05	0.64	0.04	0.01	< 0.01	5.24	100.1	11	170	21	267	99	859
	Bw1	M 2.36B	69.1	14.4	3.95	1.01	1.25	2.56	2.07	0.63	0.04	0.02	0.02	5.18	100.2	11	168	22	260	98	845
	Bw2	M 2.35B	68.3	14.4	3.93	0.98	1.3	2.61	2.1	0.63	0.04	0.01	< 0.01	5.7	100	11	174	21	276	98	886
	Bw2	M 2.34B	68.1	14.5	3.95	0.95	1.28	2.57	2.14	0.64	0.05	0.01	0.02	5.66	99.9	11	173	19	271	100	765
	Bw3	M 2.33B	68.5	14.6	4.07	1.12	1.68	2.65	2.15	0.6	0.11	< 0.01	0.02	4.72	100.3	9	169	24	294	89	788
	Bw3	M 2.32B	66.6	15	4.6	1.34	1.54	2.58	2.17	0.62	0.12	< 0.01	0.01	5.49	100.2	10	162	24	270	92	837
	Bw3	M 2.31B	66.6	14.7	4.52	1.25	1.38	2.54	2.24	0.63	0.12	0.01	0.02	6.13	100.2	10	165	23	267	94	753
	Bw4	M 2.30B	67.1	14.8	4.15	1.26	1.45	2.61	2.21	0.63	0.13	0.01	0.02	5.78	100.1	10	167	23	272	89	758
	Bw4	M 2.29B	67.3	14.8	4.16	1.24	1.41	2.63	2.3	0.62	0.11	0.02	0.01	5.44	100	10	171	23	275	92	809
8	Bw1	T 1.16	68.5	14.1	4.47	1.21	1.49	2.55	2.19	0.6	0.1	0.02	< 0.01	4.76	100.1	9	158	19	292	85	859
	Bw1	T 1.15	69.6	13.7	3.84	1.06	1.54	2.66	2.15	0.56	0.1	0.02	0.02	4.21	99.5	9	159	19	300	78	831
	Bw1	T 1.14	68.9	13.7	4.42	1.12	1.38	2.59	2.26	0.6	0.08	0.01	< 0.01	4.77	99.9	9	160	18	280	95	815
	Bw2	T 1.13	66.9	13.9	5.58	1.38	1.11	2.33	2.42	0.64	0.1	0.02	0.02	5.58	100	9	152	21	244	114	805
	Bw2	T 1.12	65.2	14.7	5.89	1.57	1.41	2.47	2.09	0.62	0.14	0.07	0.02	5.94	100.1	9	143	23	276	83	840
8	Bw1	T1.28	63.6	15.5	5.55	1.71	1.26	2.36	2.96	0.7	0.17	0.03	0.02	5.66	99.5	---	---	---	---	---	---
8	Bw2	T1.32	67.5	14.7	3.78	1.01	1.02	2.6	2.63	0.65	0.03	< 0.01	0.03	5.93	99.9	---	---	---	---	---	---
9	A	SET2-19	65.8	14.3	2.33	0.79	0.77	2.15	2.28	0.61	0.01	<0.01	0.01	9.9	99.1	12	183	26	213	96	1010
	A	SET2-18	67	15.5	2.97	0.94	0.75	2.17	2.26	0.68	0.02	<0.01	0.01	6.5	99	15	172	27	216	121	980
	Bw1	SET2-17	67.4	15.8	3.14	1.01	0.81	2.16	2.24	0.7	0.02	<0.01	0.01	5.3	98.7	17	173	29	226	124	950

	Bw1	SET2-16	67	15.9	3.29	1.05	0.84	2.16	2.23	0.7	0.03	<0.01	0.01	5	98.4	18	179	30	226	122	860
	Bw2	SET2-15	67.2	16	3.33	1.13	0.9	2.19	2.24	0.69	0.03	<0.01	0.01	4.95	98.9	15	175	27	227	120	1030
	Bw3	SET2-14	66.6	17.1	3.12	1.45	0.94	2.08	2.26	0.73	0.09	<0.01	<0.01	4.7	99.3	15	161	26	215	96	750
	Bw4	SET2-11	68.1	15.9	3.1	1.33	1.2	2.44	2.01	0.64	0.06	<0.01	0.01	3.65	98.6	15	174	25	265	85	730
	Bw4	SET2-10	67.6	16.3	3.39	1.39	1.16	2.41	2.11	0.67	0.07	<0.01	0.01	3.95	99.2	15	176	24	254	93	710
	Bw4	SET2-9	67.7	16.2	3.4	1.4	1.17	2.41	2.09	0.67	0.07	<0.01	0.01	3.95	99.2	16	182	25	255	93	750

bh= burial horizon
p= pond deposit

Appendix B: Thin Section Descriptions

Category	Sample ID	Depth (cm)	Horizon	Lithology	coarse:fine	Grain Size	Roundness	Sorting	Composition	Matrix Colour	Iron Impregnation	b-fabric	Illuvial Features	Redoximorphic Features	Notes
1	Coulee 11	18.5	Ag	fine to vf sand, silt, clay	40:60	vf sand, silt, clay	subrounded to subangular to angular	moderately poor	qtz (monocrystalline and microcrystalline), fsp, muscovite, opaques (OM)	dark grey	none observed	stipple-speckled to mosaic-speckled, some unistriations; common granostriation	none observed	possible ferruginous redoximorphic features	burrow, root trace
	Coulee 10	35	Bg1	fine to vf sand, silt, clay	40:60	vf sand, silt, clay	subangular to subrounded	moderately poor	qtz (monocrystalline and microcrystalline), fsp, muscovite, opaques (OM)	dark grey	none observed	stipple speckled to mosaic-speckled, to faintly unistriated	none observed	none observed	completely bioturbated, root traces
	Coulee 8	58	burial	some fine sand, mostly vf sand, silt, clay	40:60	vf sand, silt, clay	subangular to sunrounded	moderately well	qtz, fsp, muscovite, opaques (OM)	dark grey	none observed	mosaic-speckled with zones of well-develpped unistriated b-fabric; uncommon granostriations,	Uncommon clay coatings in groundmass	none observed	burrow? Root traces
1	Coal 1-4	0-21	Ag	mudstone	25:75	vf sand, silt, clay	subangular to subrounded	moderately	qtz (monocrystalline and microcrystalline), fsp, muscovite, opaques (OM), amber (rare)	dark grey	none observed	stipple-speckled to mosaic speckled	Common, weakly developed clay coatings along root traces and in groundmass	Rare, weakly developed, ferruginous redoximorphic features	burrow? Root trace
	Coal 1-3	21-38	BAg	sandy mudstone	25:75	vf sand, silt, clay	subangular to subrounded	moderately	qtz (monocrystalline and microcrystalline), fsp, muscovite, opaques (OM)	Greyish brown	none observed	stipple-speckled to mosaic speckled; rare granostraition	Common, weakly developed clay coatings along root traces and in groundmass	none observed	root traces
	Coal 1-2	38-66	Bg	sandy mudstone	30:75	fine sand, vf sand, silt, clay, with some fs	subangular to subrounded	moderately	qtz (monocrystalline and microcrystalline), fsp, muscovite, opaques (OM)	Dark greyish brown	none observed	mosaic speckled to stipple-speckled; rare granostriation	Common, weakly developed clay coatings along root traces and in groundmass	none observed	root traces
1	SET 5-10	33	A	mudstone	10:90	silt, clay	angular	well	qtz, weathered fsp, O.M	Dark brown	none observed	mosaic speckled to unistriated; weak granostriation.	uncommon, weakly developed clay coatings in groundmass	Rare, small ferruginous redoximorphic feature	root traces
	SET 5-8	58	Bg1	siltstone	50:50	silt, sand, clay	angular	well	qtz, weathered fsp, muscovite, O.M, but less than SET 5-10	Green-grey	none observed	stipple-speckled to mosaic speckled to faintly unistriated	none observed	Rare, small ferruginous redoximorphic feature	root traces (hand sample), thn section
	SET 5-5	94	Bg2	sandy siltstone	30:70	silt, sand, clay	angular	moderate	qtz, weathered fsp, dispersed O.M throughout, but less than SET 5-10	light grey	none observed	mosaic speckled; rare granostriations	Rare, well-developed clay coatings along root traces	none observed	rare root traces (hand sample), maybe in TS too; few, small papules
1	SET 9-2	17.5	Ag	mudstone	15:85	vf sand, silt, clay	subangular to subrounded	moderately well	mostly qtz, some fsp, minor muscovite, opaques (OM)	dark grey	none observed	well-developed mosaic-speckled	uncommon, weakly developed clay coatings in groundmass	none observed	root traces
	SET 9-1	59	Bg	mudstone	20:80	vf sand, silt, clay	subangular	moderately	mostly qtz, some fsp, minor muscovite, fairly rich opaques (OM), one lrg piece of amber (coarse)	brown	none observed	stipple-speckled to weakly developed mosaic-speckled to faintly unistriated	uncommon, weakly developed clay coatings in groundmass	none observed	possible burrows or root traces; one papule

Appendix B: Thin Section Descriptions

Category	Sample ID	Depth (cm)	Horizon	Lithology	coarse:fine	Grain Size	Roundness	Sorting	Composition	Matrix Colour	Iron Impregnation	b-fabric	Illuvial Features	Redoximor-phic Features	Notes
1	SET 11-6*	27-44	Ag	mudstone	20:80	f.u to vf sand, silt, clay	subangular to subrounded	moderately	mostly qtz, some fsp, minor muscovite, opaques (OM)	dark grey	none observed	stipple-speckled	Uncommon, weakly developed clay coatings in groundmass	none observed	few small papules, one large
	SET 11-5*	44-73	Bg	mudstone	15:85	vf sand, silt, clay	subangular to subrounded	moderately well	mostly qtz, some fsp, minor muscovite, opaques (OM)	white	none observed	Stipple speckled to mosaic speckled	Common, weakly developed clay coatings in groundmass	Uncommon ferruginous redoximorphic features around root traces; weak iron accumulation in groundmass	
	SET 11-3*	76-109	2ABg	mudstone	20:80	few M.L grains, mostly fine and vf sand, silt, clay	angular to subrounded	poorly	mostly qtz, some fsp, minor muscovite, opaques (OM). Some OM coatings in chip edges	light grey	none observed	stipple speckled to unistriated	Common well-developed clay coatings in groundmass	Rare ferruginous redoximorphic features along root trace	
	11-1*	109-196	2Bg	mudstone	2:98	vf sand, silt, clay	subangular to subrounded	well	mostly qtz, some fsp, minor muscovite, opaques (OM), one piece of amber (medium). OM is aligned	grey	none observed	very well developed mosaic-speckled	Common well-developed clay coatings in groundmass	none observed	
1	HT4.13	8	Bg1	silty mudstone	20:80	few FL, mostly vf sand, silt, clay	angular to subrounded	moderate	dominantly Qtz (mono and microcrystalline), some feldspar, msc, OM (mostly blocky fragments and some elongate strands), amber	light greyish-brown	none observed	stipple-speckled to mosaic speckled to unistriated; rare granostriation.	none observed	depletion redoximorphic features with accumulation rims and iron accumulation redoximorphic feature (orange in normal light; located within depletion redoximorphic feature-everything drained towards the centre)	papules
	HT4.12	38	Bg2	silty mudstone	25:75	few FL, mostly vf sand, silt, clay	angular to subangular	moderate	dominantly Qtz (mono and microcrystalline), some feldspar, msc, OM (few elongate strands), amber	light green-grey	none observed	stipple speckled to mosaic speckled	uncommon, weakly developed clay coatings in groundmass	depletion redoximorphic features , Fe accumulation redoximorphic features more abundant than in 4.7	root traces?
2a	SET 7-12*	0-15	Ag	Organic-rich mudstone	15:85	fine to vf sand, silt, clay	subangular	well	qtz, weathered fsp, minor muscovite, abundant opaques	Greyish brown	none observed	mosaic-speckled to unistriated, with stipple speckled in some places	Common, weakly developed clay coatings in groundmass	none observed	possible root traces
	SET 7-11*	15-41	Bg1	mudstone	15:85	vf sand, silt, clay	subangular to subrounded	moderately well	mostly qtz, some fsp, minor muscovite, less abundant than SET 7-12, but still relatively common opaques (OM)	light grey	none observed	unistriated to mosaic-speckled, to unistriated	Common, moderately developed clay coatings in groundmass	none observed	

Appendix B: Thin Section Descriptions

Category	Sample ID	Depth (cm)	Horizon	Lithology	coarse:fine	Grain Size	Roundness	Sorting	Composition	Matrix Colour	Iron Impregnation	b-fabric	Illuvial Features	Redoximorphic Features	Notes
	SET 7-10*	41-63	Bg2	mudstone	10:90	vf sand, silt, clay	subangular	well	mostly qtz, some fsp, minor muscovite, more abundant opaques (OM) than SET 7-11, amber (rare) (2 grains, M.U)	light grey	none observed	unistriated with zones of stipple-speckled between the striations	Common, moderately developed clay coatings in groundmass and along root traces	none observed	burrow, one large papule
	SET 7-9*	63-76	BC	mudstone	10:90 but up to 35:65 in "burrows or r.t"	vf sand, silt, clay	subangular to subrounded	moderate to moderately well	mostly qtz, some fsp, minor muscovite, abundant opaques (OM) (may explain why browner than overlying unit)	light brownish grey	none observed	stipple-speckled to mosaic speckled	Common, weakly developed clay coatings in groundmass and along root traces	none observed	possible burrows or root traces., few small papules
2a	M9	22	Ag	mudstone with dispersed organic matter	10:90	vf sand, silt, clay	subangular to subrounded	moderate	lots of subparallel OM, amber, qtz, fsp	dark brownish-grey	none observed	mosaic-speckled; rare granostriation	uncommon, weakly developed clay coatings in groundmass	none observed	n/a
	M8	41	Bg1	mudstone	10:90 in places, 30:70 in others	some FL, vf sand, silt, clay	angular to subrounded	moderate to moderately poor	some OM (much less abundant than above), amber, qtz, fsp	green-grey	none observed	stipple-speckled to faintly mosaic speckled	none observed	depletion redoximorphic features, papule (one, small)	burrows
	M5	68	Bg2	claystone	2: 98	vf sand, silt, clay	angular to subrounded	moderately well	some OM (~ same as M8), amber, qtz, fsp	black	none observed	very well developed mosaic speckled	iron hypocoating along void/ pore	none observed	n/a
	M4	77	Bg3	mudstone	10:90	vf sand, silt, clay	angular to subrounded	moderate	some OM (in thin elongate strands), amber, qtz, fsp, msc	dark brown	none observed	stipple-speckled to faintly mosaic speckled	uncommon, weakly developed clay coatings in groundmass; uncommon iron coatings on grains, sometimes forming bridges	none observed	root traces?
	M3	91	Bg4	mudstone	10:90	vf sand, silt, clay	angular to subrounded	moderate	some OM (in thin elongate strands), amber, qtz, fsp, msc	black	none observed	well developed mosaic speckled to faintly unistriated	rare, weakly developed clay coatings in groundmass		root traces?
	M1	138	Bg5	mudstone	40:60	some FL, vf sand, silt, clay	angular to subrounded	moderate	some OM (in blocky pieces), amber, qtz, fsp, msc	black	none observed	mosaic speckled	none observed		few small papules
2a	HT1.5	10	Bg? Ag?	very fine sandstone	30:70	Some ML, fine and vf sand, silt, clay	subangular to subrounded	poor	Qtz (mono and microcrystalline), feldspar, msc, OM (no longer elongate strands of OM in 1.2 and 1.3, but in coarse blocky fragments), amber	Greyish brown	none observed	stipple speckled	rare, weakly developed clay coatings in groundmass	depletion redoximorphic features	few small papules

Appendix B: Thin Section Descriptions

Category	Sample ID	Depth (cm)	Horizon	Lithology	coarse:fine	Grain Size	Roundness	Sorting	Composition	Matrix Colour	Iron Impregnation	b-fabric	Illuvial Features	Redoximor-phic Features	Notes
	HT1.3	50	Bg1	very fine sandstone	30:70	Some ML, fine and vf sand, silt, clay	angular to subangular	poor	Qtz (mono and microcrystalline), feldspar, msc, OM (less than 1.2)	brown	none observed	unistriated to mosaic speckled	none observed	depletion redoximorphic features	root traces
	HT1.2	75	Bg2	very fine sandstone	30:70	Some ML, fine and vf sand, silt, clay	angular to subangular	poor	Qtz (mono and microcrystalline), feldspar, msc, OM	medium brown	none observed	mosaic specled to unistriated in places	uncommon, weakly developed clay coatings along root traces	few depletion redoximorphic features	root traces, one papule
2a	HT1.42	5	Ag	mudstone	10:90	few FU, mostly vf, silt, clay	angular to subangular to subrounded	moderate	dominantly Qtz (mono and microcrystalline), some feldspar, msc, OM (elongate strands), amber	light greyish-brown	none observed	mosaic speckled to faintly unistriated; uncommon granostriation	uncommon, weakly developed clay coatings along root traces	Abundant Depletion redoximorphic features with accumulation rims and rare ferruginous redoximorphic features in groundmass	root traces, one papule
	HT1.41	15	Bg1	mudstone	10:90	few FU, mostly vf, silt, clay	sunangular to rounded	moderate	dominantly Qtz (mono and microcrystalline), some feldspar, msc, OM (elongate strands; less abundant than 1.42), amber	greyish-brown	none observed	well-developed mosaic-speckled to unistriated; Very rare granostriation	rare, weakly developed clay coatings along root traces	Smaller depletion redoximorphic features than above, less common.	root traces, one small papule
	HT1.39	45	Bg2	muddy siltstone	10:90	FL, vf, silt, clay	angular to subrounded	moderately poor	dominantly Qtz (mono and microcrystalline), some feldspar, msc, OM (blocky fragments with some elongate strands), amber (more abundant than above)	light grey	none observed	well-developed mosaic speckled to unistriated	uncommon, weakly developed clay coatings along root traces	none observed	n/a
	HT1.38	60	Bg3	sandy siltstone	10:90	few FU, FL, mostly vf, silt, clay	angular to subrounded	moderately poor	dominantly Qtz (mono and microcrystalline), some feldspar, msc, OM (blocky fragments and abundant elongate strands), amber	grey	none observed	very-well developed mosaic speckled; rare granostriations	rare, weakly developed clay coatings along root traces	few small ferruginous redoximorphic features	root traces
2b	HT4.10	53	A	mudstone	15:85	vf sand, silt, clay	angular to subangular	moderate to moderately well	dominantly Qtz (mono and microcrystalline), some feldspar, msc, OM (elongate strands, more abundant than above), amber	light brownish grey	none observed	Stipple-speckled to well-developed mosaic-speckled	Common, weakly developed clay coatings in groundmass	Uncommon redoximorphic features	root traces?
	HT4.9	23	Ag	silty mudstone	10:90	few FL, mostly vf sand, silt, clay	angular to subangular	moderately well	dominantly Qtz (mono and microcrystalline), some feldspar, OM (elongate strands, more abundant than 4.12, less abundant than 4.10), amber	grey	none observed	Well develped mosaic speckeld	Common, moderately developed clay coatings in groundmass	Common, small ferruginous redoximorphic features along root traces and ped? Surfaces	possible root traces; possible peds subangular blocky

Appendix B: Thin Section Descriptions

Category	Sample ID	Depth (cm)	Horizon	Lithology	coarse:fine	Grain Size	Roundness	Sorting	Composition	Matrix Colour	Iron Impregnation	b-fabric	Illuvial Features	Redoximorphic Features	Notes
	HT4.7	49	Bg1	silty mudstone	3:97	vf sand, silt, clay	subangular to subrounded	well	dominantly Qtz (mono and microcrystalline), some feldspar, OM (elongate strands, more abundant than 4.12, same as 4.9), amber	grey	none observed	Stipple-speckled to weakly mosaic speckled	Uncommon, well-developed clay coatings along root traces; rare, weakly developed clay coatings in groundmass	Common, small ferruginous redoximorphic features along root traces and ped? Surfaces	root traces
	HT4.5	74	Bg2	mudstone	20:80	some FL, vf sand, silt, clay	angular to subangular	moderate	dominantly Qtz (mono and microcrystalline), some feldspar, msc, OM (elongate strands, more abundant than 4.12, same as 4.9), amber	dark grey	none observed	Well-developed mosaic speckled	Very common, moderately developed clay coatings in groundmass	Uncommon ferruginous redoximorphic features along root traces	root traces
	HT4.2	124	Bg3	mudstone	20:80	some FL, vf sand, silt, clay	angular to subangular	moderately well	dominantly Qtz (mono and microcrystalline), some feldspar, OM, rare msc (elongate strands, less abundant than 4.9), amber	dark grey	none observed	Well-developed mosaic speckled	Very common, moderately developed clay coatings in groundmass and along root traces	Uncommon ferruginous redoximorphic features along root traces and in groundmass	root traces
2b	SET2-6	30	Bg1	mudstone	5:95 but up to 30:70 in the burrow/r.t	f.l, v.f sand, silt, clay	subangular	well sorted in places to, moderately sorted in others	qtz (monocrystalline and microcrystalline), fsp, muscovite, opaques (OM)-rare	Green-grey	none observed	mostly stipple-speckled with rare zones of mosaic speckled	none observed	Rare ferruginous and depletion redoximorphic features	possible sand filled burrow/ root traces
	SET2-5	60	Bg2	mudstone	2:98	few clasts of f.l sand, mostly v.f sand, silt, clay	subangular to subrounded	well sorted	qtz (monocrystalline and microcrystalline), rare fsp (if any) and muscovite, opaques (OM)-rare	Green-grey	none observed	mosaic-speckled to faintly unistrial	none observed	rare, weakly developed ferruginous redoximorphic features, very rare siderite nodules	
	SET2-3	105	Bg3	mudstone	2:98	few v.f sand clasts, silt, clay	subrounded	very well sorted	dominantly qtz, some msc, opaques (OM)-rare	Brown (base) to green-grey (top)	none observed	mosaic-speckled to faintly unistriated	none observed	rare, weakly developed ferruginous redoximorphic features. Same as above	patterns of impregnation may be due to bioturbation
	SET2-1	135	Bg3	mudstone	2:98	few v.f sand clasts, silt, clay	subrounded	very well sorted	dominantly qtz, some msc, opaques (OM)- abundant	Brown (base) to green-grey (top)	none observed	very well-developed unistriated (aligned with organic matter-possible shear) to mosaic speckled	Rare weakly developed clay coatings along root traces	redoximorphic features	patterns of impregnation may be due to bioturbation
2b	SET 7-7*	0-5	A	mudstone	<1:99	rare vf sand, silt, clay	rounded	very well	qtz, opaques (OM)	dark brown	none observed	well-developed reticulate	none observed	none observed	possible burrows or root traces.

Appendix B: Thin Section Descriptions

Category	Sample ID	Depth (cm)	Horizon	Lithology	coarse:fine	Grain Size	Roundness	Sorting	Composition	Matrix Colour	Iron Impregnation	b-fabric	Illuvial Features	Redoximorphic Features	Notes
	SET 7-6*	5-21	Bg1	mudstone	<1:99	rare vf sand, silt, clay	subrounded	very well	qtz, opaques (OM)	light grey	none observed	unistrial to reticulate in places	none observed	none observed	possible burrows or root traces. (root traces seen in hand sample)
	SET 7-5*	21-67	Bg2	mudstone	2:99	vf sand, silt, clay	subrounded	very well	qtz, opaques (OM)	green-grey	none observed	well-developed reticulate to stipple-speckled.	possible coatings along root trace or ped?	faint redoximorphic features	possible burrows or root traces. (root traces seen in hand sample)
	SET 7-3*	67-90	CBg	siltstone	10:90 to 40:60 in places	vf sand, silt, clay	subangular	moderately	qtz (monocrystalline and microcrystalline), fsp, muscovite, opaques (OM)	grey	none observed	mosaic-speckled to unistriated; rare Granostriations	Uncommon, moderately developped clay coatings in groundmass	none observed	coarser stuff could be part of burial horizon that choked underlying profile- both sand and mud deposited at the same time.
2c	SET-5	0-16	ABg	mudstone	15:85	vf sand, silt, clay	subangular	well	qtz, msc, fsp, disp OM	Dark brown	none observed	mosaic-speckled to unistriated	uncommon, weakly developed clay coatings in groundmass	none observed	
	SET-4	16-23	Bg	claystone	0:100	clay,silt	n/a	very well	?	Dark grey	none observed	stipple-speckled to mosaic speckled	none observed	Fe accumulation in groundmass	
	SET-3	23-31	CBg	claystone	0:100	clay, silt filling in channel	larger grains subangular	very well	qtz, msc, ?, disp OM		none observed	very well-developed unistriated	none observed	Fe accumulation in groundmass	root traces
3	Tree 3*	21-37	Ag	sandstone	50:50	fine (FL) sand, clay	subangular to subrounded	well	qtz (monocrystalline and microcrystalline), fsp, muscovite, opaques (OM)	White	none observed	stipple-speckled; common granostriation	Very common, well-developed clay coatings; very common iron coatings on grains, sometimes forming bridges/pendants/link cappings	none observed	n/a
	Tree 2*	37-53	Bg	sandstone	50:50	medium sand (MU), fine sand, siltclay	subangular	well	qtz (monocrystalline and microcrystalline), fsp, muscovite, opaques (OM)	White	none observed	unistriated to mosaic-speckled; common granostriation	Very common, well-developed clay coatings; common iron coatings on grains, sometimes forming bridges/pendants/link cappings	none observed	n/a
3	SET 4-3	10	A	wacke	20:80	sand, silt, clay	angular	moderate	qtz, weathered fsp, O.M	dark greyish brown	none observed	mosaic-speckled	Uncommon clay coatings in groundmass	none observed	root traces

Appendix B: Thin Section Descriptions

Category	Sample ID	Depth (cm)	Horizon	Lithology	coarse:fine	Grain Size	Roundness	Sorting	Composition	Matrix Colour	Iron Impregnation	b-fabric	Illuvial Features	Redoximorphic Features	Notes
	SET 4-2	24	Bg1	wacke	20:85	sand, silt, clay	angular	moderate	qtz, weathered fsp, O.M (less abundant than above)	dark greyish brown	none observed	mosaic-speckled to faintly reticulate	Uncommon clay coatings in groundmass	none observed	n/a
	SET 4-1	36	Bg2	wacke	20:80	sand, silt, clay	angular	moderate	qtz, weathered fsp, O.M (less abundant than SET4-3)	dark greyish brown	none observed	mosaic-speckled to faintly reticulate	rare clay coatings in groundmass	small accumulation redoximorphic feature	n/a
4	HT27B*	6	A	mudstone with dispersed organic matter	1:99 in some places, 20:80 in others	FL, vf sand, silt, clay	angular to subrounded	poor	Qtz, fsp, msc, amber, OM (elongate and blocky pieces)	Dark olive-grey	moderate with a few small clouds of weak	stipple speckled to mosaic speckled; rare granostriations	Uncommon, weakly developed clay coatings in groundmass and along root traces; rare iron hypocaotings around root traces	none observed	root traces, bioturbation; papules
	HT25B*	34	Bw	mudstone	100	silt, clay	subangular to subrounded	well	Qtz, fsp, msc, disp OM	Olive-grey	Large clouds of weak surrounded by rims of moderate	stipple speckled to mosaic speckled	Uncommon, weakly developed clay coatings in groundmass	none observed	n/a
	HT22B*	69	Bg1	mudstone	1:99	vf sand, silt, clay	subangular to subrounded	well	Qtz, fsp, msc, disp OM (more abundant than HT25B, elongate and aligned)	black	moderate iron impregantion surrounding depletion redoximorphic features	mosaic speckled to unistrated	Common, weakly developed clay coatings in groundmass	common redoximorphic features	root traces?
	HT19B*	106	Bg2	mudstone	1:99	vf sand, silt, clay	subangular to subrounded	well	Qtz, fsp, msc, rare disp OM	Olive-grey	none observed	mosaic speckled	Common, weakly developed clay coatings in groundmass	common redoximorphic features	Common sphaerosiderite, 20-30 um
	HT17B*	129	Cg	mudstone	<1:99	rare vf sand, silt clay	subangular	very well	lrgr grains are qtz, rest is clay. Lots of disp OM, some amber.	Black	none observed	stipple-speckled to mosaic speckled; rare granostriation	Common, weakly developed clay coatings in groundmass	rare redoximorphic features	papule

Appendix B: Thin Section Descriptions

Category	Sample ID	Depth (cm)	Horizon	Lithology	coarse:fine	Grain Size	Roundness	Sorting	Composition	Matrix Colour	Iron Impregnation	b-fabric	Illuvial Features	Redoximorphic Features	Notes
4	HT38B	40	Bw1	sandy mudstone	15:85	vf sand, silt, clay	subangular to subrounded	moderate	Qtz, fsp, msc, rare disp OM	olive grey	weak centre of chip with a rim that grades from strong on one side of the chip to moderate on the other. Two small patches of clay accumulation, possibly with Fe or OM.	stipple speckled, few small clay coatings		depletion redoximorphic features	papule
	HT36B	67	Bw2	sandy mudstone	2:98 in some places, 15:85 in others	vf sand, silt, clay	subangular to subrounded	moderate	Qtz, fsp, msc, rare disp OM	transitional grey green	dominantly weak in large clouds in centres of chips, thin rims of moderately weak around edges of chips	stipple speckled, few small clay coatings		depletion redoximorphic features	
	HT34B	94	Bw3	silty mudstone to mudstone	2:98 in some places, 30:70 in others	vf sand, silt, clay	subangular to subrounded	moderately poor	Qtz, fsp, msc, rare disp OM	grey	weak to moderate. Weak in zones with coarser grains and in depletion redoximorphic features. Depletion redoximorphic features have accumulation rims of stronger impregntion	stipple speckled	rare clay coatings	depletion redoximorphic features	papule
5	HT16B*	4.5	A	mudstone	2:98	some vf sand, silt, clay	angular to subrounded	well	Qtz, fsp, amber, abundant OM (elongate strands, aligned)	Dark greyish brown	Weak to moderate in subparallel, linear zones	mosaic speckled	Uncommon, weakly developed clay coatings in groundmass and along root traces; Rare iron hypocoatings alon root traces	none observed	root traces
	HT15B*	6	ABss	mudstone with dispersed organic matter	5:95	vf sand, silt, clay	mostly angular to some subrounded	well	Qtz, fsp, amber (some large (coarse) pieces), abundant OM (but not as much as HT 16; blocky to somewhat elongate, random)	light brownish grey	Weak to moderate in irregular clouds	stipple speckled to mosaic speckled; Uncommon granostriation	Uncommon, weakly developed clay coatings in groundmass and along root traces; Rare iron hypocoatings alon root traces	none observed	root traces; well developed slickensides

Appendix B: Thin Section Descriptions

Category	Sample ID	Depth (cm)	Horizon	Lithology	coarse:fine	Grain Size	Roundness	Sorting	Composition	Matrix Colour	Iron Impregnation	b-fabric	Illuvial Features	Redoximorphic Features	Notes
	HT14B*	13.5	Btss	mudstone	2:98	some vf sand, silt, clay	mostly angular to some subrounded	well	Qtz, fsp, amber (some large (coarse) pieces), some OM (blocky to somewhat elongate, random)	Very dark greyish brown	weak with narrow, irrugular zones of moderate	Stipple speckled to mosaic speckled	Rare, weakly developed clay coatings in groundmass and along root traces; Uncommon iron hypocoatings alon root traces	none observed	root traces
	HT12B*	24	Bw	mudstone	2:98	some vf sand, silt, clay	mostly angular to some subrounded	well	Qtz, fsp, amber (some large (coarse) pieces), OM (more abundant than HT14B; elongate, aligned)	Very dark greyish brown	Moderate in irregular, elongate zones separating clouds of weak	Mosaic speckled	Uncommon clay coatinga along root traces	none observed	slickensides in hand sample
5	HT11B	30	2AB	mudstone with dispersed organic matter	8:92	FL, vf sand, silt, clay	angular to subrounded	moderate	Qtz, fsp, msc amber (some large (coarse) pieces), OM (elongate)	Dark greyish-brown	strong to very strong	mosaic speckled to unistrated; Uncommon granostriation	Common, weakly developed clay coatings; Fe accumulation		n/a
	HT9B	45	2Bt	mudstone	15:85	FL, vf sand, silt, clay	angular to subrounded	poor	Qtz, fsp, msc, rare disp OM	grey	matrix moderately strong to strong with elongate clouds of weak	well developed mosaic speckled	Uncommon clay coatings		some bioturbation; papule; slickensides in handsample
	HT7B	60	2Bw1	very fine sandstone	50:50	a few ML grains, fine, vf sand, silt, clay	angular to subrounded	poor	Qtz, fsp, msc, amber, OM (elongate and blocky pieces)	brown	moderate with small ovals of moderate randomly dispersed throughout slide.	stipple speckled to faintly mosaic speckled; very rare granostriations.	some Fe accumulation		root traces?
	HT6B	75	2Bw2	very fine sandstone	50:50	FU, vf sand, silt, clay	angular to subrounded	poor	Qtz, fsp, msc, amber, OM (elongate and blocky pieces)	brown	moderate with small ovals of moderate randomly dispersed throughout slide.	stipple speckled to faintly mosaic speckled; very rare granostriation	Uncommon clay coatings	uncommon redoximorphic features	root traces?

Appendix B: Thin Section Descriptions

Category	Sample ID	Depth (cm)	Horizon	Lithology	coarse:fine	Grain Size	Roundness	Sorting	Composition	Matrix Colour	Iron Impregnation	b-fabric	Illuvial Features	Redoximorphic Features	Notes
	HT2B	128	2Bt2	mudstone	20:80	FU, vf sand, silt, clay	sunangular to subrounded	moderate	Qtz, fsp, rare amber, rare disp OM	medium olive	moderate to strong	well developed mosaic speckled	Common, well developed clay coatings	Depletion redoximorphic features	
7	HT8.11	15	A	mudstone	8:92	vf sand, silt, clay	angular to subrounded	well	Dispersed OM, large and abundant pieces of amber. Matrix is quartz, msc, fsp	dark brownish-grey	weak to strong	stipple speckled			very bioturbated
	HT8.9	39	Bw	mudstone	8:92	vf sand, silt, clay	angular to subangular	moderately well	Qtz, fsp, msc, OM, amber	olive-grey	moderate to strong	stipple speckled to mosaic speckled	Uncommon clay coatings ferruginous redoximorphic features?		burrow (circular zone of coarser fill)? With accumulation rim
	HT8.8	49	CB	sandstone	40:60	Fl and vf sand, silt, clay	angular to subrounded	moderately well	Qtz, fsp, msc, OM, amber	olive	mostly weak to moderate	stipple speckled to mosaic speckled			root traces (hand sample)
7	M2.10B	32	Bw1	mudstone	15:85	vf sand, silt, clay	angular to subrounded	moderate	Qtz, fsp, msc, rare strange green mineral with high relief and high birefringence	olive	very weak with strong	stipple speckled to mosaic speckled,	poorly developed clay coatings, accumulation rims?	possible accumulation redoximorphic feature	root traces in hand sample; uncommon Sparry, void-filling carbonate. Papule
	M2.8B	64	Bw2	mudstone	2:98	vf sand, silt, clay	subangular to subrounded	moderately well	Qtz, fsp, msc, blocky small fragments of OM, rare strange green mineral with high relief and high birefringence	light olive	moderately strong with occasional clouds of weak	stipple speckled to mosaic speckled,	poorly developed clay coatings	Some depletion redoximorphic features	root traces in hand sample; rare void-filling sparry carbonate
	M2.3B	147	Bw3	mudstone	10:90	vf sand, silt, clay	angular to subrounded	moderately poor	Qtz, fsp, msc, amber, elongate strands of OM (more abundant than above)	olive	Strong with occasional clouds of moderate	well developed mosaic speckled.	Possible poorly developed clay coatings.	Some depletion redoximorphic features	root traces? Burrow? Coarser fill
7	MB2.38B*	16	Bt	claystone	10:90	FL, vf sand, silt clay	angular to subrounded	poor	dominantly qtz and fsp, rare msc	olive-grey	Large clouds of weak surrounded by rims of moderate, with clouds of moderate within weakly impregnated	stipple speckled to mosaic speckled; uncommon granostriations in one chip, clay coatings	Uncommon clay coatings in groundmass and along ped? Surfaces; Rare iron hypocoatings along voids/ root traces	none observed	peds subangular blocky

Appendix B: Thin Section Descriptions

Category	Sample ID	Depth (cm)	Horizon	Lithology	coarse:fine	Grain Size	Roundness	Sorting	Composition	Matrix Colour	Iron Impregnation	b-fabric	Illuvial Features	Redoximorphic Features	Notes
	MB2.37B*	30	Bw1	mudstone	15:85	FL, vf sand, silt clay	angular to subrounded	poor	dominantly qtz and fsp, rare msc, rare disp OM	olive-grey	Moderate to weak	mosaic speckled	Uncommon iron coatings along voids/ along root traces	none observed	carbonate, sparry and micritic, extends along a linear trend across the slide
	MB2.35B*	55	Bw2	mudstone	20:80	some FL, vf sand, silt, clay	angular to subrounded	moderately poor	Qtz, fsp, msc, rare amber, abundant disp OM (elongate, aligned)	dark olive-grey	Large clouds of weak surrounded by rims of moderate, with clouds of moderate surrounding root traces within	stipple-speckled to mosaic speckled	Uncommon clay coatings in groundmass	none observed	Possible peds due to Fe accumulation on edges of chips
	MB2.33B*	76	Bw3	mudstone	20:80	FL, vf sand, silt clay	angular to subangular	moderate	Qtz, fsp, msc, rare amber, some disp OM	Olive-grey	Large clouds of weak surrounded by rims of moderate, with clouds of moderate within weakly impregnated area	stipple-speckled to faintly mosaic speckled	Uncommon clay coatings in groundmass	none observed	papules
	MB2.29B*	124	Bw4	sandy mudstone	20:80	FL, vf sand, silt clay	angular to subangular	moderate	Qtz, fsp, msc, rare amber, some disp OM	Olive-grey	Weak	stipple-speckled to faintly mosaic speckled; rare granostriation	rare clay coatings	none observed	papules
8	T1.16	12	Bw1	mudstone	20:80	FU, Fl and vf sand, silt, clay	angular to subrounded	moderately poor	Qtz, fsp, msc, disp OM (rare, blocky)	Olive	moderate with a few clouds of weak	mosaic speckled	Uncommon clay coatings in groundmass	none observed	
	T1.12	101	Bw2	mudstone	25:75	FU, Fl and vf sand, silt, clay	angular to subrounded	moderately poor	Qtz, fsp, msc, disp OM (common, blocky)	medium olive	mostly weak with zones of moderate	mosaic speckled	Uncommon clay coatings in groundmass	none observed	

Appendix B: Thin Section Descriptions

Category	Sample ID	Depth (cm)	Horizon	Lithology	coarse:fine	Grain Size	Roundness	Sorting	Composition	Matrix Colour	Iron Impregnation	b-fabric	Illuvial Features	Redoximorphic Features	Notes
	T1.11	120	Bw2	mudstone	10:90	vf sand, silt, clay	subangular to sub rounded	moderately well	Qtz, fsp, msc, disp OM (common, blocky)	medium olive	moderate to strong with depletion redoximorphic features having accumulation rims	mosaic speckled	Uncommon clay coatings in groundmass	none observed	
8	T1.29	10	Bw1	mudstone	5:95 in some places, up to 30:70 in others	FL sand, silt, clay	angular to subrounded	moderately poor	Qtz, fsp, msc, disp OM ? (might be Fe. Rare, dispersed)	Olive-grey	dominantly weak in large clouds in centres of chips, thin rims of moderately weak around edges of chips	stipple speckled to mosaic speckled	Uncommon, well-developed clay coatings in groundmass; Common iron coatings on grains and in groundmass	none observed	root traces, possible burrows; Small amount of sparry carbonate, papules
	T1.27	60	Bw2	mudstone	5:95	one medium grain of qtz, rest vf sand, silt, clay	subangular to subrounded	well	Qtz, fsp, disp OM (dispersed)	Olive-grey	dominantly weak in large clouds in centres of chips, thin rims of moderately weak around edges of chips	stipple speckled to mosaic speckled	Uncommon, well-developed clay coatings in groundmass; Uncommon iron coatings on grains and in groundmass	none observed	
	T1.25	100	Bw2	mudstone	10:95	FL, vf sand, silt, clay	subangular to subrounded	moderate	Qtz, fsp, disp OM (dispersed)	Olive-grey	dominantly weak in large clouds in centres of chips, thin rims of moderately weak around edges of chips	Mosaic speckled	Uncommon, well-developed clay coatings in groundmass; Uncommon iron coatings on grains and in groundmass	none observed	
8	T1.34	10	Bw1	mudstone	<1:99	rare vf sand, mostly silt, clay	subangular to subrounded	very well	Qtz, fsp, msc, OM (rare, elongate strands)	light grey	strong in thin, narrow bands surrounding clouds of weak	mosaic speckled	Rare, weakly developed clay coatings in groundmass	none observed	rare, sparry carbonate
	T1.31	95	Bw2	siltstone	20:80	Fl sand, vf sand, silt, clay	angular to subrounded	moderately poor	Qtz, fsp, msc, OM (rare, elongate strands)	olive-grey	moderately weak to moderate	mosaic speckled	Rare, weakly developed clay coatings in groundmass	none observed	papules
9	SET2-19	30-55	A	siltstone	35:65	coarse to v.f sand, silt, clay	angular to subangular	poorly	qtz (monocrystalline and microcrystalline), fsp, muscovite, opaques (OM). OM thin and aligned.	Light brownish-grey	weak to moderate	mosaic speckled to well-developed unistriated	Uncommon iron coatings on grains and hypocaotings along possible root traces	none observed	root traces? burrows?

Appendix B: Thin Section Descriptions

Category	Sample ID	Depth (cm)	Horizon	Lithology	coarse:fine	Grain Size	Roundness	Sorting	Composition	Matrix Colour	Iron Impregnation	b-fabric	Illuvial Features	Redoximorphic Features	Notes
	SET2-17	52-77	Bw1	siltstone	20:80	F.U., silt, clay	subangular to subrounded	moderately well	qtz (monocrystalline and microcrystalline), fsp, muscovite, opaques (OM)	Greyish brown	weak to moderate	well developed unistriated to faintly reticulate; uncommon granostriation	Rare clay coatings	none observed	root traces
	SET2-15	77-95	Bw2	siltstone	20:80	m.l sand to v.f sand, silt, clay		moderate	qtz (monocrystalline and microcrystalline), fsp, muscovite, opaques (OM) Much more abundant than SET 2-12 and 2-9	Greyish brown	Weak to moderate	stipple-speckled to mosaic-speckled; common granostriation	Uncommon iron coatings on grains and hypocaotings along possible root traces	none observed	burrow
	SET2-14	95-130	Bw3	mudstone	5:95	v.f. sand, silt, clay	subangular to subrounded	moderately well	qtz (monocrystalline and microcrystalline), fsp, muscovite, opaques (OM)	light brownish grey	weak to moderate	stipple-speckled	none observed	none observed	root traces (hand sample)
	SET2-12	130-200	Bw4	siltstone	20:80	f.u., silt, clay	subangular to rounded	moderate	qtz (monocrystalline and microcrystalline), fsp, muscovite, opaques (OM)	light brownish grey	Weak with a few, isolated clouds of moderate	very well developed mosaic-speckled	rare clay coatings around root traces	none observed	root traces
	SET2-9	130-200	Bw4	siltstone	20:80	one m.l clast, rest f.l to v.f sand, silt, clay	subangular to subrounded	moderate	qtz (monocrystalline and microcrystalline), fsp, muscovite, opaques (OM) (blocky fragments), piece of amber	light brownish grey	Weak with a few, isolated clouds of moderate	very well developed mosaic-speckled	rare clay coatings around root traces	none observed	n/a